



HAL
open science

Micro-fabrication of wearable and high-performing cutaneous devices based on organic materials for human electrophysiological recordings

Thomas Lonjaret

► **To cite this version:**

Thomas Lonjaret. Micro-fabrication of wearable and high-performing cutaneous devices based on organic materials for human electrophysiological recordings. Other. Université de Lyon, 2016. English. NNT : 2016LYSEM021 . tel-02003520

HAL Id: tel-02003520

<https://theses.hal.science/tel-02003520>

Submitted on 1 Feb 2019

HAL is a multi-disciplinary open access archive for the deposit and dissemination of scientific research documents, whether they are published or not. The documents may come from teaching and research institutions in France or abroad, or from public or private research centers.

L'archive ouverte pluridisciplinaire **HAL**, est destinée au dépôt et à la diffusion de documents scientifiques de niveau recherche, publiés ou non, émanant des établissements d'enseignement et de recherche français ou étrangers, des laboratoires publics ou privés.



N°d'ordre NNT : 2016LYSEM021

THESE de DOCTORAT DE L'UNIVERSITE DE LYON
opérée au sein de
l'Ecole des Mines de Saint-Etienne

Ecole Doctorale N° 488
Sciences, Ingénierie, Santé

Spécialité de doctorat : Microélectronique
Discipline : Bioélectronique

Soutenue à huis clos le 25/10/2016, par :
Thomas Edouard Lonjaret

Micro-fabrication of wearable and high-performing cutaneous devices based on organic materials for human electrophysiological recordings

Devant le jury composé de :

-	-	-	Président du Jury
Salleo Alberto	Professeur associé	Stanford University	Rapporteur
Lacour Stéphanie	Professeur	Ecole Polytechnique Fédérale de Lausanne	Rapporteuse
Yvert Blaise	Directeur de Recherche	INSERM	Examineur
Badier Jean-Michel	Ingénieur de Recherche	Aix-Marseille Université	Examineur
Malliaras George	Professeur	Ecole des Mines de Saint-Etienne	Directeur de thèse
Ismailova Esma	Ingénieure de recherche	Ecole des Mines de Saint-Etienne	Co-encadrante de thèse
Fiocchi Michel	Directeur de l'entrepreneuriat	Ecole des Mines de Saint-Etienne	Co-encadrant de thèse
Hervé Thierry	C.E.O	Microvitae Technologie	Invité

Spécialités doctorales
 SCIENCES ET GENIE DES MATERIAUX
 MECANIQUE ET INGENIERIE
 GENIE DES PROCEDES
 SCIENCES DE LA TERRE
 SCIENCES ET GENIE DE L'ENVIRONNEMENT

Responsables :
 K. Wolski Directeur de recherche
 S. Drapier, professeur
 F. Gruy, Maître de recherche
 B. Guy, Directeur de recherche
 D. Graillot, Directeur de recherche

Spécialités doctorales
 MATHEMATIQUES APPLIQUEES
 INFORMATIQUE
 IMAGE, VISION, SIGNAL
 GENIE INDUSTRIEL
 MICROELECTRONIQUE

Responsables
 O. Roustant, Maître-assistant
 O. Boissier, Professeur
 JC. Pinoli, Professeur
 X. Delorme, Maître assistant
 Ph. Lalevée, Professeur

EMSE : Enseignants-chercheurs et chercheurs autorisés à diriger des thèses de doctorat (titulaires d'un doctorat d'État ou d'une HDR)

Nom	Responsable	Grade	Spécialité	Responsable
ABSI	Nabil	CR	Génie industriel	CMP
AUGUSTO	Vincent	CR	Image, Vision, Signal	CIS
AVRIL	Stéphane	PR2	Mécanique et ingénierie	CIS
BADEL	Pierre	MA(MDC)	Mécanique et ingénierie	CIS
BALBO	Flavien	PR2	Informatique	FAYOL
BASSEREAU	Jean-François	PR	Sciences et génie des matériaux	SMS
BATTON-HUBERT	Mireille	PR2	Sciences et génie de l'environnement	FAYOL
BEIGBEDER	Michel	MA(MDC)	Informatique	FAYOL
BLAYAC	Sylvain	MA(MDC)	Microélectronique	CMP
BOISSIER	Olivier	PR1	Informatique	FAYOL
BONNEFOY	Olivier	MA(MDC)	Génie des Procédés	SPIN
BORBELY	Andras	MR(DR2)	Sciences et génie des matériaux	SMS
BOUCHER	Xavier	PR2	Génie Industriel	FAYOL
BRODHAG	Christian	DR	Sciences et génie de l'environnement	FAYOL
BRUCHON	Julien	MA(MDC)	Mécanique et ingénierie	SMS
BURLAT	Patrick	PR1	Génie Industriel	FAYOL
CHRISTIEN	Frédéric	PR	Science et génie des matériaux	SMS
DAUZERE-PERES	Stéphane	PR1	Génie Industriel	CMP
DEBAYLE	Johan	CR	Image Vision Signal	CIS
DELAFOSSE	David	PR0	Sciences et génie des matériaux	SMS
DELORME	Xavier	MA(MDC)	Génie industriel	FAYOL
DESRAYAUD	Christophe	PR1	Mécanique et ingénierie	SMS
DJENIZIAN	Thierry	PR	Science et génie des matériaux	CMP
DOUCE	Sandrine	PR2	Sciences de gestion	FAYOL
DRAPIER	Sylvain	PR1	Mécanique et ingénierie	SMS
FAVERGEON	Loïc	CR	Génie des Procédés	SPIN
FEILLET	Dominique	PR1	Génie Industriel	CMP
FOREST	Valérie	MA(MDC)	Génie des Procédés	CIS
FOURNIER	Jacques	Ingénieur chercheur CEA	Microélectronique	CMP
FRACZKIEWICZ	Anna	DR	Sciences et génie des matériaux	SMS
GARCIA	Daniel	MR(DR2)	Génie des Procédés	SPIN
GAVET	Yann	MA(MDC)	Image Vision Signal	CIS
GERINGER	Jean	MA(MDC)	Sciences et génie des matériaux	CIS
GOEURIOT	Dominique	DR	Sciences et génie des matériaux	SMS
GONDRAN	Natacha	MA(MDC)	Sciences et génie de l'environnement	FAYOL
GRAILLOT	Didier	DR	Sciences et génie de l'environnement	SPIN
GROSSEAU	Philippe	DR	Génie des Procédés	SPIN
GRUY	Frédéric	PR1	Génie des Procédés	SPIN
GUY	Bernard	DR	Sciences de la Terre	SPIN
HAN	Woo-Suck	MR	Mécanique et ingénierie	SMS
HERRI	Jean Michel	PR1	Génie des Procédés	SPIN
KERMOUCHE	Guillaume	PR2	Mécanique et Ingénierie	SMS
KLOCKER	Helmut	DR	Sciences et génie des matériaux	SMS
LAFOREST	Valérie	MR(DR2)	Sciences et génie de l'environnement	FAYOL
LERICHE	Rodolphe	CR	Mécanique et ingénierie	FAYOL
MALLIARAS	Georges	PR1	Microélectronique	CMP
MOLIMARD	Jérôme	PR2	Mécanique et ingénierie	CIS
MOUTTE	Jacques	CR	Génie des Procédés	SPIN
NIKOLOVSKI	Jean-Pierre	Ingénieur de recherche	Mécanique et ingénierie	CMP
NORTIER	Patrice	PR1		SPIN
OWENS	Rosin	MA(MDC)	Microélectronique	CMP
PERES	Véronique	MR	Génie des Procédés	SPIN
PICARD	Gauthier	MA(MDC)	Informatique	FAYOL
PIJOLAT	Christophe	PR0	Génie des Procédés	SPIN
PIJOLAT	Michèle	PR1	Génie des Procédés	SPIN
PINOLI	Jean Charles	PR0	Image Vision Signal	CIS
POURCHEZ	Jérémy	MR	Génie des Procédés	CIS
ROBISSON	Bruno	Ingénieur de recherche	Microélectronique	CMP
ROUSSY	Agnès	MA(MDC)	Génie industriel	CMP
ROUSTANT	Olivier	MA(MDC)	Mathématiques appliquées	FAYOL
STOLARZ	Jacques	CR	Sciences et génie des matériaux	SMS
TRIA	Assia	Ingénieur de recherche	Microélectronique	CMP
VALDIVIESO	François	PR2	Sciences et génie des matériaux	SMS
VIRICELLE	Jean Paul	DR	Génie des Procédés	SPIN
WOLSKI	Krzysztof	DR	Sciences et génie des matériaux	SMS
XIE	Xiaolan	PR1	Génie industriel	CIS
YUGMA	Gallian	CR	Génie industriel	CMP

Acknowledgements

Most of this work was carried out South of France, in the city of Gardanne, at the Department of Bioelectronics (BEL), part of the Microelectronics Center of Provence (CMP), research institute of the engineering school *École Nationale Supérieure des Mines de Saint-Etienne*. A lot of names to define a place where I spent most of the three years of my PhD, a place a modern research center tries to emerge from, between last century industry and wonderful surrounding forests and mountains... From my office I could see the *Sainte-Victoire* mountain, next to which the company I was part of, Microvitae Technologie, is located. Integrated as a research engineer, I discovered there the exciting world of startups and everything about medical devices.

But all of the following work would have been nothing without my colleagues, who became my friends. I will always remember the long and fruitful discussions we had (yes, about science and work, but not only), our volleyball games on Marseille's beach, hikes in the Calanques, beers in Tibbar, trips for often unsuccessful experiments in La Timone, collaborations in clean room, gossips about everything, holidays after conferences...

First, I would like to thank my advisors and scientists from BEL. George, you are a giant, and I hope that, one day, I will be able to walk in your footsteps while staying as confident and optimist as you always are. Esma, you are a wonderful person, I am sure the textile team you built up from scratch has a promising future. It was a pleasure to work with you and we had a lot of fun in Arizona. I hope I was not too terrible as your first PhD student! Michel, you are the network guy who did everything in his life, thank you for your wise advices and help. Roisin, it will always be a pleasure to discuss with you and to discover how efficient you are. I will not forget that you are the only one able to put the lab in order with a smile! Adel, tireless bike rider, we still have to talk about a lot of stuff, including the dinosaurs (I did not forget!). I really enjoyed the time I spent and giggles I had with people from the CMP, such as Thierry, Michele, Gracien, Florent, Stéphane, Bernard, Béné, Catherine, François, Hervé... I am certainly forgetting too many other people... And what to say about PhD students and postdocs from Bel, these amazing guys coming from all around the world? Many people passed by the lab and were more or less associated with my work: Xenofon, Marc, Adam, Wonryung, Bartek, Jake, Bastien, Aimie... But some names will be forever associated with my work at BEL. The crazy, manic, so-German, but efficient and funny Marcel, who will be strong and muscular, one day. The lazy but tireless and tenacious Ilke, who will be an expert in electronics and soldering, soon. The loquacious, gossipy and ink-jet printing-lover Eloïse,

Acknowledgements

who was my officemate and my companion of adventure and misfortune. The smiling Jolien, always over-excited for everything, who is snowboarding as good as she speaks French (until the bump!). The pretty and LabVIEW-expert Anna-Maria, who will never forget how to turn on a computer. The clean-room-lover, stubborn but friendly Dimitrios/is/i, who will think that, of course, this thesis is about Greek history. The member of high-society, athletic only for tennis, and Goethe-lover Shahab, who may dare start to learn *le français vulgaire de la rue*, one day. The discrete Mahmoudhy, who may coat his skis with GOPS, to avoid falling on the snow. The cell-lover, industrious and early bird Magali, who finally replaced me as youngest PhD student to cut *Galette des Rois*. The Briton, Loig, who may bet with Roisin another office and a bigger desk by playing *jeux de palets*. The enthusiastic Carol, the perpetual student who should start to kiss her probes every morning to say hello, the may become less jealous and start to work! The proud and so-Sicilian Vincenzo, who may open a micro-fluidic soap fabrication plant after postdoc. The mysterious Paschalis, who is the only one able to know what the neuromorphic devices are for. The hiker, flirty, sometimes scientific Chris, who will be able to correctly say the French *rrr*, one day. The sporty and rasta Mary, who is trying to walk barefoot in the lab as soon as Adel is not around. The naive but never mean Yi, who is actually a secret fan of Dalai-Lama. The ingenious Ussein, known as the Brother, who come to work just to have the pleasure to taste his pilaf rice. Ilke's mamma, Sahika, who chose petrol instead of never-ending post-doc positions. The kind and muscular Babis, whose actual name is unpronounceable and who is just happy of having every day his lunch cooked by Anna-Maria. I need to finish this list with Pierre, who was kind of my mentor when I started, to finish as my driver for bakery in the last months. I will not forget people from Microvitae, Valéry, Timothée. We stayed together through difficulties but I also enjoyed our chats to change the world!

Special thanks to Lucie, my girlfriend who became my wife during this PhD, for her kind advices and support, even if she still does not know what is PEDOT after hearing this word hundreds of times! To my parents who gave me the chance to become a doctor! To my brother and sister just because I love them!

Gardanne, France, September 2016

Thomas Lonjaret

Résumé

L'ensemble du corps humain est surveillé par différents capteurs médicaux connectés, que ce soit depuis une montre connectée ou par un pacemaker. Ces capteurs permettent une nette amélioration du suivi de notre santé, à l'hôpital, mais surtout dans notre vie de tous les jours, notamment en enregistrant les signaux électrophysiologiques. L'électrophysiologie consiste à étudier les signaux électriques et électrochimiques générés aussi bien par certaines cellules spécifiques que par des organes entiers. Elle donne donc aux médecins l'opportunité de suivre le fonctionnement du corps à plusieurs échelles. L'enregistrement de ces activités par des électrodes est essentiel pour le diagnostic et la compréhension de pathologies aussi diverses que les arythmies cardiaques, l'épilepsie ou la dégénération musculaire. Dans cette thèse, nous étudions différents types d'électrodes cutanées à base de matériaux organiques, de leur conception à leur évaluation préclinique. Le principal but de ce travail est de développer une interface souple et compatible avec la peau humaine, afin de réaliser des mesures électrophysiologiques performantes.

Notre approche est basée sur l'utilisation du polymère conducteur PEDOT :PSS et de gels ioniques, qui réduisent l'impédance de l'interface électrode-peau. Différents substrats fins et souples, plastiques ou textiles, composent nos électrodes. Cela leur confère une importante flexibilité et permet même de les intégrer à des vêtements. De nouvelles techniques de fabrications, adaptées à ces substrats et aux matériaux organiques, sont présentées. Afin de démontrer les excellentes performances de nos capteurs innovants par rapport aux électrodes médicales usuelles, ceux-ci sont intégralement caractérisés, puis testés sur des volontaires. L'enregistrement de signaux cutanés issus des tissus musculaires, cardiaques et cérébraux permet d'évaluer la stabilité sur plusieurs jours et la qualité de nos électrodes. Nous introduisons également le transistor organique électrochimique, utilisé pour la première fois comme une électrode cutanée microscopique dite « active ». Celui-ci permet d'amplifier et de filtrer in situ le signal afin d'augmenter sa qualité. Du fait de leurs forts potentiels industriels et cliniques, nous étudions maintenant l'intégration de nos électrodes organiques cutanées dans des produits médicaux de pointe.

Mots clefs : Dispositif Médical, électrode, électrophysiologie, électronique organique, transistor organique électrochimique, capteurs flexibles intégrés

Abstract

In our medicalized world, human-monitoring sensors can be found everywhere, from a smart-watch to a life-saving pacemaker. They facilitate direct recordings of our electrophysiological activity, in the hospital as well as in our everyday life. Electrophysiology is the study of electrical and electrochemical signals generated by specific cells or whole organs. It gives doctors the opportunity to track the physiological behavior of a single neuron, a muscle tissue or the integral brain. The recording of these activities is essential to diagnose and better understand diseases like cardiac arrhythmias, epilepsy, muscular degeneration and many more. In this thesis, we study different types of cutaneous electrodes based on organic materials, from conception to pre-clinical evaluation. The main focus of this work is to enable high-quality electrophysiological recordings through soft and flexible devices compatible with human skin. Our approach is based on the usage of PEDOT:PSS conducting polymer and ionic gels in order to reduce impedance at the skin-electrode interface. Moreover, the substrate of our electrodes is made with different materials such as thin and conformable plastics and textiles. Our devices are then flexible, motion resistant and can be integrating into clothes. We developed new fabrication processes, considering the different substrates and organic materials specifics. The electrodes were characterized and then tested on human volunteers to show their excellent performance in comparison to standard medical electrodes. The evaluation of noise reduction capabilities and possibilities to perform long-term recordings were established on signals coming from muscles, heart and brain. In order to further reduce noise and to increase wearability, we present a hundred micrometer-small “active” electrode, based on the organic electrochemical transistor. It enables in situ amplification and filtering of recorded signals. The wearable organic electrodes developed in this work are of great industrial and clinic interest. Future work will aim to integrate these technologies into state-of-the-art medical devices.

Key words: Medical Device, electrode, electrophysiology, organic electronics, organic electrochemical transistor, wearable sensor

Contents

Acknowledgements	i
Abstract (Français/English)	iii
List of figures	xi
Nomenclature	xiii
1 Introduction on electrophysiology and medical devices	1
1.1 Overview on electrophysiology	1
1.1.1 Genesis of electric biosignals	1
1.1.2 Different modalities for electrophysiology	4
1.1.3 Overview on the acquisition chain for electrophysiological recordings	10
1.2 Analysis of medical needs for electrophysiology	12
1.2.1 Electrophysiology to diagnosis pathologies	12
1.2.2 Electrophysiology to assist pathologies	14
1.2.3 Current problematics for ambulatory electrophysiology	15
1.3 Industrial vision for medical devices conception	17
1.3.1 From the idea to the mass production of medical devices	18
1.3.2 How can research and development add value to medical device conception?	19
1.3.3 CE marking	21
1.4 Bibliography	24
2 Electrodes	31
2.1 A model of the electrode and the reactions at its interface	31
2.1.1 Electrochemical model of the electrode	31
2.1.2 Noise generation	33
2.1.3 The electrolyte in electrophysiology	35
2.1.4 Skin specificities for cutaneous electrophysiology	36
2.1.5 Equivalent model of skin-electrode interface	36
2.2 Electrode characterization	37
2.2.1 Three-electrode cell and potentiostat	37
2.2.2 Impedance	38
2.2.3 DC voltage offset measurement	41
2.2.4 Cyclic voltammetry	41

Contents

2.2.5	Biocompatibility	42
2.3	Medical Electrodes for electrophysiology	43
2.3.1	Options around the conception of an electrode	43
2.3.2	Presentation of different medical electrodes	45
2.4	Bibliography	47
3	Improving skin-electrode interface with conducting organic materials	49
3.1	Introduction on organic electronics	50
3.1.1	Organic materials	50
3.1.2	Conducting polymers	50
3.1.3	Organic bioelectronics	51
3.2	The use of conducting polymers for electrophysiology	53
3.2.1	State-of-the-art on the use of conducting polymers to improve electrode interface	53
3.2.2	Fabrication processes and characterization of dry PEDOT:PSS electrodes	54
3.3	The use of ionic liquids for electrophysiology	56
3.3.1	Introduction on ionic liquids	56
3.3.2	Ion gels as solid electrolytes	57
3.3.3	Synthesis and integration of ion gels on electrodes	58
3.4	Introduction of a novel biocompatible ion gel for electrodes	58
3.4.1	Biocompatibility of cholinium-based ionic liquids	58
3.4.2	Chemical materials	59
3.4.3	Preparation of the ion gel	59
3.4.4	Characterization	60
3.4.5	Discussion	64
3.5	Bibliography	64
4	Organic conductors in wearable sensors	73
4.1	Electrodes on flexible substrates	74
4.1.1	Review of flexible electrodes to monitor internal organs	74
4.1.2	Review of flexible electrodes for cutaneous applications	74
4.1.3	Fabrication of plastic cutaneous electrodes	75
4.1.4	Discussion	77
4.2	Introduction of innovative electrodes based on textile substrate	77
4.2.1	Introduction on textile electronics	77
4.2.2	Coating of PEDOT:PSS and ion gel on knitted textile	79
4.2.3	Characterization of textile electrodes	82
4.2.4	Discussion	85
4.3	Bibliography	85

5	Cutaneous electrophysiology with organics	93
5.1	Dry electrodes	94
5.1.1	State-of-the-art on dry electrodes	94
5.1.2	Discussion	95
5.2	Ionic gel-assisted electrodes	95
5.2.1	Experimental	95
5.2.2	Electrode characterization	96
5.2.3	ECG recordings	97
5.2.4	Discussion	98
5.3	Wearable textile electrodes	99
5.3.1	Experimental	99
5.3.2	Electrode characterization on skin	100
5.3.3	ECG recording	101
5.3.4	Discussion	103
5.4	Recording and stimulation performances of textile electrodes	104
5.4.1	Experimental	104
5.4.2	Electrode characterization for stimulation	105
5.4.3	EMG recording and stimulation	105
5.4.4	Discussion	107
5.5	Bibliography	108
6	Potential of OECT for next generation electrophysiology	111
6.1	Introduction on Organic ElectroChemical Transistors	112
6.1.1	Organic transistors	112
6.1.2	The Organic ElectroChemical Transistors	112
6.1.3	Fabrication process	113
6.1.4	Applications of the OECT	116
6.2	OECT as a pre-amplifier for electrophysiological recordings	117
6.2.1	Connection set-up and Characterization	117
6.2.2	Results on ECG	118
6.2.3	Results on EOG	120
6.2.4	Results on EEG	122
6.2.5	Discussion	122
6.3	Enabling the compatibility of OECT technology with medical systems	123
6.3.1	Experimental part	123
6.3.2	Addition of a load resistor	123
6.3.3	Voltage gain in linear and saturation regimes	125
6.3.4	Voltage amplification of ECG signals	127
6.3.5	Discussion	128
6.4	Outlook: Improved OECT in direct contact with skin as active electrodes	128
6.4.1	OECT and active electrodes	129
6.4.2	Integration on flexible substrate for skin contact	129

Contents

6.4.3 Work on going	130
6.5 Bibliography	131
7 Conclusion and outlook	135

List of Figures

1.1	Anatomy of a neuron and zoom into the cell membrane	2
1.2	Generation steps of an action potential	3
1.3	10-20 system for EEG	5
1.4	Technologies to record brain activity	6
1.5	Standard ECG signal	8
1.6	EMG signal during plantar-flexion contraction	10
1.7	Acquisition chain for clinical electrophysiology	12
1.8	Medical Devices Conception Chain	20
2.1	The Galvanic electrochemical cell	32
2.2	Motion artifacts in ECG signals	35
2.3	Skin layers	36
2.4	Equivalent circuit for the electrode-skin interface	37
2.5	Schematic of a potentiostat system	38
2.6	Example of Electrochemical Impedance Spectroscopy	40
2.7	Example of Cyclic voltammetry measurement	42
2.8	List of options for electrode development	44
3.1	An example of conducting polymer: <i>trans</i> -poylacetylene	51
3.2	Chemical structure of PEDOT:PSS	54
3.3	Impedance and CV characterization of PEDOT:PSS electrodes	56
3.4	1-ethyl-3-methylimidazolium ethyl sulfate ion gel preparation	58
3.5	Cholinium lactate ion gel preparation	60
3.6	Rheological properties of cholinium lactate ion gels	61
3.7	Thermal properties of cholinium lactate ion gels	62
3.8	Electrical properties of cholinium lactate ion gels	63
3.9	Long-term stability of cholinium lactate ion gels and water absorption	64
4.1	Laser-cutting of Kapton substrates	76
4.2	Examples of Kapton-based electrodes	77
4.3	Process flow for the patterning of PEDOT:PSS on textile	81
4.4	Examples of PEDOT:PSS-patterned knitted textiles	82
4.5	Integration of ion gel on textile for cutaneous electrodes	83
4.6	Mechanical properties of the textile electrode	84
5.1	Skin impedance characterization of cholinium-based ion gels	97

List of Figures

5.2	Comparison of ECG signals between medical electrode and cholinium ion gel electrodes	98
5.3	Cholinium-based ion gel electrode evaluation for long-term ECG evaluation . .	98
5.4	Impedance spectra of textile and medical electrodes	100
5.5	Textile electrode evaluation for ambulatory ECG monitoring	102
5.6	Textile electrode evaluation for long-term ECG evaluation	103
5.7	Cyclic voltammetric measurement on textile electrode	106
5.8	EMG recording with textile electrode	107
5.9	Performance of conducting polymer textile electrode in muscular stimulation	108
6.1	Schematic of the OECT	113
6.2	OECT fabrication process with photolithography	115
6.3	Characteristics of low temperature annealed OECTs	116
6.4	Set-up of the OECT as pre-amplifier and characterization	119
6.5	ECG with OECT as pre-amplifier	120
6.6	EOG with OECT as pre-amplifier	121
6.7	Eye blinking and closing recorded with OECT as pre-amplifier	121
6.8	EEG with OECT as pre-amplifier	122
6.9	Characterization of an OECT with drain load resistor	125
6.10	Experimental data versus model for amplification gain	127
6.11	Amplification of ECG signals in saturation and linear regimes	128
6.12	Cartoon of an active electrode with an OECT	130

Nomenclature

AC	Alternative current
BCI	Brain-computer interface
CE	Counter electrode
CV	Cyclic voltammetry
DBSA	Dodecyl benzene sulfonic acid
DC	Direct current
ECG	Electrocardiography or Electrocardiograph or Electrocardiogram
ECoG	Electrocorticography or Electrocardiograph or Electrocardiogram
EEG	Electroencephalography or Electroencephalograph or Electroencephalogram
EMG	Electromyography or Electromyograph or Electromyogram
EOG	Electrooculography or Electrooculograph or Electrooculogram
FET	Field-effect transistor
GOPs	(3-glycidioxypropyl) trimethoxysilane
IL	Ionic liquid
LFP	Local field potential
MD	Medical Device (as defined by the European Medical Devices Directive (93/42/EEC))
MOSFET	Metal-oxide-semiconductor field-effect transistor
MU	Motor Unit
OECT	Organic electrochemical transistor
OFET	Organic field-effect transistor
OLED	Organic Light-emitting diode
PEDOT:PSS	poly(3,4-ethylenedioxythiophene) doped with poly(styrene sulfonate)

List of Figures

- RE Reference electrode
- RTIL Room temperature ionic liquid
- SEEG Stereoencephalography
- SNR Signal to noise ratio
- WE Working electrode

Introduction on electrophysiology and medical devices

To assess a technological challenge, an engineering approach is impossible without taking into account all constraints for the future product. Choices are then somehow limited but the solution will be directly conformable to an industrial production or utilization. A fundamental or academic approach opens more possibilities and give often rise to innovative ideas. All along this PhD, I tried to use both of these approaches (which are somehow complementary) to develop innovative cutaneous recording devices for electrophysiology.

First of all, we need to define the context and the users and technological needs of this challenge, and this is the goal of this first chapter. An overview of the field of electrophysiology, which is the main application of all the work presented in this thesis, will be given in order to show and explain which kind of signals are involved and what are the clinical ways of recording them. Then, a closer look to the daily problems occurring in clinic will be necessary to explore and understand medical needs. Finally, since this work was made with an industrial partner, the last part of this chapter will detail the industrial vision to develop a medical device. In my sense, this industrial point of view has to be taken into account, even for scientists. When developing an idea in the specific field of medical devices, it is important to know from the beginning what could be constraints for a future industrialization.

1.1 Overview on electrophysiology

1.1.1 Genesis of electric biosignals

Presentation of a neuron

The main generator of bioelectric signal is the neuron, presented on Fig 1.1a. A quick description of the neuron and its working principle will be presented here. A neuron is made of a cell body, also called soma, which contains the nucleus. The soma presents 2 extensions, the dendrites and the axon. It is possible to find thousands of dendrites branching profusely from one neuron whereas the axon is always single. The axon length varies from a millimeter to more than a meter and it is covered by myelin sheaths. At its end, it gives rise to hundred of branches, ended by synapses (contact area between the axon of a neuron and a dendrite or

Chapter 1. Introduction on electrophysiology and medical devices

soma of another one). Axons are often bundled into fascicles which can make up nerves in the peripheral nervous system.

Neurons are the support for the transmission of information, which is an electric signal called action potential (described more in depth in next Section 1.1.1). Neurons communicate each other mostly by synapses. If a neuron receives a specific amount of post-synaptic potentials from a previous neuron, a new action potential can be generated. It propagates through the axon where its speed can be increased by myelin sheaths. Then this potential is transmitted to the next neurons and so on. Neurons are used both as signal processing units and connection wires to transform and transmit electric signals between central nervous system and peripheral organs.

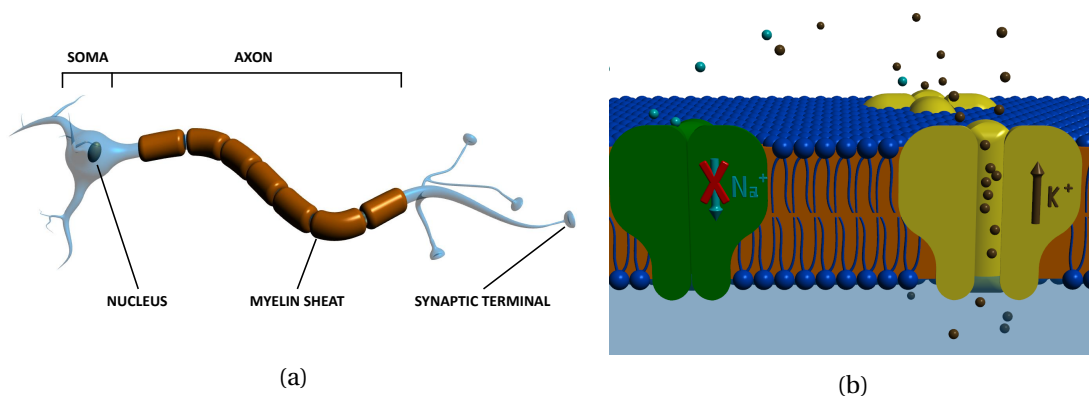


Figure 1.1 – **Anatomy of a neuron and zoom on the cell membrane.** (a) Drawing of a neuron with highlighted subdivisions. (b) Sectional view of the lipid bilayer neuron membrane separating intra- and extra-cellular medium, a closed potassium and opened sodium ion channels.

Action potential generation

In this section, we focus on the generation of this action potential. At rest, there is a negative potential difference (around -70 mV) across the neuron membrane, between the extracellular and the intracellular medium. This difference results from difference of ions concentrations across the membrane. This membrane is made of a lipid bilayer and contains ion channels, as described in the cartoon Fig 1.1b. Nerve impulses are characterized by an instantaneous modification of membrane permeability through the opening and closing of these ion channels. Fig 1.2 shows the difference steps for the changes of membrane potential at a single point of the membrane. During the resting phase, single-directional potassium (K^+) and sodium (Na^+) ion channels are closed and a constant potential is kept. The stimulation induced by the upstream propagation of the action potential opens the Na^+ ion channel which leads to a flow of sodium ions through the cell membrane, increasing the potential difference up to 35 mV. Then K^+ ion channels open and potassium ions escape the cell to the external media, leading to the depolarization state. Na^+ ion channels and then K^+ ion channels close

1.1. Overview on electrophysiology

successively and the potential difference is back to the resting state [1]. Next ion channels were stimulated during the rising phase and the same phenomenon happen. This allows the propagation of the action potential along the membrane. When the action potential reaches the axon terminal, the signal propagates from the neuron to the next one through the synapse. For mammals, the majority of synapses are chemical. The action potential causes synaptic vesicles to fuse with the membrane and to release their neurotransmitter molecules. These neurotransmitters diffuse and activate receptors on the postsynaptic neuron.

Neurons are not the only cell that can propagate action potentials. Muscle cells, also known as myocytes, can propagate action potentials as well, in the same way as neurons. They are stimulated by nerves and the propagation of an action potential involves their contraction and so the movement of the corresponding muscle (more details on the Section 1.1.2).

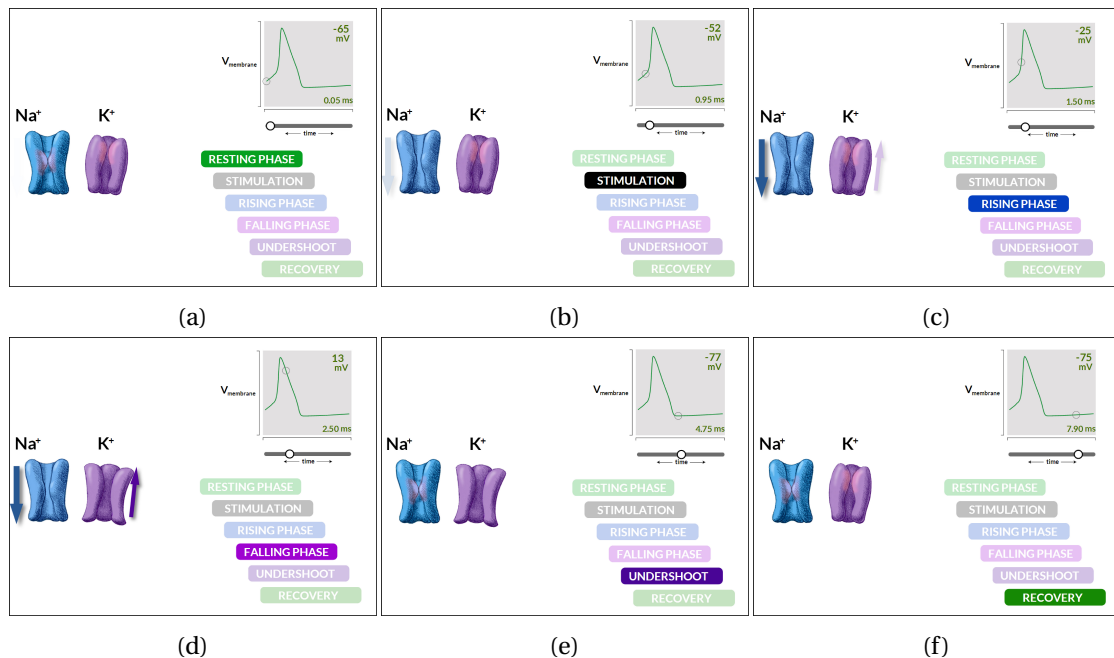


Figure 1.2 – **Generation steps of an action potential.** (a) At rest, both ion channels are closed. The potential difference between in and out of the cell is stable, around -65 mV. (b) Sodium channels are stimulated by an upstream current and start to open. (c) Sodium ions penetrate inside the cell layer and increase the membrane potential. (d) A potential peak around 35 mV triggers the opening of the potassium channels. Potassium ions are moving out of the cell, the membrane potential falls back. (e) The membrane potential reaches a low threshold which leads to the closing of sodium channels and then of potassium channels. (f) During recovery state, both ion channels are closed, membrane potential comes back to its value from resting state and ion channels cannot react to a stimulation.

Propagation in the body

The current generated by a single neuron (a small elementary current dipole) is not measurable from the skin and barely from surrounding electrodes. Signals with high-enough amplitude to be recorded from the skin are generated by a large number of synchronized active neurons and this can be modeled by an equivalent dipole. A spatial organization, that involves current addition, is also needed. This is the case for pyramidal neurons from the cortex which are aligned in a parallel way [2].

An electrophysiological recording is the measurement of the potential difference between 2 points of the body. This potential difference is generated by currents which propagate inside the volume of the body. Main factors of current propagation are the bones (especially the skull), which are less conductive than the brain or the skin. Bones are places where current are attenuated and diffused, which induces a spatial smoothing of electric potentials. In general terms, any modification of the homogeneity of the propagation medium will lightly modify the signal, and this needs to be taken into account for signal processing, especially for EEG.

1.1.2 Different modalities for electrophysiology

Electroencephalography (EEG)

Hans Berger was the first one to use EEG to record electric activity from a human brain, at the end of the 1920s [3]. However, the cerebral origin of these signals had not taken hold right away, and the neurologists started to be interested by EEG after the work of Lord Adrian in the 1930s [4]. Medical and scientific applications of EEG are now remarkably important.

As we explained previously, the opening of ion channels allows ions to move back and forth in the intra- and the extra-cellular medium. When this is happening to a large amount of neurons, an electrical field (local field potential, LFP) is created; and since the extra-cellular medium is conductive, the latter induces a secondary current which circulate in the whole volume of the head. It is important to note that glial cells, surrounding the neurons in the brain, also electroactive, could slightly influence EEG signal by generating small potential variations [5] but this is still under discussion between specialists. Potential variations at the surface of the scalp, produced by the secondary current, are recorded by electrodes placed on the scalp and the resulting signal is called an EEG. Synchrony of LFPs induces typical oscillations within specific frequency domains. The amplitude of this signal is very low (typically 25-100 μV because the scalp, the skull, the cerebrospinal fluid and the meninges are inhomogeneous media which attenuated the signal. An estimation of skull conductivity gives a result 20 to 80 lower than the conductivity of the cerebral fluid and so the skull acts ad low-pass spatial filter [6]. Although strong signal amplification is needed and spatial resolution is low, EEG is a cheap and non-invasive way to record brain activity with a good temporal resolution.

The most common set-up to record EEG is monopolar. The potential recorded by each

electrode on the scalp is compared to a common reference electrode. Usually, this reference electrode is located at the most neutral area, depending on the study, usually on mastoids, earlobes or the neck. It is also possible to use a mean reference, defined by the mean of the potential of all electrodes, especially for high-density recordings[4, 7]. Recording electrodes are placed on the scalp on standard positions: Fig 1.3 shows the 10-20 system but other high-density systems, including more than 128 electrodes, can be used.

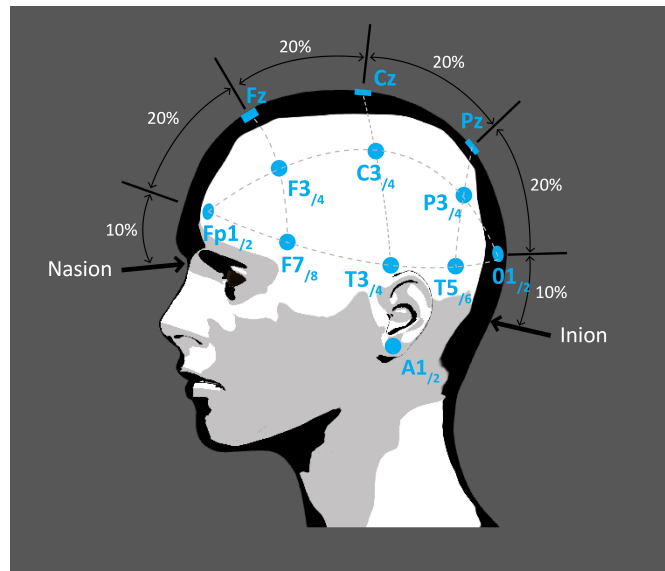


Figure 1.3 – **10-20 system for EEG** (a) Presentation of the 10-20 system which is the international standard for EEG electrodes placement. From nasion to inion, the scalp is frontally and laterally divided in 6 parts. Letters F, C, T, P and O stand for frontal, central, temporal, parietal and occipital lobes, respectively. Odd numbers are for electrodes on the left hemisphere whereas even numbers refer to those on the right hemisphere. Letters Fp, Pg and A identify frontal polar, nasaopharyngeal and earlobes sites, respectively.

Other way to record brain activity (ECoG, SEEG, MEG)

For specific clinical applications which need a better spatial resolution, it is necessary to record inside the skull. If electrodes are located at the cortex surface, the modality is called Electroencephalography (ECoG). In the case of implanted electrodes, which penetrate the brain, the term Stereoencephalography (SEEG, or also stereotactic EEG) is used. Of course, these 2 methods are highly invasive. A last possible technique is the Magnetoencephalography (MEG). Although the spatial resolution performance of invasive technique is not achieved with MEG, this method is not bound with some of the limitation associated with EEG. A cartoon of the different recording modalities for brain activity and their invasiveness is shown on Fig 1.4.

Initially, the method of ECoG (also called intracranial EEG, iEEG) was developed by Wilder Penfield and Herbert Jasper from the 1940s for epileptic patient exploration. A craniotomy is performed (scalp and skull are surgically opened) to expose the brain and an array of

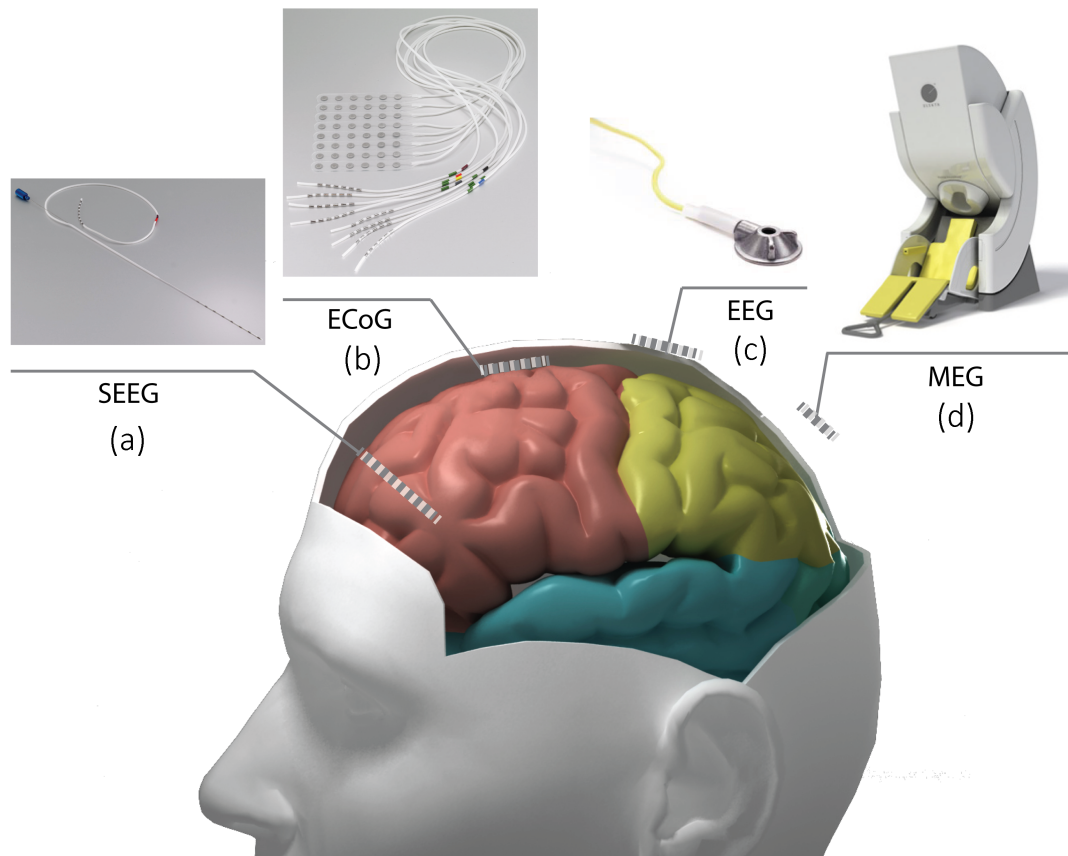


Figure 1.4 – **Technologies to record brain activity.** (a) Implantable device made of several recording electrodes used for stereoencephalography (SEEG). (b) Electrode array for applications in electrocorticography (ECoG). (c) Cup electrode used for electroencephalography (EEG). (d) System to record brain activity by magnetoencephalography (MEG).

electrodes is deposited. The device can be placed either outside of the *dura mater* (epidural ECoG), either under it (subdural ECoG). Thanks of the absence of skull, the spatial resolution of ECoG is much higher than EEG (around 1 cm [8]). However, ECoG recordings are still surface recordings and do not allow access to deep cerebral structures. Moreover, the precise and correct brain area to cover with the electrodes is hard to define. ECoG technique is used to localize epileptogenic zones during surgery but offers great promises as Brain-Machine Interface recording device.

SEEG was developed by Jean Talairach and Jean Bancaud for presurgical exploration of epileptic patients [9]. The idea is to precisely define the brain area responsible for strokes before a surgery which will remove it. EEG is first used to roughly delimit the area. Then stereotactic surgery (the brain is precisely located in a defined three-dimensional coordinate system) is performed to insert few electrode sticks which penetrate the brain. The patient keeps these implanted electrodes for few weeks in order to triangulate the location of the epileptogenic

zone.

MEG is the magnetic counterpart of EEG. Any electric current induces an associated magnetic field. It is also the case for intra-cellular currents, more dense than extracellular currents (such as the secondary current generated by neurons and recorded by EEG). This magnetic field benefits of not being affected by the homogeneity of medium. It means that MEG signals are not disturbed by the skull and source localization and identification are easier. However, MEG recordings need to be done in a specific environment, protected from external magnetic fields. Very sensitive SQUIDS (Superconducting QUantum Interference Device) are used to record up to femto Tesla magnetic field but they need to be cooled down to -269° to keep their supraconductivity state. The system is not mobile and very expensive but does not need any preparation time and does not touch the patient. If the materials are compatible, it is possible to record MEG signal in parallel to EEG or SEEG and then to study more precisely brain activity.

Electrocardiography (ECG)

The heart is a muscle (also called *myocardium*) which rhythmically contracts and induces blood circulation in the body, as pump would do. Heartbeats, or *systoles*, are triggered by specifically patterned electrical currents that spread over the heart. These currents are measurable on the body surface of a patient. The amplified and filtered resultant signal is called an electrocardiogram (ECG or EKG). If Auguste D. Waller was the first one to record on human a surface electrocardiogram in 1887, Willem Einthoven is recognized as the main contributor to the evolution of ECG, with works on the ECG signal and on the acquisition systems in the 1900s.

In the heart, there are some specific cardiac cells, called pacemakers, which possess the property of automaticity. They have the ability to spontaneously depolarize, following a specific rhythm, which lead to a self-generation of an action potential that will propagate to other cardiac cells. Unlike neurons, myocardial cells do not transmit action potentials throughout electrochemical synapses but by direct current spread from one cell to the other over a gap junction. Cells depolarize and repolarize in a precise order which gives rise to a patterned contraction of the different part of the heart. A simple modelling of the heart is a single equivalent dipole and the net dipole moment is known as the heart vector $M(t)$. This vector changes in direction and magnitude as a function of time depending on the spreading of each depolarization wave. A reasonable approximation is to consider the torso as a homogeneous isotropic conducting sphere and the heart as a single point. The ECG signal recorded by 2 electrodes placed on the torso with the heart in between is then a projection of this cardiac vector [10]. The specific placement of these electrode is called a *lead*. 12 leads were decided as standard by an international convention [11] and allow heart activity to be looked at with various points of view. Einthoven was the first to describe what is now called Einthoven's triangle, the 3 bipolar limb leads I, II, and III between right arm and left arm, right arm and left leg, left arm and left leg respectively. 3 other leads are unipolar (aVR, aVL and

Chapter 1. Introduction on electrophysiology and medical devices

aVF) and located on the right arm, the left arm and the left leg respectively. Einthoven's theory claims that the heart is located in middle of an equilateral triangle between arms and left leg. Thus, only 2 leads can be recorded and the 4 others calculated from:

- $III = II - I$
- $aVF = II - I/2$
- $aVR = -I/2 - II/2$
- $aVF = I - II/2$

6 other leads (from V1 to V6) are located on the torso and report activity in the horizontal plane. 12 leads involve some redundancies to image a 3D activity but this spatial over-sampling helps human interpretation and compensates for minor inaccuracies in electrodes placement and in body modelling (the torso is not a homogeneous sphere...). Further and detailed explanations can be found in [10]. Fig 1.5 describes a standard ECG signal obtained from limb lead I with typical patterns (PQRST complexes) whose amplitudes, axes and duration can give information about abnormal heart activity:

- **P wave** is linked with left and right atrium depolarization
- **QRS complex** is linked with left and right ventricles depolarization. An atrial T wave, corresponding with atrium repolarization is hidden by QRS complex.
- **T wave** is linked with the repolarization of ventricles.
- **U wave** can be observed after T wave but its amplitude is very low and its origin still discussed.

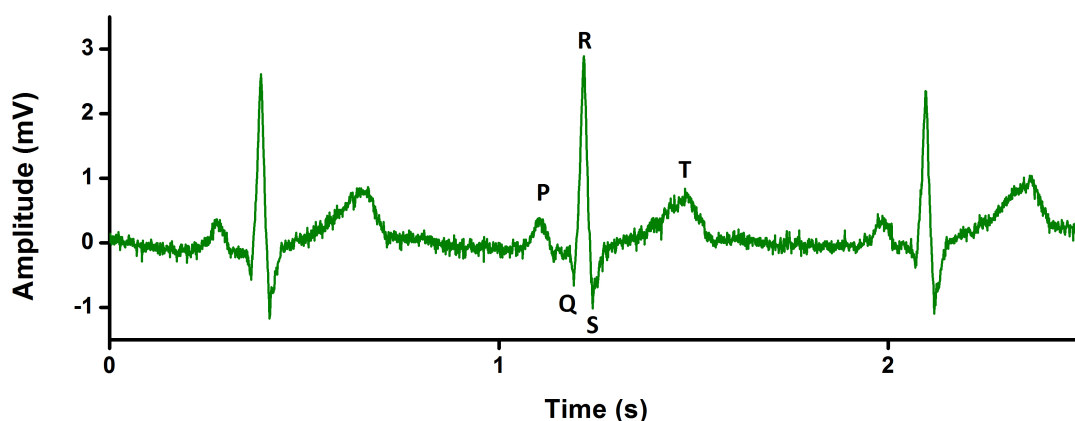


Figure 1.5 – **Standard ECG signal.** Example of an ECG signal with highlighted PQRST complex.

Electromyography (EMG)

Luigi Galvani was one of the first to highlight the fact that muscle contractions can be initiated by electricity in 1792 and he gave rise to the field of bioelectronics. Conversely, it was shown 60 years after that muscle activity induces electrical currents that can be recorded by Emil Du Bois Reymond [12]. EMG recordings and muscular stimulation are nowadays very common in clinic and sport study centers. It permits the understanding of human kinetics by studying the degree and sequence of contractions from various muscles participating in a movement while, coupled with stimulation techniques, provides insight into the mechanisms responsible for muscle force production during contraction. This technique is used in the clinical context as a diagnostic tool for nerve and muscle injury.

To understand the genesis of EMG signal, it is important to highlight the motor unit (MU) which is composed of a motor neuron in the spinal cord and the skeletal muscle fibers innervated by this motor neuron [13]. When a movement order is given from the cortex, action potentials circulate along the spinal cord to reach one or different specific motor neurons associated with the muscle to move. This induces the muscle fiber contraction. Each human muscle (composed of many muscle fibers) is associated with a various number of different MUs: from about 100 for a small hand muscle to more than 100 for large limb muscle [14]. The force and the accuracy of the muscle movement are linked with the number of associated MUs and by the number of muscle fiber in each MU. The depolarizations of muscles membrane, associated with muscle fiber contractions, can be recorded from different places. An example of EMG signal on Fig 1.5, recorded from surface electrodes, shows the rising potential associated to slowly rising force of plantar-flexion contraction on a human volunteer. Invasive techniques with penetrating electrodes allow the detection of potentials very close to the source with minimal low-pass filtering due to biological tissues between the muscle and the electrodes. Penetrating electrodes can give a precise decomposition of the MU associated with the activity and define abnormal behaviors. The muscle contraction can be voluntary or induced by an external upstream electrical stimulation. Surface EMG is performed with cutaneous electrodes. Since in this case, electrodes are further away from muscle and the signal is disturbed by biological tissue in between, MU decomposition is more difficult. However, the non-invasiveness of the technique authorized the use of large matrix of electrodes for full spatial mapping of muscle activity.

Others

If ECG is the most common electrophysiological recording in clinic examinations, EEG and EMG are also frequent. Other modalities exist but are less common and rarely used by clinicians for some very specific cases. They are still very interesting for more fundamental research on body behavior. These techniques include (non-exhaustive list):

- Electrooculography (EOG): A potential difference exists between the back (negative) and the front (positive) of the eyeball. By placing electrodes around the eye, eye move-

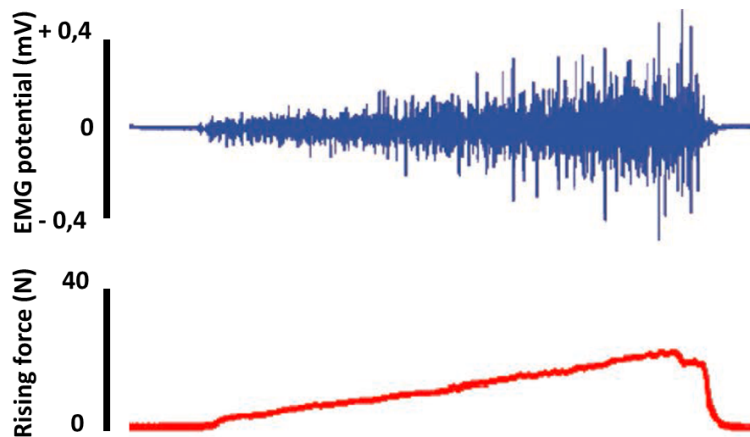


Figure 1.6 – **EMG signal during plantar-flexion contraction**. Example of an EMG signal recorded from electrodes placed on the lower limb and associated with a rising force of plantar-flexion contraction.

ments can be recorded with few degrees accuracy [15].

- **Electroretinography (ERG)**: It is the analysis of electrical answer of the retina to light stimuli. With different light intensity and frequencies, cones and rods activities are detected by electrodes placed on the cornea and the skin near the eye [16].
- **Electrocochleography (ECoChG)**: It is a technique of recording potentials generated in the inner ear after sound stimuli. Electrodes are placed inside the cochlea as a cochlear implant would do [17].
- **Electrogastrography (EGG) and electrogastroenterography (EGEG)**: They are recording of stomach and intestines muscles activities, respectively [18].

1.1.3 Overview on the acquisition chain for electrophysiological recordings

In previous sections, we defined what the electrophysiology was and explained the different modalities. It is now time to focus on the technological means to record the signals.

A general acquisition chain for electrophysiology on humans is described on Fig 1.7. The different steps, from the skin contact to data display and analysis, are described:

- **Electrode**: The electrode is the device made of conductive materials that records the potential close to the target organ or from the skin. We showed on previous sections that the placement is depending on the modality (EEG, ECG...). A minimum of 2 electrodes is required to record a potential difference but their number can be up to few hundreds. If needed, 2 specific additional electrodes (ground and reference electrodes) are placed

on the patient, if possible on an electrically neutral place. More details about electrodes will be given all along this manuscript and particularly on Chapter 2.

- **Amplification:** The recorded biological signal is very low and need to be amplified before processing. This needs to be done during the first step of the acquisition chain in order to amplify the signal of interest and not extra noise coming from the different components of the following stages. It is usually done by differential amplifiers with common ground. In case of unipolar leads, the amplifier gives the potential of each electrode compared to a common reference whereas in case of a bipolar lead, the amplifier provides the potential difference between a pair of electrodes. The gain value of the amplifier needs to be adjusted depending on the amplitude and the frequencies of the recorded signals as well as on the specifications of the following analog-to-digital converter. Efficiency of this amplifier is defined by both its own input impedance Z_{in} and electrodes impedances Z_1 and Z_2 . If V_E is the potential difference recorded between the two electrodes, the potential V_i applied at the differential inputs of the amplifier is close to:

$$V_i = V_e \cdot \frac{Z_{in}}{Z_1 + Z_2 + Z_{in}} \quad (1.1)$$

In order to lose minimal signal of interest, it induces that $Z_{in} \gg Z_1 + Z_2$ and so that input impedance of the amplifier should be higher than electrode impedance [19, 20]. In an ideal differential amplifier, the following relation is respected:

$$V_{out} = G_{amp} \cdot (V_+ - V_-) + G_{MC} \cdot \frac{V_+ + V_-}{2} \quad (1.2)$$

with G_{MC} being the common mode gain. The common mode rejection ratio is defined by $\frac{G_{amp}}{G_{MC}}$ and needs to be as high as possible [21].

- **Analog Filtering:** Even with utilization of a high-quality large bandwidth amplifier, only a specific frequency band is of interest for the analysis of the recorded signal. The frequency band of interest is defined by the targeted analysis on a specific modality (8-12 Hz for alpha waves in EEG, 1 Hz for heart beats at rest. . .) but modern components allows to keep large band of signal (0.5 to 100 Hz for ECG). High-pass and low-pass filters remove other frequencies, which are noise coming from electrodes, wires, organism of the patient and environment. A cut-band notch filter can be found in most of the acquisition systems, to remove unwanted 50 or 60 Hz frequencies coming from power lines.
- **Analog-to-Digital conversion:** After analog amplification and filtering, electrophysiological analog signals are converted to digital signals for future processing and saving. The resolution of the converter, defined by a number of bits n , is the amount of values which can be processed. An EEG acquisition system with a resolution of 12 bits can process 2^n different values of amplitude. A high sampling rate permits the converted signal to be closer from the recorded one. In the last decades, miniaturization of memories

authorized the conception of recording devices with high resolution and sampling rates, even if data recorded from many leads for a long-time can be still long to process.

- **Digital processing:** Digitalization of the signal permits many manipulations such as additional signal processing, data analysis with different algorithms and correlation with external markers (finger claps or music with EEG for instance). Some algorithms are now competing with doctors for data analysis performance.
- **Signal Transmission:** Since the rise of wireless systems, it has been possible to imagine wireless recording devices that could fit with ambulatory monitoring thanks to a reduced size. Nowadays, different wireless technologies (for instance Bluetooth Low Energy [22, 23] or Wifi [24]) exist for such recording devices to transmit signal at any step of the acquisition chain after A/D conversion.
- **Display/Storage:** Finally, recorded signal can be saved for future uses or displayed to the patient or doctors for real-time monitoring.

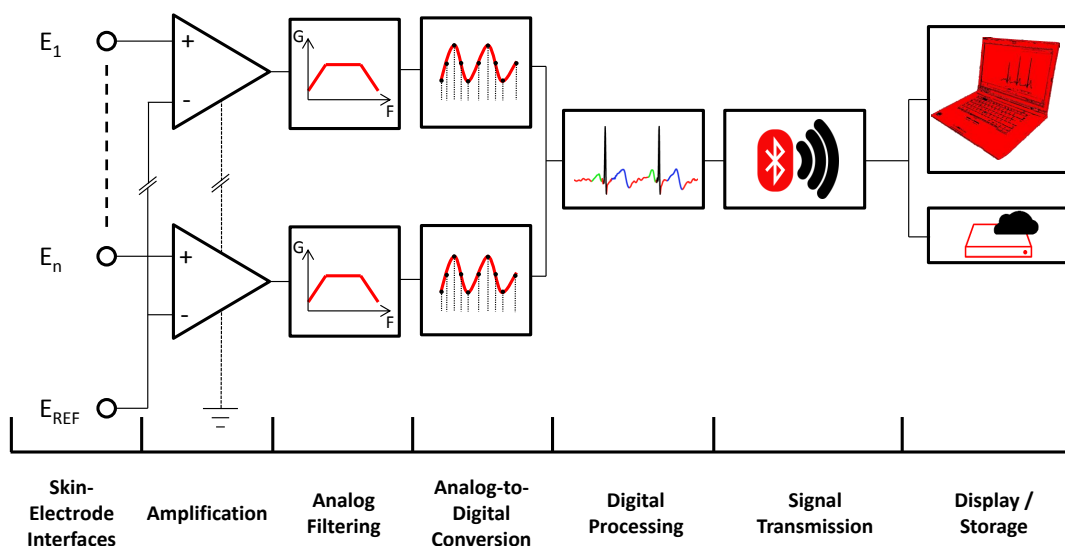


Figure 1.7 – **Acquisition chain for clinical electrophysiology.** Schematic of a usual acquisition chain for electrophysiological recording device with the different steps

1.2 Analysis of medical needs for electrophysiology

1.2.1 Electrophysiology to diagnosis pathologies

EEG, EMG or ECG recordings are very common and well known procedures in clinics. Their specific and repetitive patterns involve relatively easy observation of abnormalities. Associated with context and other medical imaging system, electrophysiological tools are essentials to clinicians.

1.2. Analysis of medical needs for electrophysiology

Imaging brain activity, an EEG would be able to give information about most of the activities of a person. But because of its poor spatial resolution and a partial comprehension of neural phenomena, EEG gives only general information of brain condition. The absence of EEG activity is strongly associated with brain death. In France, a 30-minute long flat EEG following by a second one after 4h is a one of the criteria for the declaration of patient's death. Conversely, active EEG is an important clue to define the level of consciousness of patients in coma or with total paralysis (*plegia*). Strong abnormalities in the EEG pattern can reveal brain injuries such as intracerebral hemorrhage or infraction [25]. Since brain shows very specific and well defined activity during the different steps of sleep, EEG is a common tool for sleep disorders monitoring. Brain pathologies induce modification of the EEG trace too. If EEG may be used for Creutzfeldt–Jakob disease or encephalitis (sudden inset inflammation) diagnosis [26, 27], epilepsy is certainly the most and best studied pathology with EEG. An epileptic patient presents more or less frequently sudden and strong modifications of brain activity, called seizures. A seizure is characterized by a transient functional impairment of a population of neurons: neurons localized in a specific area generate a sudden, high amplitude and synchronous electrical discharge which can propagate in one part of the brain or in its entirety. Since the brain is “short-circuited”, a seizure induces local uncontrolled muscle movements, convulsions or temporary absence which can severely disturb life of epileptic patients and even brain capacities. The duration of each seizure, their pattern and the frequency of the crisis as well as the temporal evolution of the seizure at the surface of the scalp are of great help for accurate diagnosis. EEG can be used for short-term diagnosis, or for long-term (up to 3 weeks) brain monitoring, mostly at the hospital.

Doctors can easily read ECG signals and diagnosis pathologies from the form, the amplitude and the timing of the different waves. However, some heart disorders are invisible on ECG. Heart rate is calculated from the number of QRS complexes per unit of time. At rest, it is around 70 beats per minute but it can increase up to more than 180 during sport activity (to accelerate blood circulation during exercise). An abnormal speed, called tachycardia if heart rate exceeds the normal resting rate or called bradycardia if the rate is too slow, can reveal cardiovascular diseases which involve unexpected resource consumption from the heart. In case of bradycardia, the heart pump is not efficient enough and the blood pressure is too low, inducing a lack of oxygen for the irrigated organs. If a tachycardia is detected, it may mean that the cardiac output of blood is also too low because in this case, the heart is pumping too fast and does not have to time to correctly fill. An activity faster than usual also induces strong mechanical stress and damages the tissues. The measure of the delays between remarkable ECG patterns called PR interval, ST segment or QT interval is used to check potential troubles. If short-term ECG tests are achieved at hospitals to diagnose some diseases, some other problems can only be detected from long-term (hours or even days-long) recordings, such as irregular tachycardia. A study of the general pattern of the PQRST complex and comparison from different leads is essential to the diagnosis of a cardiologist.

1.2.2 Electrophysiology to assist pathologies

If electrophysiology is mainly a passive recording procedure, it can be used to assist some specific pathologies, either by recording and recognizing specific pattern and then by warning the patient or inducing an external response, either by directly interacting with the body (stimulating probes for instance).

20 years ago, neuroscientists discovered that epileptic seizure were not as sudden and abrupt as they thought. Epileptic patients were talking about optical effects or non-usual feelings which could occur before the seizure and warn them of its imminence. EEG pattern analysis ended to convince researchers that seizures develop minutes before clinical onset. A lot of results on positive seizure predictions were claimed from intracranial EEG (SEEG) data [28]. Martinerie et al. were one of the first to show that, thanks to non-linear analysis of monitored patients, it was possible to predict seizure with high-efficiency rate up to 6minutes prior to it [29]. Other methods using linear approaches, spectral power analysis or EEG pattern classification were developed [30, 31]. Only few teams are claiming results from surface EEG [32]. However, none of the long-term post-studies were successful enough to predict seizure in any case and research is still going on. Potential applications are high: a warned epileptic patient would be able to stop his car if he is driving or to avoid falling if he is using stairs. Since repetitive seizures are crippling and can induce severe damages to the brain, a second step would be to predict a seizure and then to stop it. It was shown that it is possible to do so by electrical stimulation [33, 34, 35, 36] as well as by optical stimulation [37] even if the success rate does not yet compare with resective surgery.

Changes induced by deep brain stimulation were highlighted in 1987 by French Dr Benabid and Pollak [38] and applied to Parkinson's disease in 2003 [39]. It is now a well-established procedure to treat the debilitating symptoms such as tremor, rigidity, walking problems. . . Basically, penetrating electrodes are implanted in the brain by a stereotaxic method as close as possible of a previously-defined brain area. High-frequency (>100 Hz) potential stimulations are applied and inhibit affected neuron when the patient feels the need. Despite rare cases of infection or hemorrhage, it greatly helps patients to stop the crisis. The process is not well understood but the electrical stimulation would affect electrical and neurochemical communication between single neurons and astrocytes as well as oscillations of global structures such as thalamus [40]. Studies are now on going to find other application to deep brain stimulation. Brain connectivity is increased and patients with Alzheimer disease show some recovery [41]. It allows significant reductions in depressive symptomatology as well as encouraging rates of remission for individuals suffering from treatment-resistant depression [42]. Long-term deep brain stimulation applied to the thalamus involves a global reduction of tic without reducing intellectual performances of subjects with Tourette syndrome [43].

Brain-Computer Interfaces (BCI) are using most of time electrophysiological signals. By recording the electrical activity of neurons or muscles, they allow a disable person to act with a computer, to induce movement for instance. If titles for general audiences such as "writing

by thought” are catchy, BCI is now a broad research field and starts to have real applications for patients. 2 modalities are mainly employed for BCIs: EEG, ECoG. Signals obtained by ECoG allow commanding an effector, for instance a robotic arm [44] or an exoskeleton [45]. Despite the EEG signal inconvenient, non-invasive EEG BCIs are also promising [46] and allow a distant motor control of external devices [47]. Even if they are not literally BCIs, myoelectric prostheses grant a precise control of the artificial members. In many case, contraction of a specific existing muscle involves a specific motion of the prosthesis (for instance, biceps contraction induces the artificial hand to close), but this order is not natural for patients and implicates long training. State-of-the-art prosthesis use EMG residual activity of the amputee, mapped by high-density cutaneous matrices, to finely control the prosthesis with natural thought [48, 49, 50].

1.2.3 Current problematics for ambulatory electrophysiology

If electrophysiological recordings are now well established in clinic, some constraints, mostly coming from equipment, disable a larger use of these signals for ambulatory monitoring. Better understanding these problematics can help to conceive new ambulatory and high-performing medical devices.

Size of the acquisition systems

The presence of many wires and the weight of the acquisition system has always been a problem. In case of recordings made in the hospital on a patient at rest, there is no need for small devices. But in other cases, such as emergency or long-term monitoring recordings, a light and small device is necessary. One of the first ambulatory ECG systems was developed in 1949 by Holter [51]. It was a 34 kg-device working with radio signal. Later, lighter ECG systems authorized cardiac monitoring inside ambulances [52]. Results were sent to the hospital by cellular telephone for early diagnosis. In the last decades, the extreme miniaturization of electronics and batteries involved the development of personal ambulatory recording systems, for instance making possible epilepsy monitoring at home [53, 54, 55, 56]. Miniaturization of recording systems is also important for aesthetic appearance reasons. Reduction o size of electrodes and wires is a demand coming from patients, who do not feel comfortable with very visible equipment. However, performances (related to the quality of signal, the number of possible lead or the amount a saved data) of ambulatory systems are still limited compared to clinical devices.

Skin interface

Toxicity of materials with biological tissues is one of the main issues for sensors in contact with human body. It is obvious for penetrating electrodes but even cutaneous electrodes can induce allergic reactions of the skin. This is the main limitation for long-term studies. In

the particular case of high-density EEG recordings, other limitations for long-term studies appear. The deposition of the conductive gel on the electrodes is time-consuming. This gel dries after few hours and needs to be replaced to allow long-term recordings. Furthermore, some gel leakages can induce bridges (interconnections) between electrodes and decrease spatial resolution. More details on these problematics of electrodes are presented on Chapter 2.

Unwanted noise in the signal

The biological signal of interest is never recorded alone, but with a bench of unwanted perturbations which can affect its analysis. This noise is coming from different sources which are either biological or external:

- **biological sources:** The body is a complex and dynamic organism and the activity of a part of it has often cascaded from many other activities. Moreover, most of body components are conductive and then conduct electrical perturbations. This means that an electrophysiological recording will be always perturbed by other electrophysiological activities. A strong signal such as ECG is barely disturbed because of its high amplitude, but on the contrary, EOG and ECG highly interfere with EEG or fetal ECG recording respectively. Breathing also disturbs electrophysiological recordings by adding a low-frequency component.
- **external sources:** The interaction of the environment with the measurement is also important to take into account. First, the acquisition system itself is creating noise. For many reasons, recording electrodes are slightly moving on the skin, creating motion artifacts (see Section 2.1.2). Movement of wires and electrical components activity (power supply, thermal noise [57]...) are creating noise during propagation and processing of the signal. Power-line frequency electromagnetic field (at 50Hz in Europe and 60Hz in the USA) is a strong source of noise but other machines running close the recording system can also affect it by electromagnetic noise.

Different techniques are used in parallel to reduce this noise. The environment around the acquisition system can be adapted to reduce electromagnetic noise (for instance, patients under long-term SEEG recordings live for few weeks in a Faraday cage-bedroom at the hospital) but it is far from easy in other cases. Elements of the recording system can also be improved to reduce their noise reception. Conformable or non-contact electrodes facilitates the reduction of motion artifact, wireless systems remove disadvantages of wires and shielded electronics is less sensitive to the environment. Hardware filters are used to reduce the amplitudes of specific frequencies. Finally, digital processing highly facilitates noise removing.

Analysis of the signal

For long-time, recorded electrophysiological signals has been printed on graph paper and then manually analyzed by the doctor. The demonstration of the efficiency of analysis on computer screens [58] enable full digital processing and analysis of electrophysiological signals. It also means that a signal can be analyzed by a doctor days after the recording. This gave rise to an intense development of ambulatory systems for long-term monitoring of patients outside the hospital. Many devices facilitate electrophysiological recordings at home, with data stored for further analysis or directly sent to a specialist in case of a problem. Advanced digital processes using, among other techniques, wavelet and probabilistic approaches [59, 10], neural network [60], or chaos theory [61] assist the progress of high-speed and high-performing digital diagnosis. Thanks to an extremely large amount of data available online and the development of machine learning, it easy to imagine that soon, algorithms will be able to diagnose diseases from electrophysiological data with better performances than doctors. However, humans are still the only one able to fully understand the context of the disease and most of the digital processing methods need to be manually adjusted for each set of data.

Storage of the signal

The development of memory capacities of electronical system makes possible the storage of large amount of electrophysiological data. To guarantee interoperability between systems from different brands, to enable data exchange between research teams and to be sure that all information about an examination (signal but also specifications of the recording and the patient) is saved, standards are necessary. DICOM, a standard for handling, storing and transmitting information of most medical images can be used to encode ECG but other standard exist for ECG[62] or EEG [63]. Finally, the evolution of ambulatory recording systems raises the question of personal data safety. If information can be sent to doctors, it can also be intercepted by a third part. The necessity of data encryption has then to be integrated to standards.

1.3 Industrial vision for medical devices conception

The term Medical Device (MD) can be applied to any tool, equipment, software or material which aims to be used for diagnostic or therapeutic purposes related to any human healthcare issue, with the notable exception of medications. Conception of state-of-the-art MDs usually involves expertise from many different scientific fields such as mechanical and electrical engineering, programming, physiology, signal processing, biology... Academic and industrial research laboratories are at the first place to develop innovative ideas for MDs. In this section, we will discuss on how laboratories can have their place in the conception of such devices. We will also focus on the certification of MDs. Industrial and regulation constraints should be always in mind during the first steps of a MD development.

1.3.1 From the idea to the mass production of medical devices

In the case of applied research for MDs, one of the goals is to develop proof-of-concept devices by including state-of-the-art technologies highlighted by previous fundamental research. Since the industrial process of MD conception is very long (almost a decade is necessary before the commercialization of a heart prosthesis), it is important to know from upstream the constraints which will be applied to the future product [64, 65]. Fig 1.8 presents the general stream of MD conception, associated with the main actors of the value chain. The stream of MD development can be divided in different steps, each of them involving close relation between the MD manufacturer and other actors:

- **Idea:** Everything usually starts from a need, expressed by medical staff. The innovative work is then finding how to answer to this need, by using new technologies and materials (for example a new polymer can be developed to improve the interface of an electrode), or by recycling and adapting ideas coming from other fields (for instance, an algorithm for deblurring images of license plates on cars can be used in MRI images analysis). When an existing device or tool is improved without important change in its use, we talk about incremental innovation, which represents 70% of new products [64]. But sometimes, disruptive technologies facilitate the introduction of innovative tools and initiate the emergence of new therapeutic strategies. In this step, close collaboration between academic research centers and internal Research and Development offices are essential to have access to state-of-the-art technologies and scientific expertise on literature and techniques. A lot of “start-up” companies are actually initiated by researchers, associated with structures providing innovation support. MD companies are generally investing back a high ratio of their turnover in their Research and Development centers.
- **CE marking process:** Specific to MDs, the redaction of the technical file for the marking is an essential step, developed in parallel and in relation with all the following steps. If an international commercialization is envisaged, a lot of energy needs to be spent on the different regulatory specifications. Needs for CE marking are explained in details in Section 1.3.3.
- **Feasibility:** During this step, specifications (including performances and followed norms) of the future product are defined, as well as the different tests which will characterize its performances. For this, a judicious collaboration with medical teams is necessary, in order to be aware of precise constraints and needs of patients and medical staff. A proof-of-concept, demonstrating the main performances of the future product and validating the idea can be realized during this step, still in cooperation with the different partners. If needed, and it is often the case, redaction of patents is done at this step in order to protect the idea as soon as possible, before any advertisement. Finally, risk management studies as well as first documents for the marking are initiated.
- **Conception:** All documents needed for industrialization of the product (nomenclatures,

1.3. Industrial vision for medical devices conception

plans, specifications, fabrication processes, assembly notes...) are aggregated in a conception file and a prototype as close as possible from the final device is made. If possible, digital models and experimental validations are used to check if set out specification are respected. Pre-clinical and clinical trials (see Section 1.3.3) are made during this step to validate healthcare performances and absence of toxicity for the users. It is important to keep in mind that in case of invasive or high-risk devices, these trials can last for few years, delaying as much the industrialization of the product.

- **Industrialization:** If a clean environment is needed, this step can be done in controlled atmosphere area, where gas concentration as well as temperature and humidity are regulated to avoid contamination. First, pre-series facilitate the validation of series fabrication process. Fabrication and control ranges are defined. First devices can be sent/sell to close collaborators (= early adopters) in order to initiate and facilitate adoption and diffusion on the market. Then, mass production of the device can be launched.
- **Commercialization of the product:** An important and ramified network of distributors and users (including, hospitals, doctors, patient associations...) helps for the recognition of the device. If after-sales follow-up is supposed to be done by manufacturers and distributors for any products, a specific process need to be set up for MD and is part of the CE marking procedure. Data about long-term stability and mostly long-term absence of danger for patients and users need to be kept and studied by manufacturers and distributors. Feedbacks from patients and users are also important to collect in order to understand how to improve the next products.

1.3.2 How can research and development add value to medical device conception?

By bringing innovative ideas and techniques, fundamental research fully participates to the creation of value for medical devices. Small companies are more focused on research and development since they need to innovate to be competitive against multinational companies [66]. Mature and big companies are less focused on research, since it can be a risky field and they can afford to buy the most competitive start-ups. However, few ideas can improve the importance of research and development in the final product.

First, an early integration of MD regulation is necessary. The knowledge of the regulatory environment from the beginning of the MD conception avoids some mistakes, as the use of a material not compatible with sterilization techniques. Given the long duration of possible clinical trials, it is important to take it into account as soon as possible. Moreover, some regulatory environments (application of the MD, country of commercialization...) are more favorable for easy and short access to the market and so need to be identified. Nowadays, company and research laboratories need to be included into specific networks, also called technological *clusters*, and innovation happen between the different collaborations. This

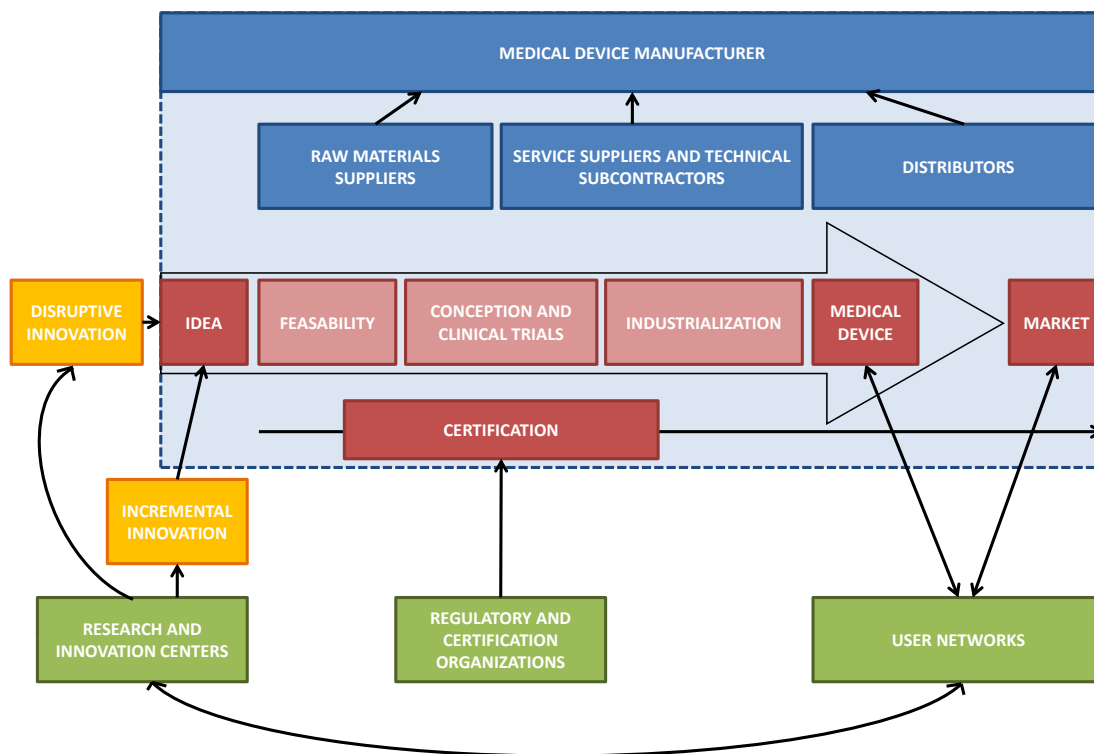


Figure 1.8 – **Schematic of the conception chain for medical devices.** The different steps of conception are marked in red. In blue are the different companies, managed by the product manufacturer, involved in the different steps of the conception chain. The different actors of the conception chain are in green, all of them are working in close collaboration with the manufacturer for inputs, advices or validation. The two different ways of innovations are highlighted in yellow.

improves the chances for the partners to get a more important access to private and public funding for both technical development and clinical evaluation. Successful partnership already exist between academic world, companies and innovation structures, such as PhD funding, creation of spin-off or common application on governmental research projects, but they need to be reinforced. In the case of MDs, working together with clinical teams helps to better identify medical needs and then better understand the market. Equilibrium on intellectual property needs to be found between the patenting of ideas and the global propagation of scientific knowledge through publications. Indeed, the development of an independent clinical research, led by academy, is essential to promote the rise of useful MDs for public health. In another hand, the mass distribution of medical devices to medical structures has to be carried out by companies.

1.3.3 CE marking

Any company that want to market a product with medical purposes needs first to certify it. The first main reason is that medical devices have short to long-term (from few seconds to life-long) and intimate (from outside of the skin to inside the body) contact with the human body and then can severely damage it. A wrong utilization or a malfunction can induce unwanted supplementary risk to a patient or diagnose an erroneous pathology. Any medical product sold in European Union countries needs to satisfy the conditions defined in the Medical Devices Directive (93/42/EEC). Two other European Directives handle with more details regulation around active implantable medical devices and medical devices for *in-vitro* diagnostics, respectively 90/385/CEE and 98/79/CEE. The other worldwide important markings for MDs is following FDA (Food and Drug Administration, USA) regulations. Despite some differences that cannot be forgotten to avoid any commercialization delay, equivalences and similarity exist between CE and FDA marking. Useful and complete information can be found on this website (in French): [67].

Classification of Medical Devices

Firstly, the class of the MD needs to be defined to know the applicable constraints to conform to the directive. 4 classes are defined and are related to possible risks for both patients and medical staff: I, IIa, IIb and III. These 4 classes are given in Annex IX of the Directive and were chosen in relation with different criteria:

- **Time of use:** The time during which a device is in contact with biological tissue is of first importance to understand the associated risks. 3 category of duration are defined: less than 1h, between 1h and 30 days, more than 30 days.
- **Invasiveness:** Any MD which needs to partially or totally penetrate inside the body by a natural orifice or through the external layer is considered as invasive and so more risky. Moreover, the device can be defined as implantable device if it is supposed to stay in the body after penetration.
- **Reusability:** A MD, particularly surgical tools, can be reused for another operation after appropriated procedures of washing and sterilization but this improves the risks of infections.
- **Active device:** Any MD which needs a non-human source of energy (mostly electricity) to be used is considered as active. In this case, the risk is that this source of energy interacts and disturbs the body.
- **Active device for therapy:** Any MD which can restore, modify or replace a biological function or structure needs to address more constraints.
- **Active device for diagnosis:** Any MD which can give information to diagnose pathology needs to address more constraints.

Chapter 1. Introduction on electrophysiology and medical devices

- **Localization of action:** Any MD in interaction with central nervous system or circulatory system needs to address more constraints.

4 different rules are applied to the devices:

- For non-invasive devices (e.g. non-invasive MDs interacting with human fluids are Class IIa or IIb)
- For invasive devices (e.g. temporary invasive devices, if they are not connected to a Class II or more MD, are Class I)
- For active devices (e.g. an active device for diagnosis and monitoring of vital parameters are Class IIb)
- Special rules (e.g. a device incorporating a blood-derived substance is Class III)

The most critical use will be the one considered for the classification as well as the most severe rule if different uses or rules can be applied to the device.

Here are few examples of MDs classification:

- **Class I:** cutaneous electrode for ECG, gloves for examination, surgical scalpel. . .
- **Class IIa:** syringe needle, thermometer, tubes for anesthesia. . .
- **Class IIb:** men condoms, incubator for baby, sterile trocar. . .
- **Class III:** heart catheter, artificial heart, prosthesis for hip articulation. . .

However, by focusing on their risks for patients and users, this classification does not reflect the variety of MDs which are included in each class. Another classification for MDs, The Global Medical Device Nomenclature, sorts them by applications and used technologies (for instance: medical software, dental materials, devices for *in vitro* diagnostic, technical textiles, active implants. . .).

Class I MD regulation

This section presents specifications for Class I MDs, since most of the devices presented in this thesis are for cutaneous applications. Class I MDs are the only MDs which can be self-certified by the manufacturer. Regulatory organisms will check if the rules were followed only in case of a problem with a user. A technical file needs to be established by the manufacturer, gathering all information about the MD. The certification will be done regarding this specific file, described in the Medical Devices Directive (93/42/EEC). Here is the list of the different kind of information that composed this technical file for Class I MDs:

- **Input information**

- **Description of the product:** In this part, a full description of the product is needed, including the main targets, the secondary targets, the functions and mechanics, the accessories, the other devices which will be connected with and the main technical performances. From the reading of this part, one is supposed to be able to understand how to use the MD and for which applications and what are the critical performances.
- **Applied norms:** In here, standards followed by the MD are described. In theory, the application of norms for the MD is not mandatory. But most of the time, the conception of the MD will follow a lot of them because it allows the manufacturer to standardize conception of different products and to ensure performances of the devices. Three different kinds of standards can be used. “General” ones are linked with safety during production, with user instructions or with risk management. “Product norms” are relevant to define and check the performances of the device. Finally, medical devices conforming to the relevant harmonized European standards (regarding biocompatibility, electromagnetic compatibility...) are considered to conform to the requirements of the directive.
- **Answers to the Directive requirements:** In this part, it is explained and detailed how the certified DM is positively answering the list of essential requirements defined in the Annexe I of the Medical Devices Directive (93/42/EEC).

- **Conception**

- **Conception documentation:** This is a technical part, where everything about the conception of the product is indicated: from reports of the first technical meetings to the fabrication of the device. From this information, one should be able to fabricate the product from scratch. All performances and related tests are supposed to be included too.
- **User manual:** The user manual is stored in this part. Usually it follows harmonized standards.
- **Labelling:** The labelling of the DM package is stored in this part. Usually it follows harmonized standards.

- **Evaluation**

- **Pre-clinical evaluation:** This part is a record of verifications done by the manufacturer and/or by external laboratories to check the compatibility of the MD with specific environment, its biocompatibility, its safety and its performances.
- **Clinical evaluation:** Depending on the device, clinical trials can be executed in order to verify the efficiency and safety of the MD on human volunteers. Clinical trials are not frequent for Class I MD, usually a literature review is enough.

- **Risk management:** All along the process of conception, fabrication and marking, a risk management procedure needs to be applied to avoid any risk for patients, users and manufacturer.

1.4 Bibliography

- [1] A. L. Hodgkin and A. F. Huxley. A quantitative description of membrane current and its application to conduction and excitation in nerve. *The Journal of physiology*, 117(4):500, **1952**.
- [2] G. Buzsáki, C. A. Anastassiou, and C. Koch. The origin of extracellular fields and currents — EEG, ECoG, LFP and spikes. *Nature Reviews Neuroscience*, 13(6):407–420, **2012**.
- [3] H. Berger. Über das Elektrenkephalogramm des Menschen. *Archiv für Psychiatrie und Nervenkrankheiten*, 97(1):6–26.
- [4] E. D. Adrian and B. H. C. Matthews. THE BERGER RHYTHM: POTENTIAL CHANGES FROM THE OCCIPITAL LOBES IN MAN. *Brain*, 57(4):355–385, **1934**.
- [5] B. N. al, et. Slow potentials of the cerebral cortex and behavior. - PubMed - NCBI.
- [6] A. Gevins, J. Le, P. Brickett, B. Reutter, and J. Desmond. Seeing through the skull: advanced EEGs use MRIs to accurately measure cortical activity from the scalp. *Brain topography*, 4(2):125–131, **1991**.
- [7] O. Bertrand, F. Perrin, and J. Pernier. A theoretical justification of the average reference in topographic evoked potential studies. *Electroencephalography and Clinical Neurophysiology/Evoked Potentials Section*, 62(6):462–464, **1985**.
- [8] E. Asano, C. Juhász, A. Shah, O. Muzik, D. C. Chugani, J. Shah, S. Sood, and H. T. Chugani. Origin and propagation of epileptic spasms delineated on electrocorticography. *Epilepsia*, 46(7):1086–1097, **2005**.
- [9] T. J. al, et. Functional stereotaxic exploration of epilepsy. - PubMed - NCBI.
- [10] G. D. Clifford, editor. *Advanced methods and tools for ECG data analysis*. Engineering in medicine & biology. Artech House, Boston, Mass., **2006**. OCLC: 255369607.
- [11] Standardization of precordial leads. *American Heart Journal*, 15(1):107–108, **1938**.
- [12] F. Isch. Histoire de l'électromyographie: Le «temps des pionniers». *Revue d'Electroencéphalographie et de Neurophysiologie Clinique*, 17:1s–8s, **1987**.
- [13] R. Merletti and P. Parker, editors. *Electromyography: physiology, engineering, and non-invasive applications*. IEEE Press series in biomedical engineering. IEEE/John Wiley & Sons, Hoboken, NJ, **2004**. OCLC: ocm56361488.

- [14] E. Henneman and L. M. Mendell. Functional organization of motoneuron pool and its inputs. *Comprehensive Physiology*, **2011**.
- [15] M. Brown, M. Marmor, Vaegan, E. Zrenner, M. Brigell, and M. Bach. ISCEV Standard for Clinical Electro-oculography (EOG) 2006. *Documenta Ophthalmologica*, 113(3):205–212, **2006**.
- [16] R. Tzekov and G. B. Arden. The electroretinogram in diabetic retinopathy. *Survey of ophthalmology*, 44(1):53–60, **1999**.
- [17] J. A. Ferraro, I. K. Arenberg, and R. S. Hassanein. Electrocochleography and symptoms of inner ear dysfunction. *Archives of Otolaryngology*, 111(2):71–74, **1985**.
- [18] THE ELECTROGASTROGRAM AND WHAT IT SHOWS. *JAMA: The Journal of the American Medical Association*, 78(15):1116, **1922**.
- [19] J. W. Osselton. Acquisition of EEG data by bipolar unipolar and average reference methods: a theoretical comparison. *Electroencephalography and clinical neurophysiology*, 19(5):527–528, **1965**.
- [20] E. S. Kappenman and S. J. Luck. The effects of electrode impedance on data quality and statistical significance in ERP recordings. *Psychophysiology*, **2010**.
- [21] B. B. Winter and J. G. Webster. Reduction of interference due to common mode voltage in biopotential amplifiers. *IEEE Transactions on Biomedical Engineering*, 30(1):58–62, **1983**.
- [22] G. Ruffini, S. Dunne, E. Farres, I. Cester, P. C. Watts, S. R. P. Silva, C. Grau, L. Fuentemilla, J. Marco-Pallares, and B. Vandecasteele. ENOBIO dry electrophysiology electrode; first human trial plus wireless electrode system. In *2007 29th Annual International Conference of the IEEE Engineering in Medicine and Biology Society*, pages 6689–6693. IEEE, **2007**.
- [23] B. Yu, L. Xu, and Y. Li. Bluetooth low energy (BLE) based mobile electrocardiogram monitoring system. In *Information and Automation (ICIA), 2012 International Conference on*, pages 763–767. IEEE, **2012**.
- [24] S. Shebi Ahammed and B. C. Pillai. Design of Wi-Fi Based Mobile Electrocardiogram Monitoring System on Concerto Platform. *Procedia Engineering*, 64:65–73, **2013**.
- [25] V. P. Continuous EEG monitoring for the detection of seizures in traumatic brain injury, infarction, and intracerebral hemorrhage: "to detect and protect". - PubMed - NCBI.
- [26] L. R. a. B. RD. Evolution of EEG and visual evoked response changes in Jakob-Creutzfeldt disease. - PubMed - NCBI.
- [27] J. Millar and A. Coey. The EEG in necrotizing encephalitis. *Electroencephalography and Clinical Neurophysiology*, 11(3):582–585, **1959**.

Chapter 1. Introduction on electrophysiology and medical devices

- [28] B. Litt and J. Echauz. Prediction of epileptic seizures. *The Lancet Neurology*, 1(1):22–30, **2002**.
- [29] J. Martinerie, C. Adam, M. L. V. Quyen, M. Baulac, S. Clemenceau, B. Renault, and F. J. Varela. Epileptic seizures can be anticipated by non-linear analysis. *Nature Medicine*, 4(10):1173–1176, **1998**.
- [30] P. Mirowski, D. Madhavan, Y. LeCun, and R. Kuzniecky. Classification of patterns of EEG synchronization for seizure prediction. *Clinical Neurophysiology*, 120(11):1927–1940, **2009**.
- [31] Y. Park, L. Luo, K. K. Parhi, and T. Netoff. Seizure prediction with spectral power of EEG using cost-sensitive support vector machines. *Epilepsia*, 52(10):1761–1770, **2011**.
- [32] M. Le Van Quyen, J. Martinerie, V. Navarro, P. Boon, M. D’Havé, C. Adam, B. Renault, F. Varela, and M. Baulac. Anticipation of epileptic seizures from standard EEG recordings. *The Lancet*, 357(9251):183–188, **2001**.
- [33] S. J. Schiff, K. Jerger, D. H. Duong, T. Chang, M. L. Spano, and W. L. Ditto. Controlling chaos in the brain. *Nature*, 370(6491):615–620, **1994**.
- [34] F. Velasco, M. Velasco, A. L. Velasco, F. Jimenez, I. Marquez, and M. Rise. Electrical Stimulation of the Centromedian Thalamic Nucleus in Control of Seizures: Long-Term Studies. *Epilepsia*, 36(1):63–71, **1995**.
- [35] R. Fisher, V. Salanova, T. Witt, R. Worth, T. Henry, R. Gross, K. Oommen, I. Osorio, J. Nazaro, D. Labar, M. Kaplitt, M. Sperling, E. Sandok, J. Neal, A. Handforth, J. Stern, A. DeSalles, S. Chung, A. Shetter, D. Bergen, R. Bakay, J. Henderson, J. French, G. Baltuch, W. Rosenfeld, A. Youkilis, W. Marks, P. Garcia, N. Barbaro, N. Fountain, C. Bazil, R. Goodman, G. McKhann, K. Babu Krishnamurthy, S. Papavassiliou, C. Epstein, J. Pollard, L. Tonder, J. Grebin, R. Coffey, N. Graves, and the SANTE Study Group. Electrical stimulation of the anterior nucleus of thalamus for treatment of refractory epilepsy: Deep Brain Stimulation of Anterior Thalamus for Epilepsy. *Epilepsia*, 51(5):899–908, **2010**.
- [36] J. D. Rolston, S. A. Desai, N. G. Laxpati, and R. E. Gross. Electrical Stimulation for Epilepsy: Experimental Approaches. *Neurosurgery Clinics of North America*, 22(4):425–442, **2011**.
- [37] X.-F. Yang, B. F. Schmidt, D. L. Rode, and S. M. Rothman. Optical suppression of experimental seizures in rat brain slices. *Epilepsia*, 51(1):127–135, **2010**.
- [38] A. L. Benabid, P. Pollak, A. Louveau, S. Henry, and J. de Rougemont. Combined (thalamotomy and stimulation) stereotactic surgery of the VIM thalamic nucleus for bilateral Parkinson disease. *Applied Neurophysiology*, 50(1-6):344–346, **1987**.
- [39] A. L. Benabid. Deep brain stimulation for Parkinson’s disease. *Current Opinion in Neurobiology*, 13(6):696–706, **2003**.

- [40] T. M. Herrington, J. J. Cheng, and E. N. Eskandar. Mechanisms of deep brain stimulation. *Journal of Neurophysiology*, 115(1):19–38, **2016**.
- [41] G. S. Smith, A. W. Laxton, D. F. Tang-Wai, M. P. McAndrews, A. O. Diaconescu, C. I. Workman, and A. M. Lozano. Increased Cerebral Metabolism After 1 Year of Deep Brain Stimulation in Alzheimer Disease. *Archives of Neurology*, 69(9), **2012**.
- [42] R. J. Anderson, M. A. Frye, O. A. Abulseoud, K. H. Lee, J. A. McGillivray, M. Berk, and S. J. Tye. Deep brain stimulation for treatment-resistant depression: Efficacy, safety and mechanisms of action. *Neuroscience & Biobehavioral Reviews*, 36(8):1920–1933, **2012**.
- [43] M. Porta, A. Brambilla, A. E. Cavanna, D. Servello, M. Sassi, H. Rickards, and M. M. Robertson. Thalamic deep brain stimulation for treatment-refractory Tourette syndrome: Two-year outcome. *Neurology*, 73(17):1375–1380, **2009**.
- [44] L. R. Hochberg, D. Bacher, B. Jarosiewicz, N. Y. Masse, J. D. Simeral, J. Vogel, S. Haddadin, J. Liu, S. S. Cash, P. van der Smagt, and J. P. Donoghue. Reach and grasp by people with tetraplegia using a neurally controlled robotic arm. *Nature*, 485(7398):372–375, **2012**.
- [45] A. Eliseyev, C. Mestais, G. Charvet, F. Sauter, N. Abroug, N. Arizumi, S. Cokgungor, T. Costecalde, M. Foerster, L. Korczowski, B. Moriniere, J. Porcherot, J. Pradal, D. Ratel, N. Tarrin, N. Torres-Martinez, A. Verney, T. Aksenova, and A.-L. Benabid. CLINATEC BCI platform based on the ECoG-recording implant WIMAGINE and the innovative signal-processing: Preclinical results. pages 1222–1225. IEEE, **2014**.
- [46] J. Höhne, E. Holz, P. Staiger-Sälzer, K.-R. Müller, A. Kübler, and M. Tangermann. Motor Imagery for Severely Motor-Impaired Patients: Evidence for Brain-Computer Interfacing as Superior Control Solution. *PLoS ONE*, 9(8):e104854, **2014**.
- [47] A. J. Doud, J. P. Lucas, M. T. Pisansky, and B. He. Continuous Three-Dimensional Control of a Virtual Helicopter Using a Motor Imagery Based Brain-Computer Interface. *PLoS ONE*, 6(10):e26322, **2011**.
- [48] Z. O. Khokhar, Z. G. Xiao, and C. Menon. Surface EMG pattern recognition for real-time control of a wrist exoskeleton. *Biomedical engineering online*, 9(1):1, **2010**.
- [49] M. Rojas-Martínez, M. Mañanas, J. Alonso, and R. Merletti. Identification of isometric contractions based on High Density EMG maps. *Journal of Electromyography and Kinesiology*, 23(1):33–42, **2013**.
- [50] T. Roberts, J. B. De Graaf, C. Nicol, T. Hervé, M. Fiochi, and S. Sanaur. Flexible Inkjet-Printed Multielectrode Arrays for Neuromuscular Cartography. *Advanced Healthcare Materials*, 5(12):1462–1470, **2016**.
- [51] N. J. Holter and J. A. Generelli. Remote recording of physiological data by radio. *Rocky Mountain Medical Journal*, 46(9):747–751, **1949**.

Chapter 1. Introduction on electrophysiology and medical devices

- [52] G. P. al, et. Cellular telephone transmission of 12-lead electrocardiograms from ambulance to hospital. - PubMed - NCBI.
- [53] M. Modarreszadeh and R. N. Schmidt. Wireless, 32-channel, EEG and epilepsy monitoring system. In *Engineering in Medicine and Biology Society, 1997. Proceedings of the 19th Annual International Conference of the IEEE*, volume 3, pages 1157–1160. IEEE, **1997**.
- [54] E. Waterhouse. New horizons in ambulatory electroencephalography. *IEEE engineering in medicine and biology magazine: the quarterly magazine of the Engineering in Medicine & Biology Society*, 22(3):74–80, **2003**.
- [55] D. C. Yates and E. Rodriguez-Villegas. A key power trade-off in wireless EEG headset design. In *2007 3rd International IEEE/EMBS Conference on Neural Engineering*, pages 453–456. IEEE, **2007**.
- [56] S. Patki, B. Grundlehner, T. Nakada, and J. Penders. Low power wireless EEG headset for BCI applications. In *International Conference on Human-Computer Interaction*, pages 481–490. Springer, **2011**.
- [57] H. Nyquist. Thermal Agitation of Electric Charge in Conductors. *Physical Review*, 32(1):110, **1928**.
- [58] K. S. Pettis, M. R. Savona, P. N. Leibrandt, C. Maynard, W. T. Lawson, K. B. Gates, and G. S. Wagner. Evaluation of the efficacy of hand-held computer screens for cardiologists' interpretations of 12-lead electrocardiograms. *American Heart Journal*, 138(4):765–770, **1999**.
- [59] M. Nitzken, N. Bajaj, S. Aslan, G. Gimel'farb, A. El-Baz, and A. Ovechkin. Local wavelet-based filtering of electromyographic signals to eliminate the electrocardiographic-induced artifacts in patients with spinal cord injury. *Journal of Biomedical Science and Engineering*, 06(07):1–13, **2013**.
- [60] J. Mateo, A. M. Torres, M. A. García, and J. L. Santos. Noise removal in electroencephalogram signals using an artificial neural network based on the simultaneous perturbation method. *Neural Computing and Applications*, 27(7):1941–1957, **2016**.
- [61] H. Adeli, S. Ghosh-Dastidar, and N. Dadmehr. A Wavelet-Chaos Methodology for Analysis of EEGs and EEG Subbands to Detect Seizure and Epilepsy. *IEEE Transactions on Biomedical Engineering*, 54(2):205–211, **2007**.
- [62] R. R. Bond, D. D. Finlay, C. D. Nugent, and G. Moore. A review of ECG storage formats. *International Journal of Medical Informatics*, 80(10):681–697, **2011**.
- [63] M. R. Nuwer, G. Comi, R. Emerson, A. Fuglsang-Frederiksen, J.-M. Guérit, H. Hinrichs, A. Ikeda, F. J. C. Luccas, and P. Rappelsburger. IFCN standards for digital recording of clinical EEG. *Electroencephalography and clinical Neurophysiology*, 106(3):259–261, **1998**.

- [64] Dispositifs médicaux : diagnostic et potentialités de développement de la filière française dans la concurrence internationale. *Pôle interministériel de prospective et d'anticipation des mutations économiques (PIPAME)*, **2011**.
- [65] Parcours du dispositif médical - guide pratique. *Haute Autorité de Santé (HAS)*, **2009, updated in 2013**.
- [66] T. Beaudet and E. Couty. La place des dispositifs médicaux dans la stratégie nationale de santé. *Avis du Conseil économique, social et environnemental - JOURNAL OFFICIEL DE LA RÉPUBLIQUE FRANÇAISE*, **2015**.
- [67] Marquage CE des dispositifs médicaux de classe I - <http://www.qualitiso.com/dispositif-medical-classe-1-declaration-ce-conformite/>.

Electrodes

Electrophysiological activities can be recorded from cellular level up to a very integrated level at the surface of the scalp. To do so, sensors, called electrodes, record a local potential generated by the activity of cells or organs and deliver it to the acquisition system for processing, displaying and saving. An electrode is made of metal or any conducting material, and records the potential at the surface, or within, the biological tissue. In case of cutaneous recordings, to improve the contact between skin and electrode, an intermediate layer of conductive gel is often used. In this chapter, electrochemical phenomenon happening at the interface between the saline media and the conducting electrode will be described and analyzed. Then, different protocols for electrode characterization will be shown. We will not forget that these results will be applied to cutaneous electrodes for recording of biological signals. And, after an overview of every available options to fit an electrode to a specific application during its conception, a list of medical electrodes used in clinic will be presented.

2.1 A model of the electrode and the reactions at its interface

2.1.1 Electrochemical model of the electrode

Definition of an electrode

An electrode is an electrical conductor which can release or capture electrons. It is in contact with the non-electronically conductive part (which can be an insulator or an ionic conductive part) of a circuit. In electrochemistry, electrodes behavior can be studied in the case of the Galvanic cell, made of two half-cells (see Fig 2.1). In the Galvanic cell, two metals are in contact to each other by a wire and are immersed in different solutions. Reduction and oxidation reactions that occur between the electrodes and corresponding ions in the electrolytes generate a potential difference between the electrode and the creation of a current. The loop is closed by a saline bridge between the two electrolyte which allows ions to flow through. A succession of such cells is forming a voltaic pile, called electrical battery. In this case, the electrode is defined as an ionic-to-electronic current transducer.

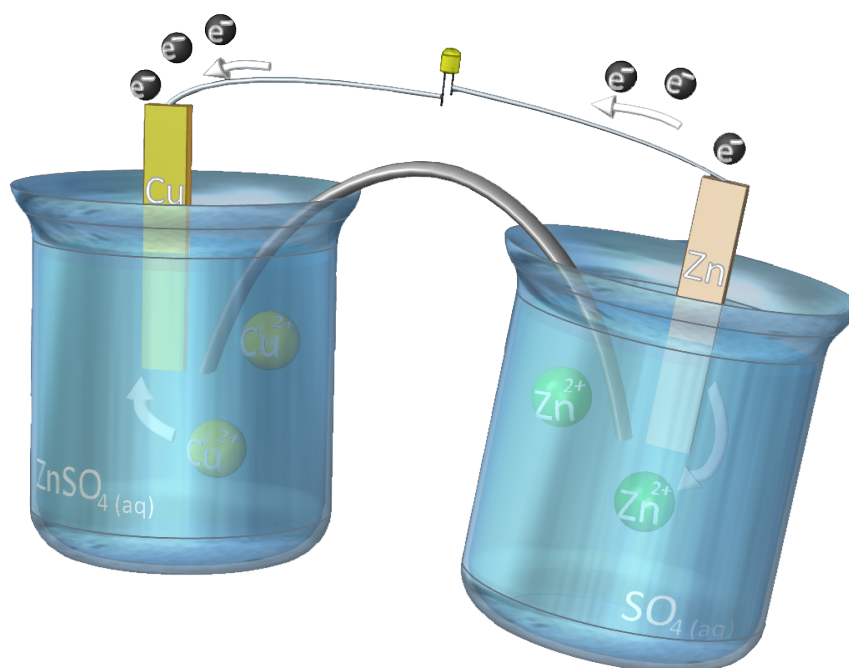


Figure 2.1 – **The Galvanic electrochemical cell.** Cartoon of a Galvanic cell. A copper (*Cu*) and a zinc (*Zn*) electrodes are immersed in copper sulfate solution ($CuSO_4$) and zinc sulfate solution ($ZnSO_4$) respectively. The two solutions are linked by a salt bridge and the two electrodes by a wire. RedOx reactions induce ions movement in the salt bridge and an electronic current is generated between the electrodes.

Reaction at the interface of the electrode

Electrodes are usually in contact with an ionic, or saline, solution called electrolyte. At the electrode-solution interface, a redox reaction occurs, allowing charge transfer: the oxidized specie C_{Ox} transforms to the reduced specie C_{Red} by transferring n electrons, following the reversible equation:



When the electrode is in contact with the electrolyte, excess of charges causes the creation of an electrical double layer to establish potential equilibrium. Metallic ions tend to leave the electrode whereas ions from the electrolyte tend to combine with the metal. Two layers of opposite polarity are formed at the interface, separated by a molecular "dielectric" layer. This creates a capacitive effect to the electrode. This simple model is called the Helmholtz model [1], and was completed by the Stern-Gouy-Chapman model, which introduces the diffusion effect of ions in the solution[2].

2.1. A model of the electrode and the reactions at its interface

In the case of electrodes for bio-recordings, the electrolyte can have a biological origin (serum, mucosa, sweat, cerebrospinal fluid, ...) or be synthesized (conductive gel like hydrogel).

2.1.2 Noise generation

Half-cell potential

In the electrochemical cell, the cell potential is the difference between the two potentials of electrodes, called half-cell potentials:

$$E_{Cell}^0 = E_{Red,Cathode}^0 + E_{Ox,Anode}^0 \quad (2.2)$$

Each of the half-cell potential is generated by an oxidation or a reduction reaction between the electrode and the corresponding metal ion in the electrolyte. These half-cell potentials are defined for a given concentration (1M) and pressure (1bar), and measured with respect to a standard hydrogen half-cell, declared to be zero. The Nernst equation is applied to correct these values if conditions are different.

In the case of biological signal recordings, if the electrodes are made with different materials, the half-cell potentials of the electrodes are not equal to each other and this adds a DC component (i.e. a continuous component) to the signal that can affect low-frequency recordings. Some acquisition systems are also sensitive to the presence of a strong DC component, which can induce the recorded signal to be out of a specific range. To reduce this effect, it is then important to measure a biological signal with the same type of electrodes even if a small half-cell potential difference is inevitable.

Polarizable electrode versus non-polarizable electrode

Depending on the conducting material used for electrode fabrication, electrodes can be polarizable or not. In the first case, for polarizable electrodes, modification of ionic concentrations in the surrounding electrolyte involves the creation of a current in the electrode without any charge crossing the electrolyte-electrode interface. In this case, the electrode acts like a capacitor. If a polarizable electrode is displaced in the electrolyte, there is a change in the charge distribution around the electrode and in its potential. This produces a strong variation in the recorded low-frequency potential, called a motion artifact, described in the next Section 2.1.2. For this reason, non-polarizable electrodes are preferred, for example made of silver/silver chloride (Ag/AgCl). In an ideal non-polarizable electrode, the current moves freely between the electrolyte and the metal, without inducing any change in the ion distribution around the electrode. In this case, the electrode acts as a resistor. In practice, non-polarizable electrodes are never perfect and have small capacitive effects.

Motion Artifacts

The term "motion artifact" covers all movements from any sources that could add noise to a recorded signal. And since some biological signals are very small, any disturbance can "hide" them. Fig 2.2 shows two ECG signals recorded from electrodes placed close to each other on a human volunteer. The purple signal is coming from a gel-assisted electrode and the green one from a dry electrode. Because of the absence of gel (discussed below), the green ECG signal is disturbed by motion artifacts. It is clear that this noise can limit the recognition of important part of the signal, like full PQRST complexes in this case.

To better understand how to prevent these motion artifacts, Webster [3] describes five movements that can cause them: , , electrode, cables and medical staff.

- **Noise created by patient's muscles:** Any muscle activity that creates unwanted EMG noise can be recorded by the electrodes. It is the main problem for ambulatory recordings since the measurement has to be done while the patient is moving. Even for recordings at resting state or during sleep or coma state, ECG potentials generated by heart beats can disturb EEG or EOG. Solutions to avoid or reduce this noise are to filter out some frequencies (for example, most of EMG noise is at higher frequency, 30-200 Hz, than significant frequencies for ECG, 0.05-100 Hz) or to place electrodes somewhere on the body where they may be less affected by muscle activity (close to a bone for instance).
- **Noise created by patient's skin:** The potential difference between the inner and the outer part of the skin can be modified by the applied pressure from the electrode and causes a noise artifact. By removing the first layer, abrasion of the external part of the skin can reduce this effect.
- **Noise created by the electrode itself:** As soon as the recording part of the electrode is moving with respect to the skin (because of a moving subject), the electrical double-layer is disturbed and a motion artifact is created. It is a real problem for clinicians since patients are active during most of the electrophysiological recordings and will most likely move, as presented in Fig 2.2. The use of gel between the skin and the electrodes highly reduces these motion artifacts: gel elastic properties involves that the two interfaces with the double layers, skin-gel and gel-electrode, are locally almost stationary but move by respect to each other.
- **Noise created by wiring:** Motion artifacts can also be generated by cables movements. Friction and deformation of the cable insulation produce triboelectric noise, like a piezoelectric movement transducer would do. Many systems are now wireless, in particular to avoid this effect.
- **Noise created by surrounding medical staff:** Friction-induced static electricity, generated by a nurse or anyone close to the patient, moving or touching him, interferes with the signal of interest.

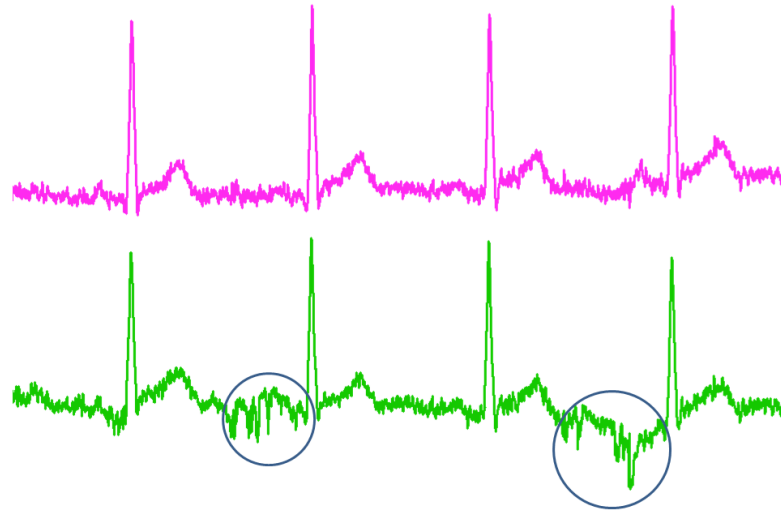


Figure 2.2 – **Motion artifacts on ECG signal.** ECG signals recorded at the same time on a human volunteer from electrodes placed close to each other on the wrists. Purple signal is coming from a wet electrode and green signal is coming from a dry electrode. Motion artifacts, generated by motion of the patient, are highlighted by circles on the green signal.

2.1.3 The electrolyte in electrophysiology

Invasive electrodes, implanted in human body, are surrounded by physiological ionic media. This aqueous media is strongly conductive and plays the role of electrolyte.

However, most of the electrodes used everyday for applications in human electrophysiology are cutaneous and contain a synthetic conductive gel as interface between metal and skin. This gel is a synthesized ionic conductor (an extreme solution could be to use sweat as saline solution) and decreases the skin impedance. Usually it is a chloride to stabilize the AgCl half-cell potential. The cation is commonly a sodium (Na), a chloride (Cl) or a potassium (K) ion. Coloring, perfume, stabilizer, humectant and antibacterial agents can also be added to commercially available conductive gel or paste. The gel is either directly included on the electrode (as it is in almost all commercial ECG electrodes), either needs to be manually added (with a syringe for most of the EEG electrodes).

To facilitate long-term recordings, the gel has to stay stable for at least few hours (to avoid evaporation) and can be adhesive. Because of his liquid or semi-liquid state, this gel grants a good and permanent contact with the skin and can cross a thin layer of hair. Moreover, by moistening, thus making more conductive the insulated external layer of the skin, the gel greatly improves the contact impedance with the electrode.

2.1.4 Skin specificities for cutaneous electrophysiology

For cutaneous electrophysiology, two interfaces are important and explain the behavior of the electrode: electrode-gel and gel-skin. Gel conductivity, skin preparation or electrode performances are parameters that modify these two interfaces, thus the global impedance of the system and the quality of the recorded signal.

A quick focus on skin composition is needed to understand the interface with an electrode and its gel. As described in Fig 2.3, the two main layers of the skin are, from the outer one to the inner one, the epidermis and the dermis. The epidermis is the first protection barrier of the human body. It is itself composed of 4 or 5 layers with different functions. The outer one, called stratum corneum and composed of dead skin cells, acts usually as an insulator. It needs to be removed most of the time (by abrasion with sandpaper) or crossed (with pins electrode) to give a low impedance interface with the recording electrode. The dermis contains most of the mechanoreceptors (to allow heat and touch senses), hair follicles, sweat and sebaceous glands as well as blood vessels to feed the epidermis. The hypodermis, or subcutaneous layer, is not part of the skin. Its purpose is to attach the skin to the bones muscles and it is mainly composed of fat.

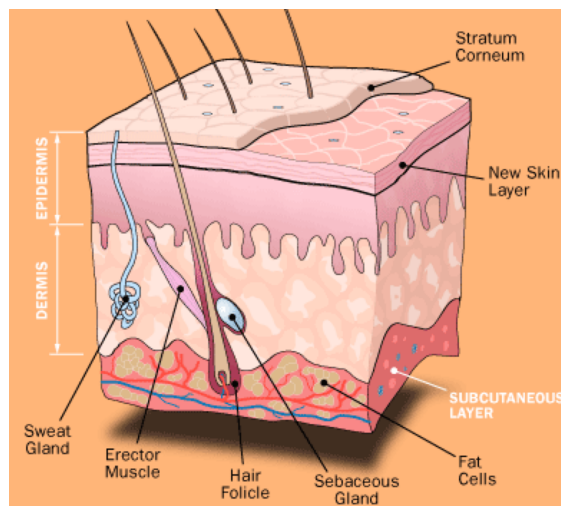


Figure 2.3 – **Skin layers.** The outer layer, the stratum corneum, is made of dead cells and can be removed by abrasion

2.1.5 Equivalent model of skin-electrode interface

To explain the electrical behavior of the interaction between electrode, electrolyte and skin, it is possible to model all the interfaces with an equivalent circuit. This equivalent circuit is based on mathematical models of each “components” which characterize the system and facilitates the fit of the system behavior with R(RC) models.

Fig 2.4 shows an equivalent circuit for the interfaces electrodes-electrolyte-epidermis-dermis

[4]. The potential source E_{hc} models the half-cell potential of the electrode (see Section 2.1.2), thus the additional DC component on the recorded signal. As described in Section 2.1.2, any electrode presents both capacitive and resistive effects, modeled by R_{el} and C_{el} . These two last components can be defined with impedance measurements (see following Section 2.2.2). R_e is the effective resistance associated with the gel between the electrode and the skin. E_{hc} , R_{el} , C_{el} and R_e are mainly depending on the materials of the electrode, and then can be tuned during electrode conception. The potential difference E_{se} can be found from the Nernst equation for the electrolyte, and is due to the semipermeability of the stratum corneum. The epidermal circuit acts as a parallel RC circuit, with a high resistance due to the stratum corneum. The dermis and subcutaneous layers are conductive and represented as a single series resistor.

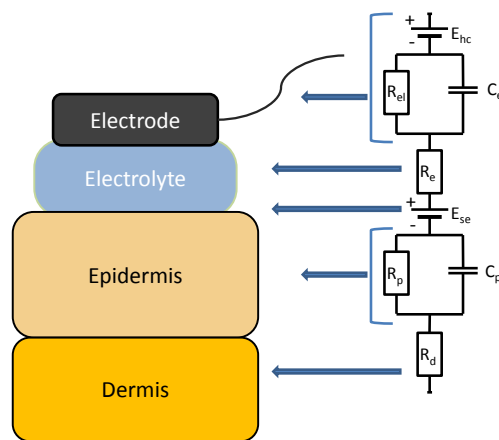


Figure 2.4 – Equivalent circuit for the electrode-skin interface.

2.2 Electrode characterization

2.2.1 Three-electrode cell and potentiostat

Presentation of the three-electrode system

Most of electrode characterizations (electroanalytical experiments) are done by a potentiostat connected to a three-electrode cell. The potentiostat is an electronic device which controls voltage between a working electrode (WE, the electrode to characterize) and a reference electrode (RE) through the injection of current from a counter electrode (CE). For a specific potential applied between WE and RE, the current between WE and CE is measured. In the following sections, impedance and cyclic voltammetry characterizations performed with a potentiostat and a three-electrode cell will be presented more in details. RE is able to keep a constant electrochemical potential if no current is flowing through it. The most common RE is a saturated calomel electrodes or a Ag/AgCl electrode. CE is usually made of an inert conductor such as platinum and preferably presents a bigger surface area than the WE. The

three electrodes are immersed in an electrolyte, such as NaCl.

Working principle of a potentiostat

Fig 2.5a presents the schematic of a potentiostat electric circuit with a simple operational amplifier. This circuit is equivalent to the one shown on Fig 2.5b, with Z_1 related to the recording resistance R_m in series with the interface impedance of CE and the electrolyte resistance between CE and WE. Z_2 is related to the interface impedance of WE and the electrolyte resistance between WE and RE. Because we make the hypothesis that no current is flowing through RE, we can write at the output of the op amp:

$$E_r = \frac{Z_2}{Z_1 + Z_2} \cdot E_{out} = \beta \cdot E_{out} \quad (2.3)$$

with β as the feedback factor. As we work with a non-inverting amplifier (with a gain A), we then obtain:

$$\frac{E_r}{E_i} = \frac{\beta \cdot A}{1 + \beta \cdot A} \quad (2.4)$$

When $\beta \cdot A$ is very large with respect to one, we obtain $E_i = E_r$, which proves that the control amplifier works to keep the voltage between RE and WE as close as possible from the input source voltage [5].

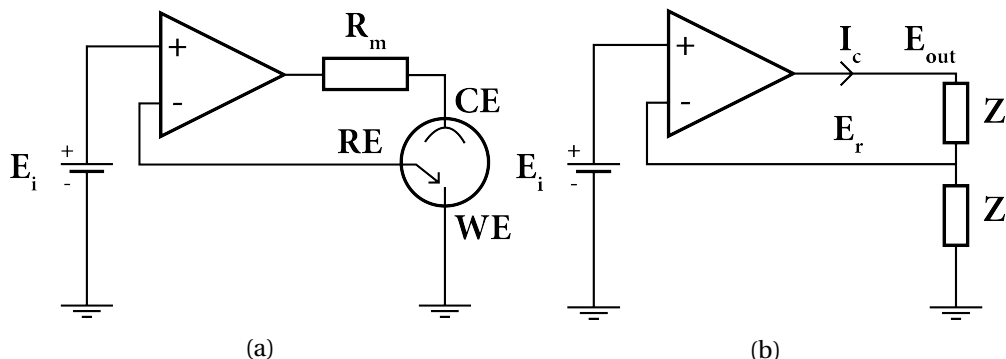


Figure 2.5 – **Schematic of a potentiostat system**(a) with the electrochemical cell, (b) with electrochemical cell replaced by two impedances.

2.2.2 Impedance

Electrochemical Impedance Spectroscopy

The concept of electrical resistance is defined by Ohm's law: $R = V/I$. However, this relation is limited to one element, the resistor. For more complex elements or systems, the concept of impedance Z replaces the resistance: $Z = V_{AC}/I_{AC}$. Impedance is a complex function expressed in terms of a magnitude and a phase. To measure impedance, an AC voltage (usually

sinusoidal) is applied to the electrochemical cell. The phase is the time shift between the potential input and the current output. The last important parameter for impedance is the frequency at which it is measured.

These three parameters are often plotted on a Bode plot, with both magnitude and phase logarithmically plotted against frequency. Impedance can also be plotted in polar form in the Nyquist plot. Magnitude is then the length of the vector and phase is its angle. An example of both Bode plot is presented on Fig 2.6. More details on electrochemical impedance spectroscopy theory and application can be found here: [6, 7].

Simple equivalent circuits can be used to characterize an electrode after impedance measurement (see previous Section 2.1.5. When a sine wave potential is applied to an ideal simple resistor, the current through it is a sine wave with no time shift. A system acting similarly to a resistor presents on Bode plot a constant phase at 0° and a constant magnitude R over all frequencies. Another element very common in electrodes equivalent circuits is the capacitor. In Bode plot, it matches with a horizontal line at 90° for phase and magnitude is linear to frequencies with a slope of -1 . As it can be analyzed in Fig 2.6, the Ag/AgCl electrode (in black) is close to be a perfect non-polarizable electrode with a constant and low impedance and a phase close to 0° . Impedance analysis of bare gold electrodes shows that they behave as resistor at high frequencies but behave as polarizable electrodes below 1 kHz. However, one gold electrode has a surface area 6.25 times bigger than the other one, and shows an impedance approximately one order of magnitude lower. Indeed, the surface area of the WE is directly linked with impedance magnitude.

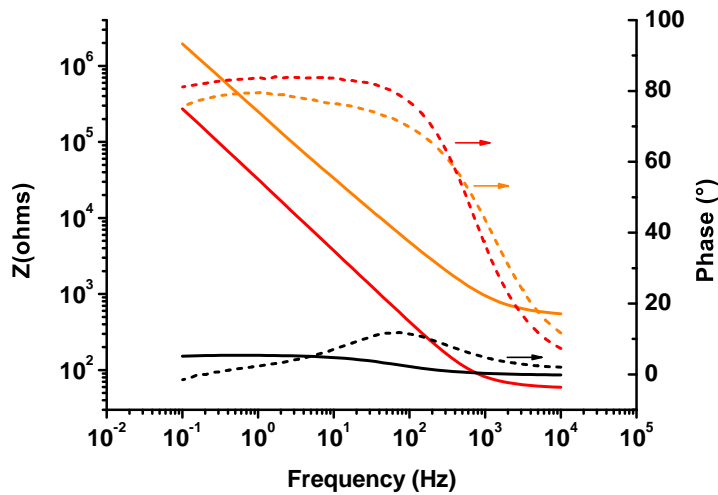
To resume, impedance can be defined by a combined measurement of the opposition to current through the electrode interface (resistance) and the ability to store charge at the interface (capacitive reactance), in response to a sinusoidal current [8].

Importance of impedance for bio-signal recordings

For bio-medical applications, extracellular signals are very low (from microvolts to millivolts) and can be hidden by the ion-based noise fluctuations surrounding the electrode or by environmental noise such as breathing or electromagnetic interferences. If the electrode impedance is not low enough, the interesting signal may be lost [9]. In the same way, a high current density is necessary to induce activity during electrical stimulation. In this case, low impedance involves low applied electrode potential, leading to less unwanted electrochemical reactions which could damage the surrounding cells [10]. It is explained on Eq 1.1 how impedance of electrodes interacts with input impedance of the acquisition system.

Application to cutaneous electrodes

If electrodes are usually characterized with an electrochemical cell, that is to say in contact with a liquid electrolyte, a part of most of the cutaneous electrodes is made of gel or hydrogel



(a)

Figure 2.6 – **Example of Electrochemical Impedance Spectroscopy.** Results are displayed for a 18.8 mm² Silver/Silver Chloride electrode (in black), for a 50 mm² Gold electrode (in red) and a 0.8 mm² Gold electrode (in orange). Impedances are plotted with full lines and phases with dash lines. The electrolyte was a 0.1 M NaCl.

which could dissolve in water. It is then impossible to characterize the gel-skin interface. Two other ways of measuring impedance are then possible:

- **Gel-to-gel impedance:** Accordingly to the ANSI/AAMI EC12:2000/(R)2005 standard, impedance can be measured by placing active areas of two electrodes in contact to each other, in gel-to-gel configuration. In this case, the electrochemical cell is formed by two electrodes and one electrolyte (made of the two gels together). If this configuration has the merit of being simple and fast to set up, it gives the opportunity to study only the electrode-gel interface and is not as accurate as a measurement with three electrode electrochemical cell. The norm recommends to apply a 10 Hz sinusoidal current which does not exceed 100 μ A peak-to-peak and to measure the resulting voltage for at least 12 electrode pairs. The resulting impedance of each pair should not exceed 3 k Ω and the mean impedance over the 12 pairs should not exceed 2 k Ω [8].
- **Impedance on skin:** Since cutaneous electrodes are in contact with skin, which cannot be considered as a purely conductive electrolyte, an impedance test on skin was developed by Leleux et al. [11]. It facilitates the test of different gels and electrodes by inducing characterization of both electrode-gel and gel-skin interfaces. To do so, the three-electrode configuration is kept and these electrodes are placed on a healthy volunteer. Working and counter electrodes are placed 2 cm away from each other on the forearm, and the reference electrode is placed 30 cm away on the arm. Both reference and counter electrodes are medical gel electrodes in order to keep stability over

measurements. Then, a regular potentiostat can be used in the same way as for an electrochemical cell. This method is more adapted to cutaneous sensors but the resulting impedances cannot be qualitatively compared to each other without decomposition to equivalent models. This is because subject-to-subject skin impedance variations are too important, as well as time variation of skin hydration over a subject.

2.2.3 DC voltage offset measurement

As explained previously, the half-cell potential difference between the two recording electrodes (bipolar measurement) or between the recording electrode and the reference (unipolar measurement) generates a DC offset. Depending on the acquisition system, a too high DC offset can hinder a correct recording because the resulting signal is too high compared to ground and the range of the amplifier. It has to be as low as possible. Accordingly to the ANSI/AAMI EC12:2000/(R)2005 norm, DC offset is characterized by placing two electrodes in a gel-to-gel configuration and applying a continuous 200 nA current. The DC change should not exceed 100 mV over at least 8 hours [8].

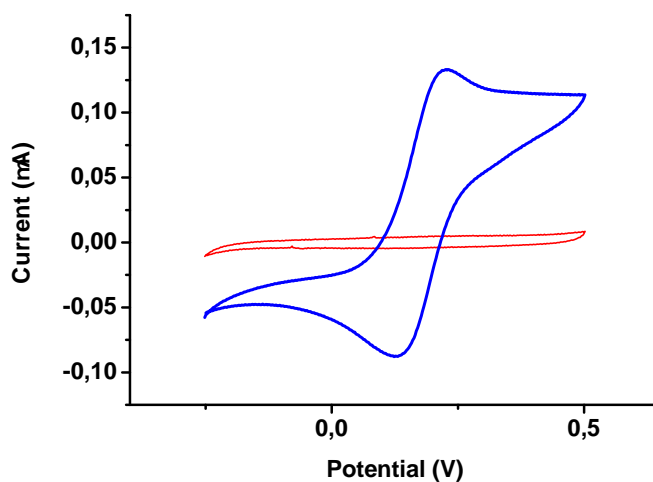
2.2.4 Cyclic voltammetry

During a cyclic voltammetry (CV), the potential of an electrode, immersed in an unstirred electrolyte, is cycled and the resulting current is measured [12]. This characterization is performed in a three-electrode cell, as defined in previous Section 2.2.1. The potential of the WE is controlled versus the RE and is considered as the excitation signal. For CV, the excitation signal is ramped versus time at a specific scan rate (unit: Vs^{-1}) with a triangular waveform. Multiple cycles are usually performed. A cyclic voltammogram is the plot of the measured current between WE and CE during the potential scan.

CV is mainly used to study electrochemical properties of an analyte in the electrolyte. Indeed, reduction-oxidation reactions occur during the potential scan. These reactions are characterized by peaks in the CV at specific potentials. During negative potential scan, the reduction peak is reached when all the substrate at the surface of WE has been reduced or when all species in the electrolyte have been reduced. After the switching potential, the potential is scanned positively and the oxidation peak is reached when all the substrate at the surface of WE has been oxidized (or when all species in the electrolyte has done so). Stopping the CV after one of the redox peak can facilitate a cleaning of the WE for specific applications. Usually, the potential scan is usually limited by water electrolysis potential (around 1.23 V in pure water). Indeed, unwanted reaction between WE and the water contained in the electrolyte can damage the WE. However, such reaction is used to define water window limits (as well as electrochemical window), to characterize what is the maximum voltage that can be applied to an electrode for stimulation without damaging the electrode and the surrounding tissues (or to avoid spoiling energy that is intended for another reaction). Finally, CV facilitates the characterization of charge storage capacity of the WE. Cathodic charge storage capacity is cal-

culated by integration of the cathodic current (current generated during the negative potential scan) over one cycle of CV.

An example of CV measurement is shown on Fig 2.7. The potential was scanned from -0.25 to 0.5 V at a speed rate of 0.25 Vs^{-1} and a bare gold electrode was used as WE. In presence of redox neutral electrolyte, such Phosphate buffer solution (PBS), no redox reaction is detected during the scan (in red). However, if this electrolyte is mixed with a 1 mM solution of the $[\text{Fe}(\text{CN})_6]^{3-/4-}$ couple, composed of ferrocyanide $[\text{Fe}(\text{CN})_6]^{4-}$ and ferricyanide $[\text{Fe}(\text{CN})_6]^{3-}$, typical oxidation and reduction peaks are detected by the CV at 0.12 V and 0.28 V (in blue) [13].



(a)

Figure 2.7 – **Example of Cyclic voltammetry measurement.** The CV was performed with a 0.25 μm^2 gold electrode. For the red curve, electrolyte was a 0.1 M phosphate buffer solution, neutral for redox reactions. For the blue curve, a 1 mM $[\text{Fe}(\text{CN})_6]^{3-/4-}$ solution was mixed with the previous solution.

2.2.5 Biocompatibility

Definition of Biocompatibility

Ideally, any material in contact with or close to a living tissue should not disturb its regular behavior. Obviously, any foreign material in contact with a biological tissue will induce an immune (defense) response and the goal is to minimize it. Biocompatibility is then the ability of a material to induce an appropriate host response in a specific situation [14]. This term is ambiguous because biocompatibility does not mean no damage at all, and a biocompatible material in a specific situation could be very toxic in another situation: if it is no problem to manipulate plastic parts with our fingers for a long time, it is not recommended to swallow them. The multiple interactions of a living tissue with the rest of the body and the presence of multiple different materials in modern medical devices make the determination of their

toxicity increasingly complicated. However, specific standards such as ISO 10993, have to be respected in order to get a FDA-approved, or a CE marked, medical device.

Application to cutaneous electrodes

Because the purpose of cutaneous electrodes is to be in contact with the skin, it is important that none of the materials and parts of the electrode would harm it. The ANSI/AAMI/ISO 10993 list of standards define the necessary tests to prove the safety of electrodes and to be able to sell them for medical purpose. The ANSI/AAMI EC12:2000/(R)2005 [8] standard for disposable ECG electrodes addresses few important tests in the case of any cutaneous electrodes (not only for ECG). First, cytotoxicity of the electrode has to be tested: the electrode is brought together with cultured cells (from the organ which will be in contact with the electrode) and should not disturb their growth. Then, tests using an appropriate model validate the absence of sensitization and irritation of the skin because of the device, which means the absence (or a minimum) of any allergic response.

2.3 Medical Electrodes for electrophysiology

2.3.1 Options around the conception of an electrode

When a research team is about to start the development of new kind of electrodes, many possibilities are offered, depending on the needs. All these options have to be considered because they influence each other and they can change the design, the structure, the properties and the constraints of the new device. A summary of these options is presented as a cartoon on Fig 2.8:

- **Spatial organization of the recording areas.** The device can offer a single recording site or multiple ones. Usually, matrices of electrodes are used for spatiotemporal analysis of a signal recorded on a large area (surface of a muscle for instance). But if this area is too large (e.g., entire scalp) many single devices will provide a better contact than a single matrix. In the case of depth probes, one single device with many different recording sites is used in order to reduce the invasiveness.
- **Materials.** The choice of materials is important to define mechanical properties of the device. They can be soft and thin to be light and to comply with the contact surface or harder and thicker to allow easy manipulation by the users. For cutaneous and external applications, less invasive or even invisible device are the new trend, patients need to forget that they are wearing cutaneous devices. Each material will affect the biocompatibility of the final device and need to be accordingly chosen.
- **Environment around the device.** For invasive probes or devices, the biologic fluids (e.g., cerebrospinal fluid, blood), but also sweat in case of cutaneous devices, will surround

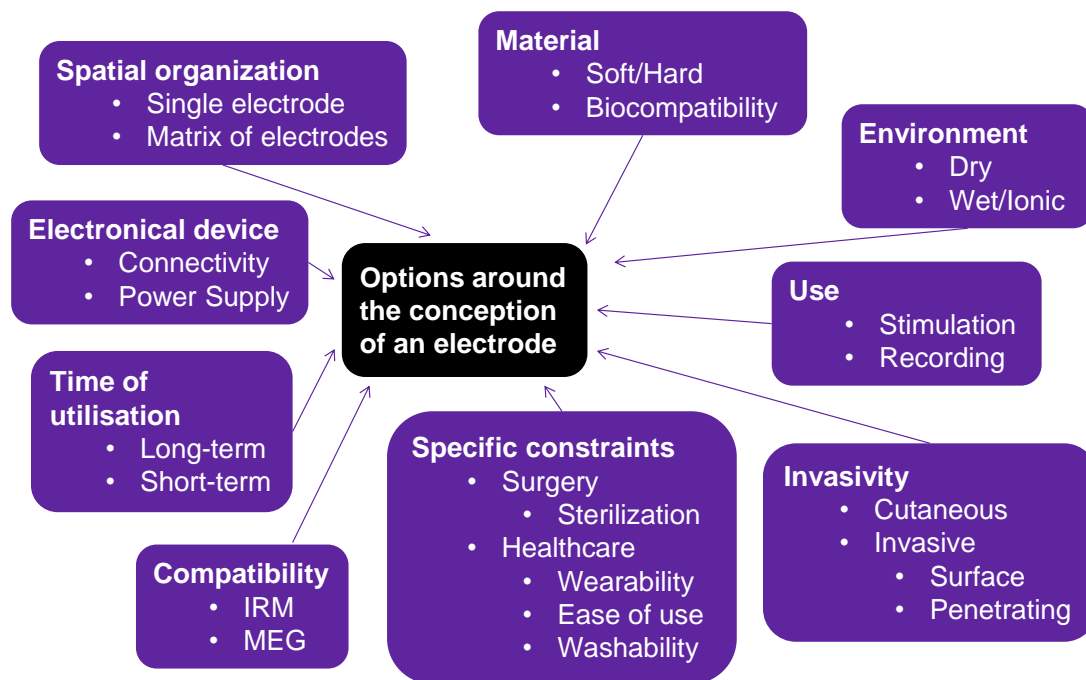


Figure 2.8 – **List of options for electrode development.** Arbitrary list of choices and constraints that need to be taken into account at a first stage of electrode development.

the active sites. Because biological fluids are conductors, an electrolyte may be not necessary.

- **Monitoring or Therapy?** If electrodes are usually made to record bio-signals, it is also possible to use them to modify the local electrical field and then to interact with a specific organ. Depending on the passivity of the electrodes, certification can be changed as well as materials in order to be able to deliver high potentials or currents.
- **Invasivity.** It is obvious than the biocompatibility of a cutaneous device, only in contact with the skin, will be easier to certificate than the biocompatibility of an invasive device that penetrates a living tissue. But some subtleties exist: if the device is meant to stay outside of a tissue but is still in contact with fluids coming from the tissue, the non-contamination of theses fluids has to be demonstrated. For invasive devices, its penetration (and so the materials) need to be defined since an ECoG does not need to be thick to penetrate the brain compared to a depth probe.
- **Clinic specifications.** In the hospital, most of devices need to be sterilized in order to avoid any extra contamination. Autoclave, radiation or chemical sterilization involve a high-level of constraints for the components of the device that need to keep their

properties. If the device is meant to be used during surgery, surgeon and nurses may have specific constraints to handle the device since he is wearing gloves and little space to move around the patient.

- **Out of clinic specifications** If the devices is intended to be used in a normal environment, it has to comply with high wearability standards. It has to be easy to handle, to be washable or at least waterproof, to be as invisible as possible for the user and to resist to high mechanical constraints because of motion.
- **Compatibility with other recording modalities.** To learn more about the patient state, doctor can try to use an MRI (Magnetic Resonance Image) or a MEG (MagnetoEncephalograph) at the same time as an electrophysiological recording device. High magnetic fields applied by the MRI can damage some materials whereas the extreme sensitivity of the MEG to magnetic fields forbids the use of some other materials.
- **Time of utilization.** The time of utilization and the time of the contact between living tissue and the device are another parameter. The immune response can be different after some time and long-term devices are more difficult to certificate. Usually, devices for short-term utilization are consumables, they are meant to be used only once.
- **Electronics.** Some electrodes, called active, include close by electronics for filtering and amplification. Stimulation device also need a power source. The presence of electronics modifies the size, the mechanical properties, the price and the compatibility of the devices.

2.3.2 Presentation of different medical electrodes

A quick overview of some commercially available electrodes which are used in clinic is important to fully understand what the needs of medical staff are. It is important to notice that only few technologies that will be presented later in the thesis are commonly used by clinicians, even if they were already developed years ago. This means it is difficult to convince clinicians to use new devices. There is a big technology gap between medical devices developed in research institutes and devices used at the hospital. In this section, we aim to present couples of common cutaneous and invasive electrodes. Choices are of course biased and limited but give a general idea.

Cutaneous electrodes

Most of the cutaneous electrodes are for ECG or EMG examinations, and Ambu (Denmark) and 3M (USA) are the main worldwide suppliers, even if other brands exist. Usually big (with a surface area in contact with skin up to 50 mm of diameter), most of them are made of large adhesive part which ensure a strong contact with skin and less motion artifacts, and of foam soaked in a Sodium Chloride Hydrogel. The sensor material, place beside the foam, is usually Silver/Silver Chloride, to obtain an electrode as non-polarizable as possible. The electrode

Chapter 2. Electrodes

is either delivered with an integrated connection wire, either with a connector which can be clipped to wires.

EEG electrodes are usually called cup electrodes. Indeed, they are made of a Silver/Silver Chloride- or Gold-coated metal cup with a hole in the middle axis and wire to be connected to an acquisition system. The diameter of the electrode is around 10 mm and the diameter of the hole is around 2 mm. The hole enables clinicians to fill the space between the scalp and the electrode, often full of hair, with a gel electrolyte. To fill the electrodes with gel is a time-consuming step but this allows the electrodes to be reusable for many patients after cleaning.

Stainless steel, sterile, subdermal electrodes are also very common in clinics, to be used as reference cutaneous electrodes during surgery or to record EMG or EEG in specific case. However, they are painful for patients and trigger a fast immune response which avoids a recording longer than few days.

Invasive electrodes

Depth electrodes are the only invasive electrodes widely used in clinic; even if the applications are few and recent. As an example, we can examine sterile SEEG depth electrodes from Ad-Tech (USA). They are around 15 cm long, to facilitate connection outside of the brain, with a diameter between 0.8 and 2 mm to reduce brain damage during insertion. Between 5 and 10 electrode pads are distributed along the stick. Each pad is coated with platinum or irridium-platinum and in direct contact with brain. Figures of these electrodes can be found on this website. Sterile, single-use and silicone-based ECoG (subdural) grids can be found on Ad-Tech Medical website. These ECoG grids can be linear or in the form of a matrix. Electrode pads are with a diameter of 4 mm, with a 10 mm spacing and coated with stainless steel or platinum. Color codes on the connecting wires facilitate electrode identification.

Electrodes arrays developed for artificial retina give patients the ability to distinguish big patterns with strong contrast or few pixels on a computer screen. The Argus II retinal prosthesis (from Second Sight Medical Products, USA) was the first to receive both FDA and UE approvals after certification. They provide a matrix of $6 * 10$ stimulation electrodes, coated with platinum gray, with diameter of $200 \mu\text{m}$. The substrate is made of silicone and the grid is inserted in the eye and applied on top of the retina, as showed in this movie. More information can be found on this website. Another retinal implant, called Alpha-IMS Implant and conceived by Retina Implant AG(Germany) consists of a $3\text{mm} * 3\text{mm} * 70\mu\text{m}$ silicon chip mounted on a $20 \mu\text{m}$ -thick polyimide substrate with gold-coated circuits. A matrix of 1500 pixels transduces photon signal to an electrical stimulation. The $50 \mu\text{m}^2$ stimulation electrodes are made of titanium nitride. More information can be found on this website.

2.4 Bibliography

- [1] H. v. Helmholtz. Ueber einige Gesetze der Vertheilung elektrischer Ströme in körperlichen Leitern mit Anwendung auf die thierisch-elektrischen Versuche. *Annalen der Physik*, 165(6):211–233, **1853**.
- [2] O. Stern. Zur theorie der elektrolytischen doppelschicht. *Zeitschrift für Elektrochemie und angewandte physikalische Chemie*, 30(21-22):508–516, **1924**.
- [3] J. C. Webster. Interference and motion artifact in biopotentials. In *Region Six Conference Record, 1977. IEEE 1977*, pages 53–64. IEEE, **1977**.
- [4] N. Meziane, J. G. Webster, M. Attari, and A. J. Nimunkar. Dry electrodes for electrocardiography. *Physiological Measurement*, 34(9):R47–R69, **2013**.
- [5] A. J. Bard and L. R. Faulkner. *Electrochemical methods: fundamentals and applications*. Wiley, New York, 2nd ed edition, **2001**.
- [6] E. Barsoukov and J. R. Macdonald, editors. *Impedance spectroscopy: theory, experiment, and applications*. Wiley-Interscience, Hoboken, N.J, 2nd ed edition, **2005**.
- [7] D. Loveday, P. Peterson, and B. Rodgers. Evaluation of organic coatings with electrochemical impedance spectroscopy. *JCT coatings tech*, 8:46–52, **2004**.
- [8] American National Standards Institute and Association for the Advancement of Medical Instrumentation. *Disposable ECG electrodes*. Association for the Advancement of Medical Instrumentation, Arlington, VA, **2000**. OCLC: 47749236.
- [9] M. E. Spira and A. Hai. Multi-electrode array technologies for neuroscience and cardiology. *Nature Nanotechnology*, 8(2):83–94, **2013**.
- [10] M. Tykocinski, Y. Duan, B. Tabor, and R. S. Cowan. Chronic electrical stimulation of the auditory nerve using high surface area (HiQ) platinum electrodes. *Hearing research*, 159(1):53–68, **2001**.
- [11] P. Leleux, C. Johnson, X. Strakosas, J. Rivnay, T. Hervé, R. M. Owens, and G. G. Malliaras. Ionic Liquid Gel-Assisted Electrodes for Long-Term Cutaneous Recordings. *Advanced Healthcare Materials*, 3(9):1377–1380, **2014**.
- [12] P. T. Kissinger and W. R. Heineman. Cyclic voltammetry. *J. Chem. Educ*, 60(9):702, **1983**.
- [13] M. B. Rooney, D. C. Coomber, and A. M. Bond. Achievement of Near-Reversible Behavior for the $[\text{Fe}(\text{CN})_6]^{3-/4-}$ Redox Couple Using Cyclic Voltammetry at Glassy Carbon, Gold, and Platinum Macrodisk Electrodes in the Absence of Added Supporting Electrolyte. *Analytical Chemistry*, 72(15):3486–3491, **2000**.
- [14] G. W. Hastings. *Definitions in biomaterials: progress in biomedical engineering 4*, Editor: DF Williams. Elsevier, Amsterdam, 1987, pp viii+ 72, US \$63.50. Elsevier, **1989**.

Improving skin-electrode interface with conducting organic materials

Most of the work to improve the performance of an electrode has to be done at the interface with the skin. The skin-electrode interface is subject to motion which can increase noise level of the recording signal. Different materials can be used to modify and improve the usual interface. In this chapter, we first suggest to work with conducting polymers, coated on top of the surface of electrodes, to improve electrode/skin interfaces. Then, in addition to conducting polymers, we present the use of ionic liquid-based gel to replace the common conducting hydrogels in electrodes for cutaneous applications. The interests of these two approaches are evaluated.

Data presented in this chapter were included in the following publications :

M. Isik, T. Lonjaret, H. Sardon, R. Marcilla, T. Herve, G. G. Malliaras, E. Ismailova, and D. Mecerreyes, *Cholinium-based ion gels as solid electrolytes for long-term cutaneous electrophysiology*, J Mater Chem C, 3, 8942–8948 (2015)

S. Takamatsu, T. Lonjaret, D. Crisp, J.-M. Badier, G. G. Malliaras, and E. Ismailova, *Direct patterning of organic conductors on knitted textiles for long-term electrocardiography*, Sci. Rep. 5, 15003 (2015)

M. Papaiordanidou, S. Takamatsu, S. R. Mazinani, T. Lonjaret, A. Martin, and E. Ismailova, *Cutaneous Recording and Stimulation of Muscles Using Organic Electronic Textiles*, Adv. Health. Mater., doi: 10.1002/adhm.201600299 (2016)

3.1 Introduction on organic electronics

3.1.1 Organic materials

Organic materials are chemical species made of at least two different chemical elements, one of which is carbon. Only few elements can be associated with carbon in organic compounds: hydrogen (*H*), oxygen (*O*), nitrogen (*N*), sulfur (*S*), silicium (*Si*) and halogen elements. A covalent bond is the share of two valence electrons by two atoms. Carbon atoms are linked together by directional covalent bonds almost indefinitely. Thus, long and various covalent chains characterize organic molecules. Two categories of organic compounds can be distinguished, depending on their size and weight: the small molecules and the polymers. In opposition, inorganic compounds are any other compounds, mostly made of ionic bonds. Allotropic forms of carbon, such as graphite or diamonds, are only composed of carbon atoms and so are classified as inorganic compounds. Some simple carbon compounds, such as carbon oxides (*CO*, *CO*₂...) and inorganic carbonates and bicarbonates are also classified as inorganic compounds, following a European Union directive [1].

3.1.2 Conducting polymers

Polymers are macro-molecules made of a sequence of polymerized (i.e. covalently bonded) subunits, also called small molecules or monomers. These polymers can have a natural origin (such as the cellulose, main constituent of wood) or can be made via synthetic reactions (as the polystyrene, one of the most widely used plastic for packaging). Conductive polymers, also called intrinsically conducting polymers, are able to conduct electricity. The electronic structure of semiconducting organic materials were first introduced in the 1960s [2, 3] with polypyrrole and anthracene molecules. Polyacetylene is a good example to study the conducting behavior of some polymers, as described by Shirakawa, Heeger and MacDiarmid, who won in 2000 the Nobel Prize for the discovery of conducting polymers [4]. Fig 3.1a shows the chemical representation of *trans*-polyacetylene. Most of the chemical representations omit the direct figuration of carbon and hydrogen atoms, as in Fig 3.1b and a polymer can also be represented with the monomer into brackets (Fig 3.1c). The double bond symbolize covalent bonding but it is easy to imagine an equivalent representation, as shown in Fig 3.1d. The alternation of single and double bonds is known as conjugation (such a polymer is then known as conjugated-polymer) where single and double bonds are called σ and π bonds respectively. This is similar to semi-conducting behavior. The second electron of the π bond is actually delocalized and moves almost freely without encountering resistance, thus giving to the polymer a good conductivity. Shirakawa showed that it was possible to dope the polyacetylene and then to obtain metallic properties with a massive increase of conductivity. Even if polyacetylene is not easy to process and lacks of stability, its study facilitated the development of new families of conducting polymers [5].

The main property of conducting polymers is their ease to be processed. Stable and repro-

ducible dispersions are commercially available and can be deposited as films by straightforward processes like spin coating, dip-coating, doctor-blading, ink jet-printing. This allows large-scale and low-cost fabrication of flexible devices [6]. Moreover, most of the conducting polymers can be stored for long periods in non-controlled environment without degradation. First applications of conducting polymers rose with the development of organic photoconductors for copying and printing [7]. Flexibility, low-cost and variety of families explain the omnipresence of organic materials in nowadays copier systems. Electroluminescence properties [8] of organic materials facilitated the conception of light-emitting devices such as the OLED (Organic Light-Emitting Diode) [9], which enabled the conception of the first flexible screens [10]. Conductive polymers are also very present in conception of state-of-the-art photovoltaics cells, flexible and cheaper than inorganic cells, as well as field-effect-transistor.

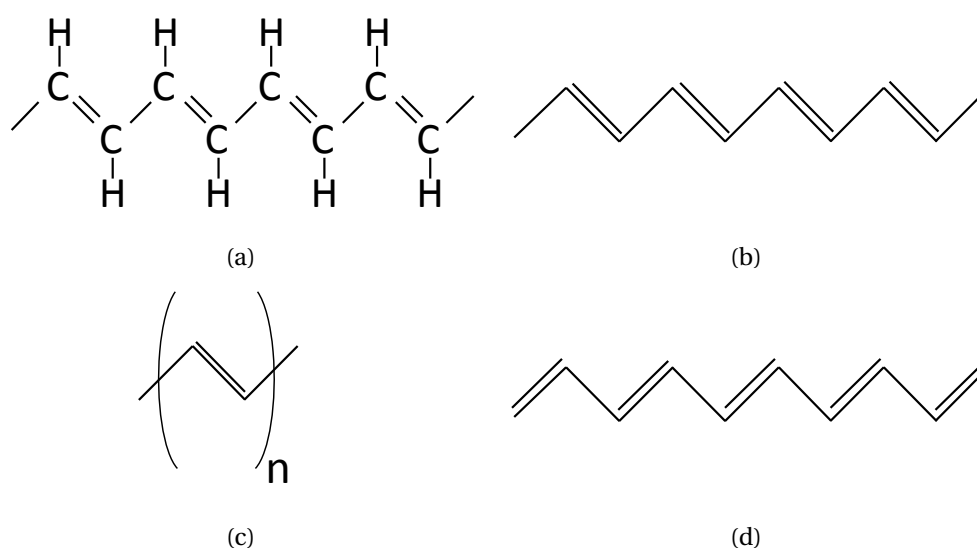


Figure 3.1 – An example of conducting polymer: *trans*-polyacetylene. (a) Lewis structure of the organic polymer. (b) Skeletal representation, omitting carbon and hydrogen atoms. (c) Short representation of the polymer with the monomer into brackets. (d) Equivalent representation of the *trans*-polyacetylene, highlighting the possibility for electrons to move along the chain.

3.1.3 Organic bioelectronics

The term “organic bioelectronics” was recently introduced by Berggren and Richter-Dahlfors [11]. It describes the coupling, which works in two directions, between organic devices (such as OLEDs, polymers electrodes, organic transistors. . .) and biological systems (cultured cells, tissues such as muscles, fluids such as blood, organites such as proteins, organs. . .) [12]. To better understand the bidirectional coupling of bioelectronics, we can imagine the interface of a futuristic ideal hand prosthesis with the arm of a patient. If the patient wants to manipulate an egg, neural information from the brain to control fingers needs to be transferred to the prosthesis. Pressure sensors from the prosthesis need to send back the information of

Chapter 3. Improving skin-electrode interface with conducting organic materials

“touching” to the brain through neurons to let the patient adapt the applied pressure. [13]. This feedback loop is only possible via a bidirectional neural-robotic, or bioelectronic, interface.

Soft nature of organic electronics facilitates the interface with living tissues [14], with better mechanical and material compatibilities with biology than “hard” electronics materials. Polypyrrole and PEDOT:PSS proved their great biocompatibilities in many studies [15, 16]. The ability of conducting polymers to conduct ions as well as electrons and holes is a big advantage to match with ion fluxes from biology. Furthermore, conjugated polymers can be functionalized by the immobilization of specific bio-agents (such as enzymes, anticoagulants. . . .) that interact with biochemical reactions [17].

Example of the biology-to-electronics interface

Biosensors are made of a biomaterial layer (with enzymes, antigens. . . .) that constitutes the recognition element, providing specificity, and of an electronic device that acts as a transducer to create a measurable signal from the recognition event. Glucose and lactate monitors are perfect examples of biosensors [18, 19]. These metabolite sensors use a specific enzyme that get oxidized with glucose or lactate in an analyte (the sample to test, blood, saliva. . . .) and then a mediator (such as ferrocene or glucose oxidase) to transfer electrons to an electrode. Organic conducting materials are then used as supports to immobilize these reacting chemical compounds and as electrodes to record the resulting signal. As explained in the following Section 3.2.1, conducting polymers has been extensively used to improve the electrode interface for better recording of electrical signals from biological origin. They facilitate the translation of ionic currents to electronic currents. The bioelectronic transducer can also be made of an OLED, with optical properties changing in accordance to recognition events [20].

Example of the electronics-to-biology interface

In the reverse way, biological events can be controlled by electronics. 3D macroporous scaffolds made of conducting polymer can support cell growth. The application of a potential to the scaffold offers the possibility to better control the conformation of adsorbed proteins as well as cell adhesion [21]. It is already possible to control proliferation and differentiation of cells [22] and then to imagine the future of wound healing with tissues repairing themselves. In another field, our team recently showed the possibility to control epileptic activity of brain slices with organic electronic ion pumps, by the very local delivery of drugs, contained in a reservoir, induced by an applied potential [23].

3.2 The use of conducting polymers for electrophysiology

3.2.1 State-of-the-art on the use of conducting polymers to improve electrode interface

An improved interface for electrophysiology

The coating of an electrode with conducting polymers grants lower impedance to the interface, which is a great advantage to improve recorded signals quality. Two elements can explain this decrease. Thanks to ability of conducting polymers to conduct ions, the biotic/abiotic interface is improved; ions can penetrate inside the conducting polymer and increase the effective surface area of contact between electrode and media [24, 25]. Moreover, the surface of the polymer films is slightly structured, which again means that the effective surface area with the media is increased and so does the capacitance effect [26, 27]. A large charge storage capacity renders polymer-coated electrodes very efficient for electro-stimulation [28, 29]. Finally, the flexibility of conducting polymers facilitates their conformability to the different organs for accurate local recordings. However, other inorganic thin diamond- or graphene-based materials, often micro- or nano-structured, can provide biocompatibility, flexibility, improved interface and deposition ease properties similar to conducting polymers, and then are their first competitors [30, 31, 32].

Polypyrrole and PEDOT-coated electrodes

Two conducting polymers are mainly coated on electrodes for electrophysiology. Polypyrrole is usually electrochemically deposited on metal electrodes [33, 15, 28]. In electropolymerization, current is driven through a three-electrode cell (see Section 2.2.1) with a working electrode immersed in an electrolyte containing the monomer and counterions. As a result, monomers form polymer chains including counterions. The resulting coating is stable in water. Recently, it was shown that another conducting polymer, PEDOT could provide better impedance and above all, better long-term stability. Poly(3,4-ethylenedioxythiophene) (PEDOT) is a conjugated polymers that carries positive charge. Doped PEDOT, for example with poly(styrene sulfonate) (PSS), provides high hole conductivity ($> 1000 \text{ S cm}^{-1}$) [34]. A PEDOT layer can be deposited on electrodes by polymerization of the EDOT monomer with vapor phase polymerization (VPP) [35] or electropolymerization [26] techniques. PEDOT:PSS is also commercially available as a dispersion and this facilitates its coating with various methods, which need to be following by a hard-bake. Blau et al. proposed to design micro-channels in poly(dimethylsiloxane) (PDMS) and then to coat them with PEDOT:PSS [36]. Khodagholy et al. developed a process based on photolithography, which makes possible the spin-coating of PEDOT:PSS on an etched electrode site and then to remove a sacrificial layer to get rid of the excess of polymer coating [37]. It is also possible to cast the solution usign doctor-blade, as well as to draw accurate pattern with ink-jet printing [38]. To form a thick layer of PEDOT:PSS, the conducting polymer dispersion can be drop-casted [39, 40] or spray-casted.

Great performances in various applications

Thanks to their excellent biocompatibility and ion/electron transduction, conducting polymers coat most of state-of-the-art electrodes for *in vivo* experiments with neural probes [41, 42]. They facilitate long-term recordings with minimal immune response [26]. Polypyrrole as well as PEDOT are used on silicone shanks which penetrate the brain to record neurons activities [15, 43]. Taking advantage of conformability properties of polymers, PEDOT:PSS electrodes are successfully able to record LFPs and even action potentials from an ECoG array [44]. Thanks to a thick layer of PEDOT:PSS, dry coated-electrodes are also able to record electrophysiological activity from the skin, such as ECG [45], EMG [40] or EEG [39].

3.2.2 Fabrication processes and characterization of dry PEDOT:PSS electrodes

Presentation of PEDOT:PSS

PEDOT:PSS is a mixture of two electrically charged polymers, also called ionomers. The sodium polystyrene sulfonate carries a negative charge. The other component, poly(3,4-ethylenedioxythiophene), is a polythiophene-based conjugated polymer that carries positive charges. PSS is doping PEDOT chains to improve the conductivity of the whole. Fig 3.2 shows the chemical structure of the PEDOT:PSS. PEDOT is a hole conductor by the ion transport is far to be negligible when the polymer is hydrated. Recently, Rivay et al. studied how the structure of a PEDOT:PSS layer facilitate the high ionic conductivity that characterize this polymer [25].

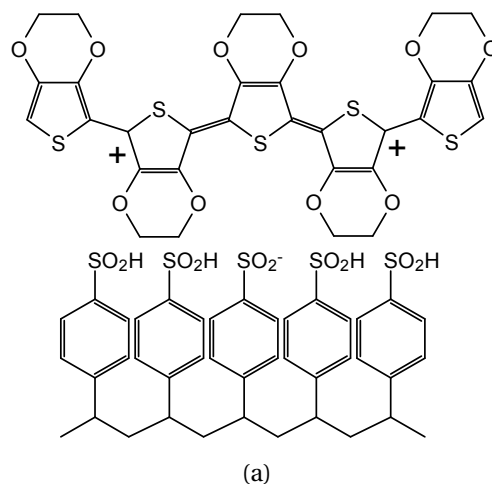


Figure 3.2 – Chemical structure of PEDOT:PSS.

Fabrication process of PEDOT:PSS solution

The PEDOT:PSS solution is prepared by mixing an aqueous dispersion (19 ml, Clevios PH 1000 from Heraeus Holding GmbH) with ethylene glycol (1 ml) and dodecyl benzene sulfonic

3.2. The use of conducting polymers for electrophysiology

acid (50 μl), to improve conductivity and enhance film formation. The resulting solution is sonicated for 40 min, then (3 glycidyloxypropyl) trimethoxysilane (1 wt%) is added to prevent delamination of the film. The solution is finally sonicated for another 5 min.

Coating methods of PEDOT:PSS

To form a homogeneous and solid PEDOT:PSS film on top of a substrate, the PEDOT solution needs to be spin-coated. Spin-coating speed and time define the thickness of the film, for instance a speed of 3000 rpm for 90 s allows to target a thickness of 90 nm. The film is then soft-baked at 90° for 90 s. An hour long hard-baking at 125°C is the last step of PEDOT:PSS deposition. This solution is compatible with a fabrication process by photolithography in clean room environment and facilitate the coating of a PEDOT:PSS layer with a defined thickness. In this thesis, we also used drop-casting, deep-coating and brushing techniques, followed by hard-baking, to cover the active areas of our electrodes.

Characterization of dry electrodes with a PEDOT:PSS interface

As defined in Section 2.2.2, an impedance measurement was performed with a potentiostat (Autolab equipped with FRA module, Metrohm B.V.) to highlight properties of the addition of a PEDOT:PSS layer on top of an electrode. In Fig 3.3a, orange and red curves show impedance measurements performed on bare gold electrodes with a diameter of 1 mm and 8 mm, respectively. Cyan and blue curves show results from PEDOT:PSS-coated gold electrodes with a diameter of 1 mm and 8 mm, respectively. Bare gold electrodes present typical behavior of polarizable (i.e. capacitive) electrode below 10 kHz signals: phase is close to 90° and impedance exponentially increases. If a fit with the R(RC) model developed in Section 2.1.5 is applied to these electrodes, high interface resistance (4.48 M Ω and 1.11 M Ω for the 1 mm and 8 mm electrodes respectively) explain why only few electrons can cross the interface.

For both sizes, the addition of a drop-casted PEDOT:PSS layer highly decreases the impedance of gold electrodes. They show almost pure non-polarizable behavior above 10 Hz (which is low enough for many electrophysiological signals) and still very low impedance (up to 3 order of magnitude compared to bare gold electrodes) at below 10 Hz.

The CV presented on Fig 2.2.2 highlights the capacitive properties difference between bare gold electrode and PEDOT:PSS-coated gold electrode of same size (8 mm diameter). Because the electrolyte is NaCl, so neutral for redox reactions, no oxidation or reduction peak is visible for Gold and PEDOT-coated electrodes (still, small peaks are visible on PEDOT-coated electrode, certainly due to some impurities). By integrating the cathodic current over one cycle of CV, the charge injection capability can be found. For the bare gold electrode it is 0.012 mCcm⁻² whereas the charge injection capability of the PEDOT-coated electrode is 39.6 mCcm⁻², conforming with results from other studies [46, 29]. This shows the high performance of PEDOT:PSS coating for stimulation electrode.

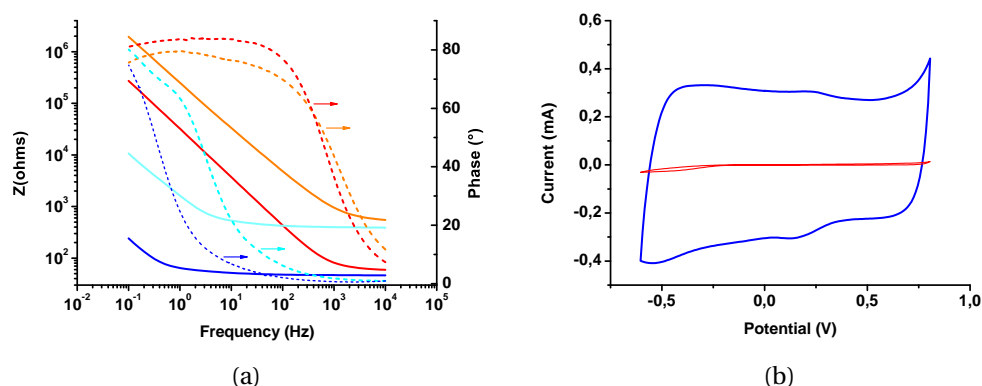


Figure 3.3 – **Impedance and CV characterization of PEDOT:PSS electrodes.** Results are displayed for 50 mm² electrodes coated with bare gold (in red) and gold + PEDOT:PSS (in blue) and for 0.8 mm² electrodes coated with bare gold (in orange) and gold + PEDOT:PSS (in cyan). The electrolyte was a 0.1 M NaCl solution. (a) Impedances are plotted with full lines and phases with dash lines. (b) CV was performed for the 8 mm diameter electrodes, at a sweep rate of 0.5 V s⁻¹.

3.3 The use of ionic liquids for electrophysiology

3.3.1 Introduction on ionic liquids

Definition and properties of ionic liquids

Ionic liquids (ILs), also called Room Temperature Ionic Liquids (RTILs) or room temperature molten salts, are ionic compounds with negligible vapor pressure and evaporation rate [47]. They are free of any molecular solvent and are liquid at room temperature or below. The first truly ionic liquid, ethylammonium nitrate, [EtNH₃][NO₃], was discovered by Walden in 1914 [48], but ionic liquid started to be extensively studied after the 1970s. Quickly, ionic liquids with groups combined with imidazolium cations proved their great performances in terms of melting point and electrochemical stability [49]. Complete reviews devoted to RTILs can be found in the literature [47, 50, 51, 52, 53]. They are nowadays a key tool for emerging technologies using electrochemical reactions, since they allow the electrodeposition of water-sensitive metals or semi-conductors at low temperature [54, 55]. Thanks to their remarkable large electrochemical window, RTILs are also perfect solvents for the electrodeposition of reactive elements such as tantalum for the coating of biomedical implants [56]. In the actual context of the fast growing development of “green” technologies, lithium batteries are a key solution to store energy and power systems. Because they are non-flammable, ionic liquids could be a future common and safe electrolyte for these batteries [57, 58], to replace the conventional flammable and volatile electrolyte which can lead to thermal runaway and non-wanted explosion reactions. Other applications of RTILs are in the field of bioscience. More specifically, they are used to replace the traditional media for enzymatic reactions or to

dissolve biomaterials. For instance, the properties of ionic liquids allow them to be a good solvent for the dissolution of cellulose, the most common polymer found in nature used as “green” polymer for fabricating new attractive materials [59].

Toxicity of Ionic Liquids

Although ionic liquids were initially defined as green solvents, one of the most actual concerns regarding ionic liquids is their toxicology [60]. It is widely accepted that among all the different types of ionic liquids, some of them are toxic and hence should not be released to the environment, while some others are not toxic [61, 62]. As a general rule, even though there is a certain contribution from the anion [63], the toxicity of the ionic liquid is largely determined by the headgroup of the cation [64, 65, 66].

3.3.2 Ion gels as solid electrolytes

Integration into a gel matrix

Ionic liquids are usually immobilized in gels to provide them solid-like mechanical properties while preserving their ionic conductivity and other unique properties [67, 68]. Ion gels are already introduced as solid electrolytes in different devices such as batteries and supercapacitors [69], fuel cells [70], electrochemical and biochemical sensors [71], actuators [72], or drug delivery systems [73]. Compared to solids, ionic liquids lack mechanical properties such as persistent structure and mechanical integrity. This absence can be supplied by mixing them with polymeric components. The polymer network acts then like a sponge filled of ionic liquid with comparable ionic conductivity as the neat ionic liquid. It is worth to note that ion gels can be prepared using different types of polymeric matrices such as cellulose, poly(ethylene oxide), or even inorganic siloxane networks made by sol-gel chemistry.

However, poly(ionic liquid) networks are usually preferred due to their excellent compatibility with the free ionic liquids preventing their future leaching problems. For instance, polymer ionic liquids have been successfully used as polyelectrolyte in supercapacitors and batteries [74, 75] or fuel cells [76].

Ion gels for cutaneous electrodes

As we explained in previous Section 2.1.3, a gel improves the contact between the skin and commonly used medical electrodes. Usually, it is a hydrogel mixed with NaCl or KCl solution. The main problem for long-term recordings is coming from leakage of the gel (that can involve a short-cut between 2 nearby electrodes) and from the evaporation of water. Moreover, in some case of EEG studies, this gel has to be added manually to each cup electrode. The presented ion gels could solve these problems. They can be integrated during fabrication of the electrodes and they do not leak or dry out. The first presentation of such an ion gel

integrated on top of the active area of a cutaneous electrode was made by Leleux et al. in 2014[77]. By regularly measuring the impedance of gel-assisted electrodes in constant contact with the skin of a human volunteer, it was proven that long-term (more than 3 days) recordings were possible, unlike recordings from medical electrodes.

3.3.3 Synthesis and integration of ion gels on electrodes

In a first time, we used the ion gel conceived by Leleux et al. [77]. The IL gel was prepared by mixing the IL (1-ethyl-3-methylimidazolium ethyl sulfate) and the polymer poly(ethylene glycol) diacrylate (30% of the total weight solution). The latter facilitates the formation of a matrix encapsulating the ionic liquid. We then added 0.3% of the photoinitiator 2-hydroxy-2-methylpropiophenone (see Fig 3.4). We mixed until no phase separation was visible. For an electrode with a diameter of 8 mm, ten microliters of the solution was pipetted onto the electrode. Finally, the gel was cross-linked using exposure to UV light for approximately 1 min, directly on top of the electrode to improve the attachment. As a result, the gel-assisted electrode can be stored as it is without too much constraints, and the gel can be reused weeks after. Results obtained from this gel are presented on Sections 5.3 and 5.4.

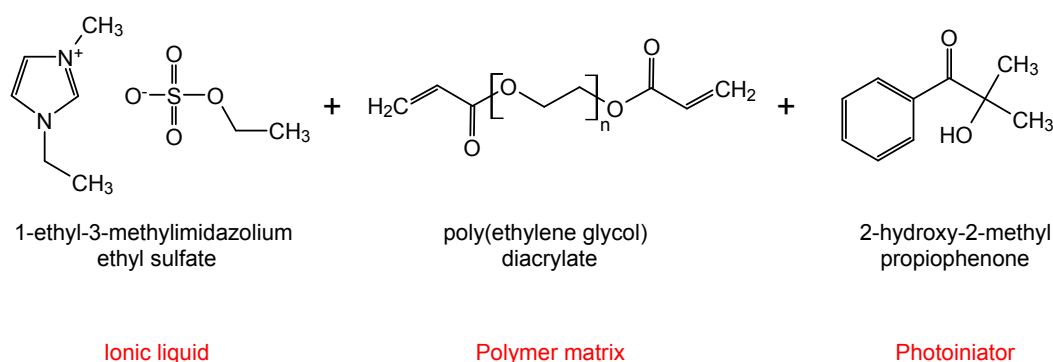


Figure 3.4 – 1-ethyl-3-methylimidazolium ethyl sulfate ion gel preparation. General pathway for the preparation of the ion gel.

3.4 Introduction of a novel biocompatible ion gel for electrodes

3.4.1 Biocompatibility of cholinium-based ionic liquids

Choline based ionic liquids seem to present a promising low toxicity[78, 79] but cholinium family is even more favorable. Cholinium refers to trimethylethanol ammonium cation and it is an essential micronutrient assisting several biological functions. For this reason, cholinium cation-based ionic liquids are known also as bio-ionic liquids due to their biocompatibility, biodegradability and low toxicity[80, 81]. Since the gel is continuously in contact with the skin for cutaneous applications, these properties made a cholinium-ionic liquid-based gel promising.

3.4.2 Chemical materials

2-Dimethylaminoethyl methacrylate (98%, Aldrich), 2-bromoethanol (95%, Aldrich), cholinium hydroxide (80% by weight in methanol, Aldrich), lactic acid (85% solution in H₂O, Aldrich), 2-hydroxy-2-methyl propiophenone (97%, Aldrich), ethyl acetate (99.5%, Aldrich), methanol (99%, Aldrich) were all reagent grade and used without further purification.

3.4.3 Preparation of the ion gel

In this section, we report the preparation and the characterization of cholinium-based ion gels (with different ratio of ionic liquid content) that will be used as solid electrolytes for cutaneous electrophysiology.

Synthesis of the 2-cholinium lactate methacrylate monomer and cholinium lactate IL has been explained in detail in previous studies[82, 83]. Ion gels were prepared through photopolymerization of the ionic liquid monomer (cholinium lactate methacrylate) with the ionic liquid (cholinium lactate) and a small amount of a commercially available crosslinker such as ethylene glycol dimethacrylate. The amount of free IL with respect to the polymer matrix was varied from 0 wt% to 60 wt%. Fig 3.5 shows a representation of the preparation method of the ion gels. Calculated amounts of IL, IL monomer and ethylene glycol dimethacrylate crosslinker were mixed in a vial. Appropriate amount (1.5% by weight *vs* monomer) of photoinitiator was introduced before exposure to UV light. Dymax UVC-5 conveyor belt system with 800 mWcm⁻² intensity operating at a wavelength of 365 nm was used for photopolymerization. Photopolymerization is a common technique to produce polymers at room temperature and short reaction times. Sample to lamp distance was 10 mm and the belt speed was fixed at 1 mm⁻¹. Five repetitive cycles were applied to achieve a full photopolymerization. The mixture was casted into a mold, photopolymerized and then gently removed from the molds to be characterized. The ion gels were coded as cholinium IG-0, IG-10, IG-20, IG-30, IG-40, IG-50 and IG-60 where the number represents the weight percentage of the free ionic liquid. One of the important parameters regarding the synthetic reproducibility and proper design of ion gels through photopolymerization is the conversion of the monomer to form the polymer matrix. Uncontrolled polymerization will yield non-reproducible ion gels which will result in gels with incoherent properties. The conversion of the polymerization was controlled by ¹H NMR and ATR-FTIR spectroscopy. The crosslinked structures of ion gels prevent their dissolution and make it impossible to obtain direct ¹H NMR spectra from solution. Therefore, to evaluate non-polymerized content of the monomer, the ion gels were immersed into D₂O for 1 day. The soluble fraction was then analyzed by ¹H NMR spectroscopy. Since the cholinium lactate methacrylate ionic liquid monomer is highly soluble in water, any unreacted monomer will be dissolved in the aqueous phase. The signals associated with the reactive methacrylic group disappeared for all the ion gel compositions after exposure to UV light, indicating the complete photopolymerization of the monomer. The further studies using ATR-FTIR spectroscopy affirm the full conversion of the monomer in solid ion gel samples.

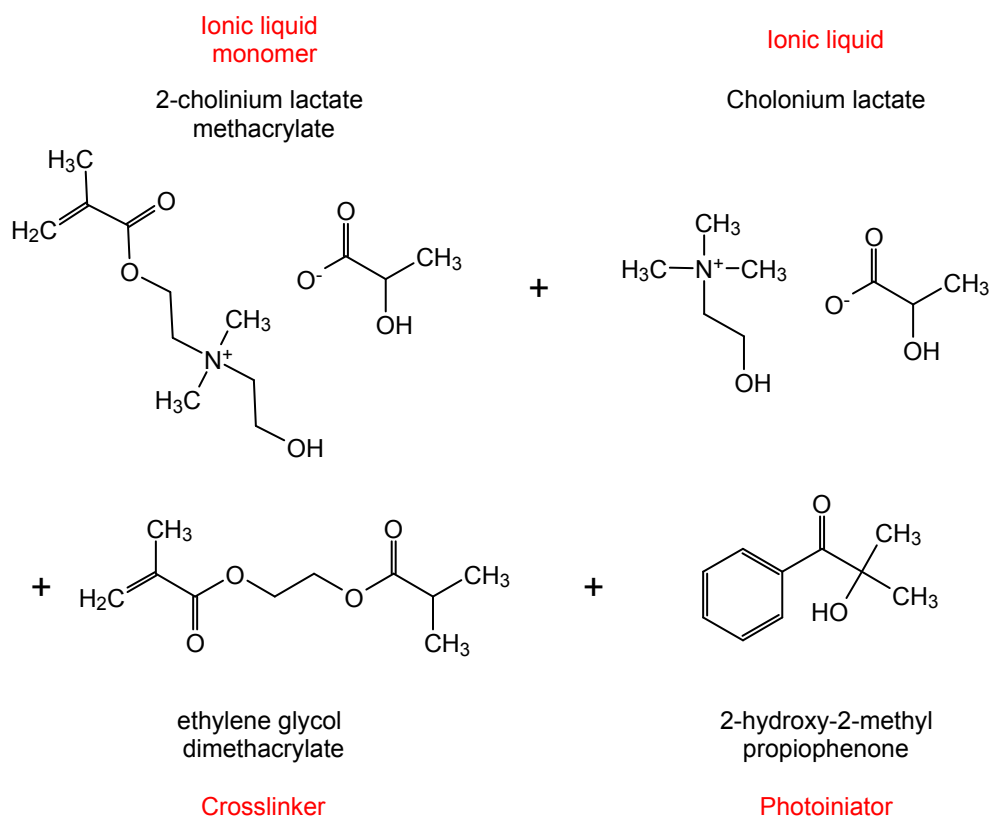


Figure 3.5 – **Cholinium lactate ion gel preparation.** General pathway for the preparation of the ion gel.

3.4.4 Characterization

Rheological properties of the ion gels

The mechanical properties of ion gels are one of the most important properties for their practical application as part of the electrode in contact with the skin. This interface has to be soft to conform to skin surface and hair, as well as flexible to absorb mechanical shocks. Therefore, rheological properties of the ion gels were analyzed by frequency sweep measurements. Elastic (G') and viscous (G'') moduli of the ion gels were examined as a function of angular frequency at 25°C as shown in Fig 3.6 for 3 different ion gel formulations. Ideal gels display almost purely elastic response where the elastic modulus is higher than the viscous modulus and is independent of angular frequency. For the sample that does not contain any free IL (IG-0), highest elastic modulus (G') was obtained which is around 4.08 MPa and is approximately four times greater than the loss modulus (G'') throughout the entire frequency range. Both G' and G'' were frequency independent until 1 rads^{-1} and after there was a very weak dependency. This confirms that the sample was a gel network of rubbery nature. As expected, introduction of free ionic liquid into the polymer network acts as plasticizer and reduces the mechanical strength of the ion gels as revealed by the decreased G' and G''

3.4. Introduction of a novel biocompatible ion gel for electrodes

values. With the introduction of 10% IL into the structure, the G_0 value decreased to 0.83 MPa at 100 rad s^{-1} . The G_{00} was lower than G_0 over the entire angular frequency range and both moduli were slightly frequency dependent indicating that the material behaves as a soft solid material. Although increasing the IL content further reduced the elastic modulus down to 0.55 MPa, G_{00} was lower than the G_0 over the entire angular frequency range and dependence of both moduli was similar to the previous formulation indicating a soft solid ion gel. The gradual decrease of both moduli was observed while increasing free IL content in the ion gel formulations. All the ion gels until 50% IL displayed similar frequency behavior over the entire measured angular frequency range. In all cases, the elastic moduli of the ion gels were higher than loss moduli suggesting that the elastic components of the dynamic moduli were greater. The ion gel IG-60 is the sample that contained the highest amount of free IL and displayed the lowest mechanical property with respect to the samples containing less IL. At high angular frequencies, the G_0 and G_{00} values were almost the same, around 0.02 MPa. The G_{00} became higher than G_0 over the entire lower angular frequency range and both moduli were frequency dependent indicating that the sample was a pregel. These findings indicated the gel type behavior of the ion gels due to the crosslinked poly(ionic liquid) matrix blended with ionic liquid. All in all, these cholinium ion gels presented soft solid and elastic behaviors which are ideal mechanical properties for the application as cutaneous electrodes.

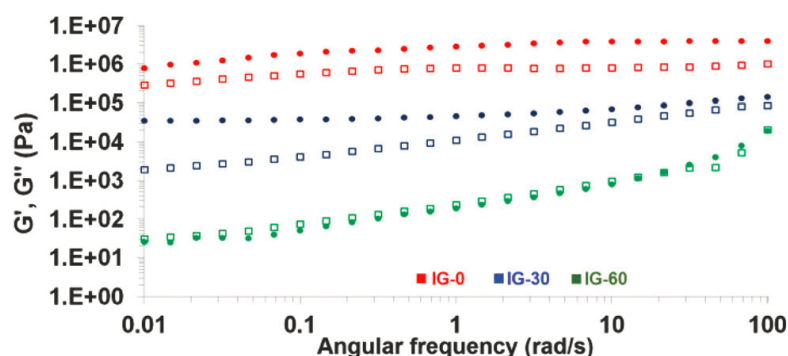


Figure 3.6 – **Rheological properties of cholinium lactate ion gel.** Frequency dependences of dynamic storage G' (circular symbols) and loss G'' moduli (square symbols) of the ion gels.

Thermal properties of the ion gels

Thermal properties of the ion gels were analyzed by differential scanning calorimetry (DSC) and thermogravimetric analysis (TGA). DSC signals are provided in Fig 3.7a. The glass transition temperature (T_g) of the homopolymer of 2-cholinium lactate methacrylate is around -50°C [82]. Similarly, DSC analysis of the sample IG-0 revealed a T_g around -40°C which is slightly higher due to the crosslinked nature of the sample. Introduction of free IL acts as a plasticizer to the polymer matrix, decreasing the T_g of the ion gel. Therefore, T_g values gradually decrease with the increasing IL content. The lowest glass transition being found was around -70°C for IG-60 in which 60% free IL content was blended. Additionally, the change

in the glass transition temperature with changing ionic liquid content is provided in Fig 3.7b. As clearly seen from the figure, addition of ionic liquid plasticizes the material resulting in a gradual decrease of the glass transition temperature with increasing amount of free ionic liquid in the polymeric matrix. Low T_g behaviour of ion gels provides a broad operational window from -70°C to higher temperatures. To determine the thermal stability of ion gels, TGA measurements were carried out. The TGA signals are provided in Fig 3.7c, d. As reported in literature, cholinium based ionic liquids display onset temperatures starting from 170°C [81]. For the ion gels composed of cholinium cation combined with lactate anion, the trend observed for the thermal stabilities were similar to the glass transition temperatures. Although the onset temperatures were similar to one another for all the ion gel formulations at around 180°C , the weight loss after that point were distinctive as it can be seen from Fig 3.7d. Samples containing higher amounts of free IL displayed a sharper weight loss compared to the samples with low IL contents. The sample IG-0 showed a decomposition temperature (50% weight loss) at 292°C and this temperature gradually dropped down to 250°C for IG-60. To better demonstrate the change in the decomposition temperature of the ion gels with changing ionic liquid content, Fig 3.7e is provided. As clearly seen, introduction of ionic liquid into the solid matrix gradually decreases the decomposition temperature as the amount of ionic liquid increases. To summarize, the ion gels showed in general glass transition temperatures way below room temperature and good thermal stability up to 200°C which provides a flexible operational window.

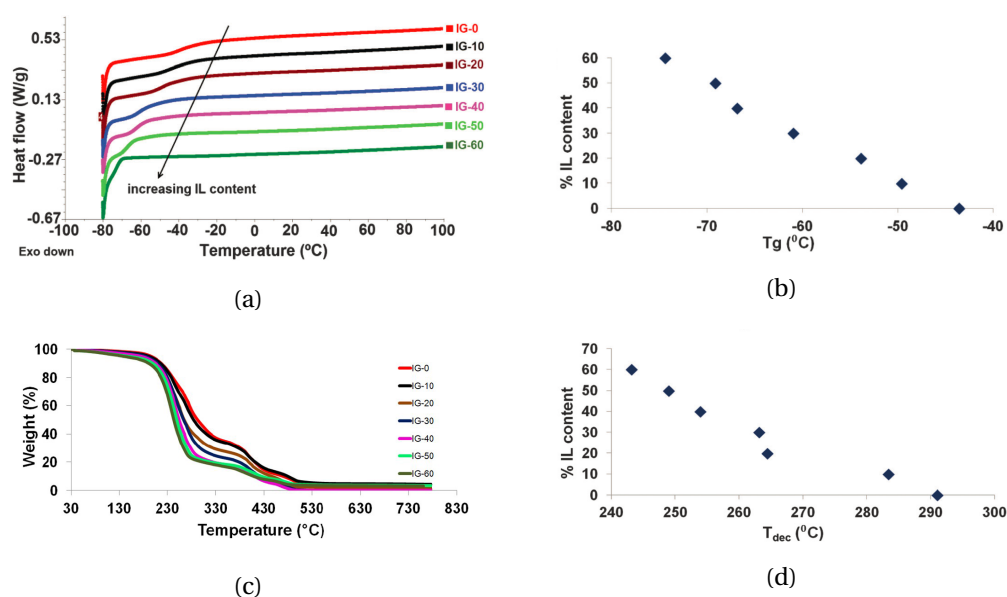


Figure 3.7 – **Thermal properties of cholinium lactate ion gel.**(a) Differential scanning calorimetry (DSC) curves of the ion gels containing different amounts of IL. (b) Glass transition temperature change *vs* free ionic liquid %. (c) Thermal gravimetric analysis (TGA) profiles of the cholinium ion gels. (d) Decomposition temperature *vs* free IL content in the gels (the temperature at which 50% weight loss was observed and was taken as the decomposition temperature).

Electrical properties of the ion gels

Due to the presence of the free IL embedded in the polymer matrix, ion gels present higher ionic conductivities than other solid polymer electrolytes[75]. Therefore, the ionic conductivity of an ion gel becomes one of the most characteristic properties and is usually responsible for its good performance in the different device application. For this reason, the ionic conductivities of ion gels were determined by impedance spectroscopy from 0°C to 110°C as shown in Fig 3.8. As expected, the ionic conductivities change dramatically with the introduction of free ionic liquid and its weight content. The slight curvature observed in the Arrhenius plot is in good accordance with the Vogel–Tamman–Fulcher (VTF) model which is commonly seen in amorphous polymer electrolytes due to the amorphous nature of the polymer matrix. The conductivity values were gradually increasing with the increasing free ionic liquid amount in the ion gel. The ionic conductivity reached values between 10^{-8} S cm⁻¹ for the pure poly(ionic liquid) and 10^{-3} S cm⁻¹ for ion gels having 60 wt% of free IL. Values range from 10^{-8} S cm⁻¹ at 20°C to 10^{-4} S cm⁻¹ at 110°C for the sample that does not contain any free IL. When 20 wt% of cholinium lactate is introduced into the ion gel, the ionic conductivity at 20°C was 10^{-6} S cm⁻¹ which gradually increased to 10^{-3} S cm⁻¹ at 110°C. As expected, the highest ionic conductivity values were obtained for the ion gel which contained 60 wt% free ionic liquid IG-60, values ranging from 10^{-3} S cm⁻¹ at 20°C to 10^{-2} S cm⁻¹ from 20°C to 110°C, respectively.

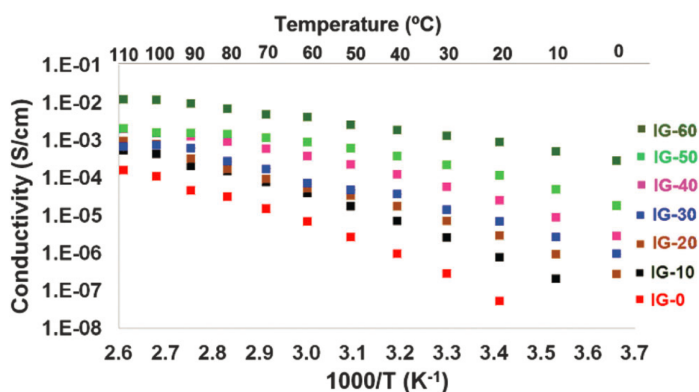


Figure 3.8 – **Electrical properties of cholinium lactate ion gel.** Ionic conductivity of the ion gels from 0°C to 110°C.

Long-term stability of the ion gels

It is worth to mention that the ion gels are composed of water soluble ingredients. Therefore, direct exposure of the ion gels to water or excessive sweat will result in loss of gel integrity. However, the exposure of the ion gels to environmental humidity does not affect their integrity. The % weight gain due to moisture uptake was limited up to 4% and did not cause any integrity issues of the gels during the evaluated time period, as shown in Fig 3.9. The water uptake from the environment was more important for the ion gels containing higher amount of free ionic liquid.

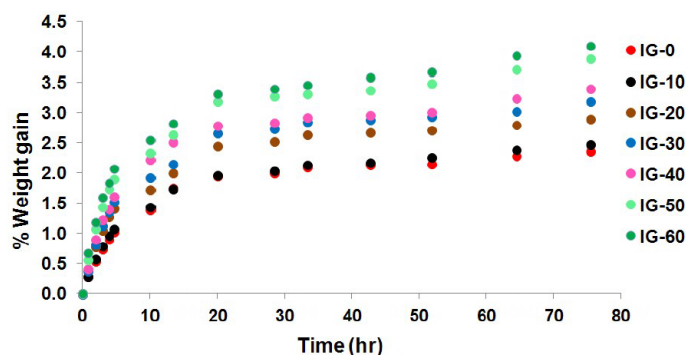


Figure 3.9 – [Long-term stability of cholinium lactate ion gels and water absorption. This graph represents % weight gain of the ion gels when they are left at ambient humidity. The ion gels were left at ambient temperature (24°C) having relative humidity values set between 60-70%. Environmental humidity seems to not affect the integrity of the ion gels. The water uptake was evaluated gravimetrically over 80hrs. We observe that the water uptake was more important for the ion gels containing higher amount of free ionic liquid. The highest % weight gain being around 4.

3.4.5 Discussion

New cholinium-based ion gels were synthesized by photopolymerization in less than two minutes. The ion gels showed mechanical properties of an elastic gel soft solid and low glass transition temperatures and thermal stability. As an important property, the ion gels showed values of ionic conductivity values at 20°C up to 1 mS cm^{-1} . It can be directly polymerized on top of a cutaneous electrode and be used later. These properties make the cholinium-based ion gel good candidates to be used as the electrolytic interface with the skin in transcutaneous electrophysiology. However, more experiments would be needed to compare properties of this cholinium-based ion gel with hydrogels contained in commercial medical electrodes. On top of that, full cutaneous biocompatibility should be run before to consider commercialization.

3.5 Bibliography

- [1] Limitation of emissions of volatile organic compounds due to the use of organic solvents in certain activities and installations - <http://eur-lex.europa.eu/legal-content/en/all/?uri=celex:31999l0013>.
- [2] R. McNeill, R. Siudak, J. H. Wardlaw, and D. E. Weiss. Electronic conduction in polymers. I. The chemical structure of polypyrrole. *Australian Journal of Chemistry*, 16(6):1056–1075, **1963**.
- [3] M. Pope, H. Kallmann, and J. Giachino. Double-Quantum External Photoelectric Effect in Organic Crystals. *The Journal of Chemical Physics*, 42(7):2540, **1965**.
- [4] H. Shirakawa, E. J. Louis, A. G. MacDiarmid, C. K. Chiang, and A. J. Heeger. Synthesis of

- electrically conducting organic polymers: halogen derivatives of polyacetylene, (CH)_x. *Journal of the Chemical Society, Chemical Communications*, (16):578–580, **1977**.
- [5] M. Geoghegan and G. Hadziioannou. *Polymer Electronics*. Oxford University Press, Oxford, 1st edition, **2013**.
- [6] Y. Diao, B. C.-K. Tee, G. Giri, J. Xu, D. H. Kim, H. A. Becerril, R. M. Stoltenberg, T. H. Lee, G. Xue, S. C. B. Mannsfeld, and Z. Bao. Solution coating of large-area organic semiconductor thin films with aligned single-crystalline domains. *Nature Materials*, 12(7):665–671, **2013**.
- [7] A. R. Melnyk and D. M. Pai. Organic photoreceptors: an overview. In *SC-DL tentative*, pages 141–154. International Society for Optics and Photonics, **1990**.
- [8] A. Bernanose. Electroluminescence of organic compounds. *British Journal of Applied Physics*, 6(S4):S54, **1955**.
- [9] C. W. Tang and S. A. VanSlyke. Organic electroluminescent diodes. *Applied Physics Letters*, 51(12):913, **1987**.
- [10] G. Gustafsson, Y. Cao, G. M. Treacy, F. Klavetter, N. Colaneri, and A. J. Heeger. Flexible light-emitting diodes made from soluble conducting polymers. *Nature*, 357(6378):477–479, **1992**.
- [11] M. Berggren and A. Richter-Dahlfors. Organic Bioelectronics. *Advanced Materials*, 19(20):3201–3213, **2007**.
- [12] R. M. Owens and G. G. Malliaras. at the Interface with Biology. *MRS bulletin*, 35, **2010**.
- [13] D. W. Tan, M. A. Schiefer, M. W. Keith, J. R. Anderson, J. Tyler, and D. J. Tyler. A neural interface provides long-term stable natural touch perception. *Science Translational Medicine*, 6(257):257ra138–257ra138, **2014**.
- [14] G. G. Malliaras. Organic bioelectronics: A new era for organic electronics. *Biochimica et Biophysica Acta (BBA) - General Subjects*, 1830(9):4286–4287, **2013**.
- [15] P. M. George, A. W. Lyckman, D. A. LaVan, A. Hegde, Y. Leung, R. Avasare, C. Testa, P. M. Alexander, R. Langer, and M. Sur. Fabrication and biocompatibility of polypyrrole implants suitable for neural prosthetics. *Biomaterials*, 26(17):3511–3519, **2005**.
- [16] D. Khodagholy, T. Doublet, P. Quilichini, M. Gurfinkel, P. Leleux, A. Ghestem, E. Ismailova, T. Hervé, S. Sanaur, C. Bernard, and G. G. Malliaras. In vivo recordings of brain activity using organic transistors. *Nature Communications*, 4:1575, **2013**.
- [17] B. Garner, A. Georgevich, A. J. Hodgson, L. Liu, and G. G. Wallace. Polypyrrole-heparin composites as stimulus-responsive substrates for endothelial cell growth. *Journal of Biomedical Materials Research*, 44(2):121–129, **1999**.

Chapter 3. Improving skin-electrode interface with conducting organic materials

- [18] G. Scheiblin, A. Aliane, X. Strakosas, V. F. Curto, R. Coppard, G. Marchand, R. M. Owens, P. Mailley, and G. G. Malliaras. Screen-printed organic electrochemical transistors for metabolite sensing. *MRS Communications*, 5(03):507–511, **2015**.
- [19] A.-M. Pappa, V. F. Curto, M. Braendlein, X. Strakosas, M. J. Donahue, M. Fiocchi, G. G. Malliaras, and R. M. Owens. Organic Transistor Arrays Integrated with Finger-Powered Microfluidics for Multianalyte Saliva Testing. *Advanced Healthcare Materials*, 5(17):2295–2302, **2016**.
- [20] O. Hofmann, X. Wang, J. C. deMello, D. D. C. Bradley, and A. J. deMello. Towards microalbuminuria determination on a disposable diagnostic microchip with integrated fluorescence detection based on thin-film organic light emitting diodes. *Lab on a Chip*, 5(8):863, **2005**.
- [21] A. M.-D. Wan, S. Inal, T. Williams, K. Wang, P. Leleux, L. Estevez, E. P. Giannelis, C. Fischbach, G. G. Malliaras, and D. Gourdon. 3d conducting polymer platforms for electrical control of protein conformation and cellular functions. *J. Mater. Chem. B*, 3(25):5040–5048, **2015**.
- [22] C. E. Schmidt, V. R. Shastri, J. P. Vacanti, and R. Langer. Stimulation of neurite outgrowth using an electrically conducting polymer. *Proceedings of the National Academy of Sciences*, 94(17):8948–8953, **1997**.
- [23] A. Williamson, J. Rivnay, L. Kergoat, A. Jonsson, S. Inal, I. Uguz, M. Ferro, A. Ivanov, T. A. Sjöström, D. T. Simon, M. Berggren, G. G. Malliaras, and C. Bernard. Controlling Epileptiform Activity with Organic Electronic Ion Pumps. *Advanced Materials*, 27(20):3138–3144, **2015**.
- [24] E. Stavrinidou, P. Leleux, H. Rajaona, D. Khodagholy, J. Rivnay, M. Lindau, S. Sanaur, and G. G. Malliaras. Direct Measurement of Ion Mobility in a Conducting Polymer. *Advanced Materials*, 25(32):4488–4493, **2013**.
- [25] J. Rivnay, S. Inal, B. A. Collins, M. Sessolo, E. Stavrinidou, X. Strakosas, C. Tassone, D. M. Delongchamp, and G. G. Malliaras. Structural control of mixed ionic and electronic transport in conducting polymers. *Nature Communications*, 7:11287, **2016**.
- [26] K. A. Ludwig, J. D. Uram, J. Yang, D. C. Martin, and D. R. Kipke. Chronic neural recordings using silicon microelectrode arrays electrochemically deposited with a poly(3,4-ethylenedioxythiophene) (PEDOT) film. *Journal of Neural Engineering*, 3(1):59–70, **2006**.
- [27] J. Bobacka, A. Lewenstam, and A. Ivaska. Electrochemical impedance spectroscopy of oxidized poly(3,4-ethylenedioxythiophene) film electrodes in aqueous solutions. *Journal of Electroanalytical Chemistry*, 489(1–2):17–27, **2000**.
- [28] T. Nyberg, O. Inganäs, and H. Jerregård. Polymer hydrogel microelectrodes for neural communication. *Biomedical microdevices*, 4(1):43–52, **2002**.

- [29] A. A. Guex, N. Vachicouras, A. E. Hight, M. C. Brown, D. J. Lee, and S. P. Lacour. Conducting polymer electrodes for auditory brainstem implants. *J. Mater. Chem. B*, 3(25):5021–5027, **2015**.
- [30] A. Bendali, L. H. Hess, M. Seifert, V. Forster, A.-F. Stephan, J. A. Garrido, and S. Picaud. Purified Neurons can Survive on Peptide-Free Graphene Layers. *Advanced Healthcare Materials*, 2(7):929–933, **2013**.
- [31] D.-W. Park, A. A. Schendel, S. Mikael, S. K. Brodnick, T. J. Richner, J. P. Ness, M. R. Hayat, F. Atry, S. T. Frye, R. Pashaie, S. Thongpang, Z. Ma, and J. C. Williams. Graphene-based carbon-layered electrode array technology for neural imaging and optogenetic applications. *Nature Communications*, 5:5258, **2014**.
- [32] G. Piret, C. Hébert, J.-P. Mazellier, L. Rousseau, E. Scorsone, M. Cottance, G. Lissorgues, M. O. Heuschkel, S. Picaud, P. Bergonzo, and others. 3d-nanostructured boron-doped diamond for microelectrode array neural interfacing. *Biomaterials*, 53:173–183, **2015**.
- [33] X. Cui, V. A. Lee, Y. Raphael, J. A. Wiler, J. F. Hetke, D. J. Anderson, and D. C. Martin. Surface modification of neural recording electrodes with conducting polymer/biomolecule blends. *Journal of Biomedical Materials Research*, 56(2):261–272, **2001**.
- [34] A. Elshchner, S. Kirchmeyer, W. Lovenich, U. Merker, and K. Reuter. PEDOT. Principles And Applications Of An Intrinsically Conductive Polymer. *ResearchGate*, **2011**.
- [35] B. Winther-Jensen and K. West. Vapor-Phase Polymerization of 3,4-Ethylenedioxythiophene: A Route to Highly Conducting Polymer Surface Layers. *Macromolecules*, 37(12):4538–4543, **2004**.
- [36] A. Blau, A. Murr, S. Wolff, E. Sernagor, P. Medini, G. Iurilli, C. Ziegler, and F. Benfenati. Flexible, all-polymer microelectrode arrays for the capture of cardiac and neuronal signals. *Biomaterials*, 32(7):1778–1786, **2011**.
- [37] D. Khodagholy, T. Doublet, M. Gurfinkel, P. Quilichini, E. Ismailova, P. Leleux, T. Herve, S. Sanaur, C. Bernard, and G. G. Malliaras. Highly Conformable Conducting Polymer Electrodes for In Vivo Recordings. *Advanced Materials*, 23(36):H268–H272, **2011**.
- [38] E. Bihar, Y. Deng, T. Miyake, M. Saadaoui, G. G. Malliaras, and M. Rolandi. A Disposable paper breathalyzer with an alcohol sensing organic electrochemical transistor. *Scientific Reports*, 6:27582, **2016**.
- [39] P. Leleux, J.-M. Badier, J. Rivnay, C. Bénar, T. Hervé, P. Chauvel, and G. G. Malliaras. Conducting Polymer Electrodes for Electroencephalography. *Advanced Healthcare Materials*, 3(4):490–493, **2014**.
- [40] T. Roberts, J. B. De Graaf, C. Nicol, T. Hervé, M. Fiocchi, and S. Sanaur. Flexible Inkjet-Printed Multielectrode Arrays for Neuromuscular Cartography. *Advanced Healthcare Materials*, 5(12):1462–1470, **2016**.

Chapter 3. Improving skin-electrode interface with conducting organic materials

- [41] R. A. Green, N. H. Lovell, G. G. Wallace, and L. A. Poole-Warren. Conducting polymers for neural interfaces: Challenges in developing an effective long-term implant. *Biomaterials*, 29(24-25):3393–3399, **2008**.
- [42] M. Asplund, T. Nyberg, and O. Inganäs. Electroactive polymers for neural interfaces. *Polymer Chemistry*, 1(9):1374, **2010**.
- [43] K. A. Ludwig, N. B. Langhals, M. D. Joseph, S. M. Richardson-Burns, J. L. Hendricks, and D. R. Kipke. Poly(3,4-ethylenedioxythiophene) (PEDOT) polymer coatings facilitate smaller neural recording electrodes. *Journal of Neural Engineering*, 8(1):014001, **2011**.
- [44] D. Khodagholy, J. N. Gelinias, T. Thesen, W. Doyle, O. Devinsky, G. G. Malliaras, and G. Buzsáki. NeuroGrid: recording action potentials from the surface of the brain. *Nature Neuroscience*, 18(2):310–315, **2014**.
- [45] D. Pani, A. Dessi, J. F. Saenz-Cogollo, G. Barabino, B. Fraboni, and A. Bonfiglio. Fully Textile, PEDOT:PSS Based Electrodes for Wearable ECG Monitoring Systems. *IEEE Transactions on Biomedical Engineering*, 63(3):540–549, **2016**.
- [46] S. Wilks. Poly(3,4-ethylene dioxythiophene) (PEDOT) as a micro-neural interface material for electrostimulation. *Frontiers in Neuroengineering*, 2, **2009**.
- [47] M. Galiński, A. Lewandowski, and I. Stępnia. Ionic liquids as electrolytes. *Electrochimica Acta*, 51(26):5567–5580, **2006**.
- [48] P. Walden. Aus den Erinnerungen eines alten chemischen Zeitgenossen. *Naturwissenschaften*, 37(4):73–81, **1950**.
- [49] J. S. Wilkes and M. J. Zaworotko. Air and water stable 1-ethyl-3-methylimidazolium based ionic liquids. *Journal of the Chemical Society, Chemical Communications*, (13):965–967, **1992**.
- [50] M. Armand, F. Endres, D. R. MacFarlane, H. Ohno, and B. Scrosati. Ionic-liquid materials for the electrochemical challenges of the future. *Nature Materials*, 8(8):621–629, **2009**.
- [51] J. D. Holbrey and K. R. Seddon. Ionic Liquids. *Clean Technologies and Environmental Policy*, 1(4):223–236, **1999**.
- [52] T. Welton. Room-Temperature Ionic Liquids. Solvents for Synthesis and Catalysis. *Chemical Reviews*, 99(8):2071–2084, **1999**.
- [53] J. Lu, F. Yan, and J. Texter. Advanced applications of ionic liquids in polymer science. *Progress in Polymer Science*, 34(5):431–448, **2009**.
- [54] S. Caporali, A. Fossati, A. Lavacchi, I. Perissi, A. Tolstogousov, and U. Bardi. Aluminium electroplated from ionic liquids as protective coating against steel corrosion. *Corrosion Science*, 50(2):534–539, **2008**.

- [55] A. Ispas and A. Bund. Electrodeposition in ionic liquids. *The Electrochemical Society Interface*, 23(1):47–51, **2014**.
- [56] C. Arnould, J. Delhalle, and Z. Mekhalif. Multifunctional hybrid coating on titanium towards hydroxyapatite growth: Electrodeposition of tantalum and its molecular functionalization with organophosphonic acids films. *Electrochimica Acta*, 53(18):5632–5638, **2008**.
- [57] D. M. Piper, T. Evans, K. Leung, T. Watkins, J. Olson, S. C. Kim, S. S. Han, V. Bhat, K. H. Oh, D. A. Buttry, and S.-H. Lee. Stable silicon-ionic liquid interface for next-generation lithium-ion batteries. *Nature Communications*, 6:6230, **2015**.
- [58] A. Basile, A. I. Bhatt, and A. P. O'Mullane. Stabilizing lithium metal using ionic liquids for long-lived batteries. *Nature Communications*, 7:ncomms11794, **2016**.
- [59] Y. Fukaya, K. Hayashi, M. Wada, and H. Ohno. Cellulose dissolution with polar ionic liquids under mild conditions: required factors for anions. *Green Chem.*, 10(1):44–46, **2008**.
- [60] T. P. Thuy Pham, C.-W. Cho, and Y.-S. Yun. Environmental fate and toxicity of ionic liquids: A review. *Water Research*, 44(2):352–372, **2010**.
- [61] S. Stolte, M. Matzke, J. Arning, A. Bösch, W.-R. Pitner, U. Welz-Biermann, B. Jastorff, and J. Ranke. Effects of different head groups and functionalised side chains on the aquatic toxicity of ionic liquids. *Green Chemistry*, 9(11):1170, **2007**.
- [62] S. Stolte, J. Arning, U. Bottin-Weber, A. Müller, W.-R. Pitner, U. Welz-Biermann, B. Jastorff, and J. Ranke. Effects of different head groups and functionalised side chains on the cytotoxicity of ionic liquids. *Green Chem.*, 9(7):760–767, **2007**.
- [63] S. Stolte, J. Arning, U. Bottin-Weber, M. Matzke, F. Stock, K. Thiele, M. Uerdingen, U. Welz-Biermann, B. Jastorff, and J. Ranke. Anion effects on the cytotoxicity of ionic liquids. *Green Chemistry*, 8(7):621, **2006**.
- [64] A. Romero, A. Santos, J. Tojo, and A. Rodríguez. Toxicity and biodegradability of imidazolium ionic liquids. *Journal of Hazardous Materials*, 151(1):268–273, **2008**.
- [65] A. Cieniecka-Rosłonkiewicz, J. Pernak, J. Kubis-Feder, A. Ramani, A. J. Robertson, and K. R. Seddon. Synthesis, anti-microbial activities and anti-electrostatic properties of phosphonium-based ionic liquids. *Green Chemistry*, 7(12):855, **2005**.
- [66] A. García-Lorenzo, E. Tojo, J. Tojo, M. Teijeira, F. J. Rodríguez-Berrocal, M. P. González, and V. S. Martínez-Zorzano. Cytotoxicity of selected imidazolium-derived ionic liquids in the human Caco-2 cell line. Sub-structural toxicological interpretation through a QSAR study. *Green Chemistry*, 10(5):508, **2008**.
- [67] T. P. Lodge. MATERIALS SCIENCE: A Unique Platform for Materials Design. *Science*, 321(5885):50–51, **2008**.

Chapter 3. Improving skin-electrode interface with conducting organic materials

- [68] J. Le Bideau, L. Viau, and A. Vioux. Ionogels, ionic liquid based hybrid materials. *Chem. Soc. Rev.*, 40(2):907–925, **2011**.
- [69] X. Li, Z. Zhang, L. Yang, K. Tachibana, and S.-i. Hirano. TiO₂-based ionogel electrolytes for lithium metal batteries. *Journal of Power Sources*, 293:831–834, **2015**.
- [70] F. Wu, N. Chen, R. Chen, Q. Zhu, J. Qian, and L. Li. “Liquid-in-Solid” and “Solid-in-Liquid” Electrolytes with High Rate Capacity and Long Cycling Life for Lithium-Ion Batteries. *Chemistry of Materials*, 28(3):848–856, **2016**.
- [71] D. Khodagholy, V. F. Curto, K. J. Fraser, M. Gurfinkel, R. Byrne, D. Diamond, G. G. Malliaras, F. Benito-Lopez, and R. M. Owens. Organic electrochemical transistor incorporating an ionogel as a solid state electrolyte for lactate sensing. *Journal of Materials Chemistry*, 22(10):4440, **2012**.
- [72] S. Imaizumi, H. Kokubo, and M. Watanabe. Polymer Actuators Using Ion-Gel Electrolytes Prepared by Self-Assembly of ABA-Triblock Copolymers. *Macromolecules*, 45(1):401–409, **2012**.
- [73] L. Viau, C. Tourné-Péteilh, J.-M. Devoisselle, and A. Vioux. Ionogels as drug delivery system: one-step sol–gel synthesis using imidazolium ibuprofenate ionic liquid. *Chem. Commun.*, 46(2):228–230, **2010**.
- [74] G. Ayalneh Tiruye, D. Muñoz-Torrero, J. Palma, M. Anderson, and R. Marcilla. All-solid state supercapacitors operating at 3.5 V by using ionic liquid based polymer electrolytes. *Journal of Power Sources*, 279:472–480, **2015**.
- [75] A. S. Shaplov, R. Marcilla, and D. Mecerreyes. Recent Advances in Innovative Polymer Electrolytes based on Poly(ionic liquid)s. *Electrochimica Acta*, 175:18–34, **2015**.
- [76] M. Díaz, A. Ortiz, M. Isik, D. Mecerreyes, and I. Ortiz. Highly conductive electrolytes based on poly([HSO₃-BVIm][TfO])/[HSO₃-BMIm][TfO] mixtures for fuel cell applications. *International Journal of Hydrogen Energy*, 40(34):11294–11302, **2015**.
- [77] P. Leleux, C. Johnson, X. Strakosas, J. Rivnay, T. Hervé, R. M. Owens, and G. G. Malliaras. Ionic Liquid Gel-Assisted Electrodes for Long-Term Cutaneous Recordings. *Advanced Healthcare Materials*, 3(9):1377–1380, **2014**.
- [78] R. Kemp, K. Fraser, K. Fujita, D. MacFarlane, and G. Elliott. Biocompatible Ionic Liquids: A New Approach for Stabilizing Proteins in Liquid Formulation. In *ASME 2008 Summer Bioengineering Conference*, pages 947–948. American Society of Mechanical Engineers, **2008**.
- [79] K. D. Weaver, H. J. Kim, J. Sun, D. R. MacFarlane, and G. D. Elliott. Cyto-toxicity and biocompatibility of a family of choline phosphate ionic liquids designed for pharmaceutical applications. *Green Chemistry*, 12(3):507, **2010**.

- [80] M. Petkovic, J. L. Ferguson, H. Q. N. Gunaratne, R. Ferreira, M. C. Leitão, K. R. Seddon, L. P. N. Rebelo, and C. S. Pereira. Novel biocompatible cholinium-based ionic liquids—toxicity and biodegradability. *Green Chemistry*, 12(4):643, **2010**.
- [81] Y. Fukaya, Y. Iizuka, K. Sekikawa, and H. Ohno. Bio ionic liquids: room temperature ionic liquids composed wholly of biomaterials. *Green Chemistry*, 9(11):1155, **2007**.
- [82] M. Isik, R. Gracia, L. C. Kollnus, L. C. Tomé, I. M. Marrucho, and D. Mecerreyes. Cholinium-Based Poly(ionic liquid)s: Synthesis, Characterization, and Application as Biocompatible Ion Gels and Cellulose Coatings. *ACS Macro Letters*, 2(11):975–979, **2013**.
- [83] M. Isik, H. Sardon, M. Saenz, and D. Mecerreyes. New amphiphilic block copolymers from lactic acid and cholinium building units. *RSC Adv.*, 4(96):53407–53410, **2014**.

Organic conductors in wearable sensors

We showed that organic materials are the best candidates for the skin-electrode interface. But another way of modifying the electrode to improve the recorded signal is to look after the substrate. This main component of the electrode, that supports the conductive materials as well as adhesives and interconnections, gives to the device its main mechanical characteristics. Since the skin and other organs are soft materials, rigid devices in contact with them are unacceptable after few minutes. New devices should be flexible, even stretchable and should allow the skin to breath in order to able long-term and painless recordings. If plastic electrodes, with Kapton as substrate, will be presented, the main interest of this work is in the development of innovative textile electrodes, detailed in the last section of this chapter.

Data presented in this chapter were included in the following publications :

M. Isik, T. Lonjaret, H. Sardon, R. Marcilla, T. Herve, G. G. Malliaras, E. Ismailova, and D. Mecerreyes, *Cholinium-based ion gels as solid electrolytes for long-term cutaneous electrophysiology*, J Mater Chem C, 3, 8942–8948 (2015)

S. Takamatsu, T. Lonjaret, D. Crisp, J.-M. Badier, G. G. Malliaras, and E. Ismailova, *Direct patterning of organic conductors on knitted textiles for long-term electrocardiography*, Sci. Rep. 5, 15003 (2015)

S. Takamatsu, T. Lonjaret, E. Ismailova, A. Masuda, T. Itoh, and G. G. Malliaras, *Wearable Keyboard Using Conducting Polymer Electrodes on Textiles*, Adv. Mater., 28(22):4485-8 (2016)

M. Papaiordanidou, S. Takamatsu, S. R. Mazinani, **T. Lonjaret**, A. Martin, and E. Ismailova, *Cutaneous Recording and Stimulation of Muscles Using Organic Electronic Textiles*, Adv. Health. Mater., doi: 10.1002/adhm.201600299 (2016)

4.1 Electrodes on flexible substrates

4.1.1 Review of flexible electrodes to monitor internal organs

There is a deep mismatch between soft and curvilinear biological tissues and the hard and planar surfaces of silicon devices. Regular electronic devices are wafer-based, thus made of silicon with very high Young's modulus (between 130 and 188 GPa [1]). In comparison, living tissues are much softer and more elastic since they present low Young's modulus: between 0.5 kPa and 6 kPa for brain tissues [2, 3], around 1 MPa for human radial artery [4] and even between 3.2 and 18.6 GPa for bones [5]. It is then important that electrode substrates for surface recordings are at least as elastic as the organ to record. This facilitates a better conformity with the 3D micro-structure of the living tissues and thus a better surface contact with active area of the device to lower impedance contact. Polymer materials such as parylene, easily synthesizable, are often used as substrate for invasive devices. Parylene films are usually created by vapor deposition. It is also possible to encapsulate and insulate sensors with such a film. Strong but flexible at the time (4 GPa) and with low thickness (800 nm to 3 μm), parylene film induces minimum invasivity [6, 7, 8]. Polyethylene terephthalate (PET) and polydimethylsiloxane (PDMS) are inert and flexible polymer films, also well known in invasive devices fabrication [9, 10]. Polyimide substrates offer a cheap and easy-to-process solution for thin and flexible arrays of electrodes, adapted to in-vivo studies [11, 12]. In order to minimize as much as possible the invasivity of the device, Kim et al. [13] even suggested making the substrate disappearing inside the body, once in place. To do so, a dissolvable film of silk fibroin is used, and once the latter dissolved, only metal lines and insulating are in contact with the living tissues. In the case of penetrating probes, materials need to be harder than the brain in order to pierce through the tissues without flexing and deviating. This produces of course tissue damage and disrupt neural network but the probe has to penetrate. In case of a chronic implantation, microscale movements of the brain can induce forces between the depth probe and the tissue. However, a rigid shuttle can be used to allow a flexible thin probe to penetrate and then removed to minimize long-term damages [14]. If organic materials offer many advantages for invasive flexible devices, silicon devices have not lost yet. Far away from the success of the rigid and damaging Utah array [15], semi-conductor nanomembrane/ribbons (known as NMs) technologies [16] allow conformable and high-speed multiplexing ECoG recordings [17].

4.1.2 Review of flexible electrodes for cutaneous applications

To improve the interface of state-of-the-art cutaneous sensors with skin, two visions confront each other. In order to penetrate the first very insulating layer of the skin and avoid long skin-preparation or painful invasive probes, electrodes with micro-structured interface are developed (see Section 5.1.1). Usually, the overall impedance is decreased for better quality recordings. Other researches focus on thin and flexible substrates which conform intimately to skin roughness. One of the disadvantages of micro-structured electrodes is the fact that

the external part is usually solid and thick, preventing the conception of “invisible” sensors for the user. A solution could be to fabricate micro-structured electrodes area on ultra-thin substrates. In this part we will focus on flexible technologies. To improve the contact area with skin but enable easy handling by clinicians, conformable electrodes or matrices of electrodes can be integrated to polyimide or polyester substrates thinner than 125 μm [18, 19, 20]. On an even smaller scale, electronic skin, or e-skin, is a recent concept: new thin and conformable substrates facilitate the integration of sensors and electronics to record biological activities, or to replace some skin properties in an imperceptible way [21, 22, 23, 24, 25, 26]. Flexible and thin electrodes for cutaneous electrophysiological recordings are obviously one of the important e-skin components for healthcare applications. Indeed, new generation of medical devices has to take advantages of new materials properties, beyond traditional standards, for a better answer to the recent request of the ambulatory monitoring market [27, 28, 29]. For intimate contact with skin, repeating its surface topology, ultra-thin substrates ($<10 \mu\text{m}$) facilitate the development of stamp or tattoo-like electrodes [30, 31, 32]. These sensors are even able to wrap around usually inaccessible area such as hair [33] or auricle [34] for high-performing BCI applications. They possess mechanical properties which give them the ability of being crushed [6] or highly stretched [35] and then to follow all skin motions. Silicon (usually PDMS) or parylene layers are adapted substrates for these applications, but exotic substrates such as bioresorbable bioscaffolds in poly(L-lactide-co-glycolide) (PLGA) [36] or hydrogel [37] are even more compatible with the skin for long-term monitoring. Finally, a last sort of flexible substrate, based on textile, is developed for human health monitoring and aim to be integrated to clothes (more details in Section 4.2.1).

4.1.3 Fabrication of plastic cutaneous electrodes

An easy process was developed to able reliable and quick fabrication of cutaneous electrodes. A polyimide, Kapton (from DuPont), was used as substrate. Kapton is flexible but still easy to handle, which is important for manual fabrication process. It also helps when the final electrode needs to be placed on the body of the subject. The protocol was previously described by Leleux et al. [18]. Briefly, a 125 μm thick Kapton was cut by a LPKF ProtoLaser S equipment. It is also possible to pre-cut the polyimide to enable post process on an easy to handle-substrate as shown in Fig 4.1a. 10 nm of chromium and 100 nm of Gold were then deposited on the polyimide by metal evaporation. This evaporation can be done on the whole substrate (in case of an electrode with a single active area) or just on specific area define by a shadow-mask (as in Fig 4.1b). PEDOT:PSS solution (see Section 3.2) was then drop-casted (or spin-coated) on the active area and baked (110°C for 1 h) and an insulator (such as polish nail) was casted on the non-active parts, as for the electrodes presented on Fig 4.2a. Then a defined quantity of ion gel (see Section 3.3) was drop-casted and polymerized. The cartoon on Fig 4.2c describes the final electrode with the different layers.

We also developed another protocol to fabricate a matrix of small electrodes for cutaneous applications. To improve the contact of the electrode with the skin a thinner Kapton is used

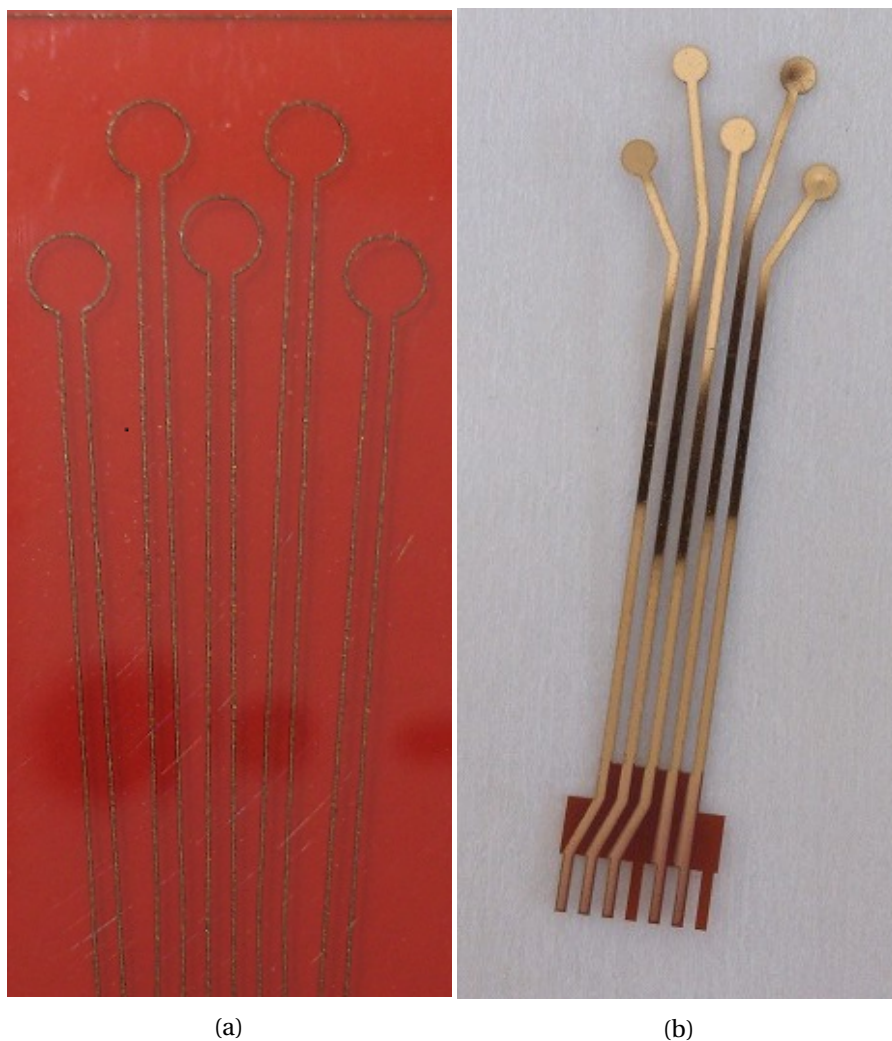


Figure 4.1 – **Laser-cutting of Kapton substrates.**(a)Pre-cut polyimide. (b) Gold-coated polyimide substrate patterned through shadow-mask.

(12,5 μm as substrate. Then, a photolithographic process facilitates the conception of small insulated gold lines for the connection of the matrix. This process is presented on Section 6.1.3 but basically, a first lithography enable the patterning of gold lines, 2 layers of parylene are deposited and etched after lithography. PEDOT is spin-coated and the second layer of parylene is removed. The final flexible matrix is shown on Fig 4.2b. We could imagine using this protocol to make flexible EEG matrices.

4.2. Introduction of innovative electrodes based on textile substrate

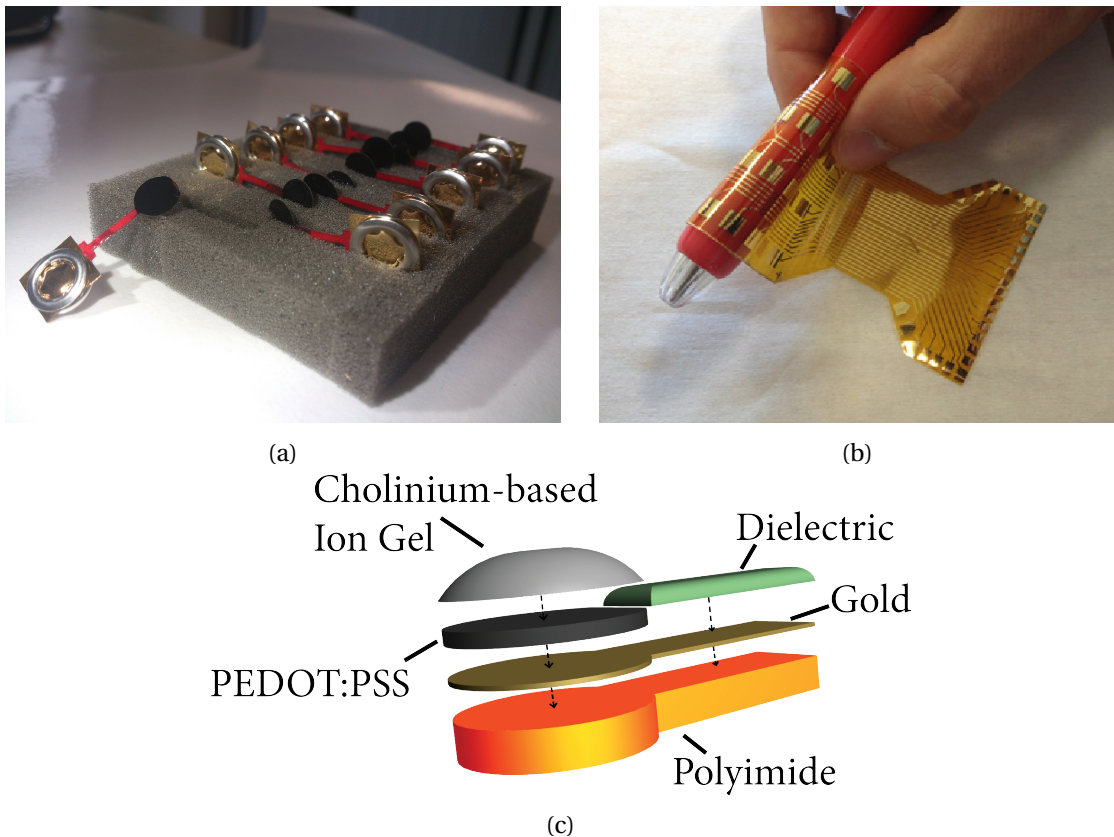


Figure 4.2 – **Examples of Kapton-based electrodes.**(a) Exploded view of the different layers of a cutaneous electrode with a 120µm thick Kapton substrate. (b) Electrode matrix developed by photolithography for EMG applications with a 12,5µm thick Kapton substrate.

4.1.4 Discussion

4.2 Introduction of innovative electrodes based on textile substrate

4.2.1 Introduction on textile electronics

If most of the actual electronics is still made of hard and planar materials, the recent emerging field of flexible electronics is now merging with the fields of connected and wearable embedded sensors. Textile is one of the new target substrate. Textile as substrate offers many advantages such as well-known and low-cost mass fabrication process, broad presence in everyday life (clothes, sheets, car seats. . .) and direct contact with a large area of human skin (in the case of healthcare applications). To be integrated into fabric, conductive parts and components need to fulfill textile characteristics: flexibility, stretchability, high porosity, fiber orientation, resistance of the structural integrity to treatments such as washing [38, 39]. The most common materials and techniques used for textile electronics are presented in this section as well as possible applications.

Materials to coat fibers with

The choice of materials is of first importance for textile electronics conception. These materials need to confer high carrier mobility even under important mechanical stress, together with safety and time stability. Carbon-based materials are widely used for flexible electronics due to their unique properties coming from the different allotropes of carbon such as high conductivity, possible transparency and high elastic modulus. For instance, single-walled carbon nanotubes are mechanically flexible and can conform to the shape of the fibers. They exhibit large Van der Waals forces with many polymers but also with cellulose, as well as strong hydrogen bonds with the latter [40, 41]. Intrinsically flexible and easily tunable, conducting polymers are other promising conductive materials for e-textile. Various conducting polymers are reported in the literature to be coated on textile: Polypropylene [42], PEDOT [43, 44, 45, 46], PEDOT:PSS [47, 48, 49, 50], Poly(styrene- β -isobutylene- β -styrene)-poly(3-hexylthiophene) (SIBS-P3HT) [51], P3HT only [52], polypyrrole and polyaniline [53, 54, 55, 56, 57]. Thanks to their high conductivity, metallic nanowires, nanoparticles or nanolayers are also good candidates for fiber-based electronics. Aluminium or gold alone are used to create conductive lines [58, 52] but the addition of metallic nanoparticles in a conductive solution allow to highly increase the conductivity of the created film (for instance combination of gold nanoparticles with tosylate-doped PEDOT [49] or silver nanoparticles with carbon nanotubes [59]).

Coating fabrication processes

Once one's has matched the material properties with the specific application, the integration into textile has to be performed. For textile electronics, 2 ideas are competing. The first one is to integrate external fibers (or flexible ribbons) into the textile mesh. These external fibers are either conductive on their own, either used as a substrate for embedded electronics. If the strip has similar elastic and bending radius properties as the yarns of the fabric, the former can be woven into it. For instance, few woven polyimide strips with embedded LED chips [60] or patterned electronics [61] or woven optical fibers [62] give new properties to a textile while keeping its properties. A fabric can also be fully made of electronically improved PET ribbons, woven to form a sheet [63]. Another method is to use the textile as a direct substrate for the conducting materials. 2 solutions are then possible: coating of the single yarn, or coating of the full fabric surface. Single yarn coating allows each fiber to be independently coated before weaving. This usually induces a stronger conductivity for the resulting textile since the repartition of conductive material is more homogeneous on the fabric, especially in its bulk. It gives also the possibility of using different fibers in the same fabric to obtain patterns or different functionalities. However, the fiber coating process needs to be done upstream fabric conception. If vapor-phase polymerization (VPP) can be used to polymerize EDOT monomer at the surface of the thread [43, 49], coating from a solution by dipping the fiber [48, 52, 49, 41, 64] may be more adapted to an integration to large-scale textile fabrication process. Takamatsu et al. present a die-coating system that can be easily integrated in a roll-to-roll process [65]. Surface coating of fabrics gives some different advantages: it is a

4.2. Introduction of innovative electrodes based on textile substrate

low-cost and large scale downstream process that can be done after textile fabrication by different ways. The easiest way is to soak the fabric in a solution of conducting materials for fully coating [47, 44, 40, 54, 45, 55, 56]. Vapor phase polymerization of conducting polymer is also possible [54] but seems difficult to adapt to large scale needs. Techniques compatible with roll-to-roll processes able industrial surface coating of fabric: spraying [54], blade-coating [57], screen-printing [66] or ink-jet printing [67, 68]. Nonetheless, if the usual hydrophilic behavior of textile fabric allows a good absorption of solution, it avoids the possibility of precise patterning. Moreover, conducting materials coated in between fibers can reduce flexibility of the fabric.

Textile electronics applications

Because textile is everywhere, applications for textile electronics are various and promising. Similarly to more common sensors that are included in our electronic devices as smartphone or watches, functionalized or coated fibers are able to sense their environment [61], to interact with humans by displaying information using electrochromic properties of conducting polymers [47]. It is possible to use these improved fabrics for very specific applications such as energy storage elements [40] or as local heater [69] and take advantage of the flexibility of the textile substrate. But because clothes offer a large area of contact with the skin and offer a maintained conformal contact, a lot of interest is brought to textile embedded sensors that could monitor health parameters while being invisible [70, 62]. Textile electronics allows already the monitoring of electrophysiological parameters [71, 64, 72, 73], for nerve electrical stimulation [66] or for the analysis of living samples such as blood or sweat to detect pathogens [56, 74] or specific proteins [41]. Indeed, shirts [75], gloves [39], and wristbands [76] outfitted with sensors have been used to demonstrate the potential of this technology. Furthermore, the way is now paved for the conception of elemental electronic components [77]: fiber-based OFET and OECT were developed [58, 49] and elements such as multiplexers, inverters or AND operators were made from textile transistors [48, 52].

4.2.2 Coating of PEDOT:PSS and ion gel on knitted textile

An innovative fabrication process to coat PEDOT:PSS on knitted textile

Despite the large interest in cutaneous electrodes, patterning conducting materials on stretchable fabrics has been hampered by their three-dimensional nature, which makes difficult to apply conventional patterning processes. The fibers in knitted textiles are assembled in a snake shape that can be altered by applying a mechanical force to the knit varying its design. Such wave-form fibers mimic a mechanical spring design, providing the textile with a considerable resisting force when its shape is changing. We previously showed that technique such deep-coating, inkjet or screen-printing can be used for making conductive patterns on textiles. If the creation of a precise pattern is impossible in deep-coating (because of the ink diffusion), the controlled transfer of a pattern using the other techniques on thick knitted fabrics can

Chapter 4. Organic conductors in wearable sensors

be obstructed. The conductive materials need to be coated not only on the surface of the knitted structure but also inside, providing continuous contact between the yarns during its mechanical deformation. Micro-contact and inkjet printing allow direct pattern transfer which is usually done on thin textiles since a small amount of the ink can be transferred at the time. The coating happens only on the top layer of the textile however the pattern conductivity is maintained even under stretch. In the screen printing, additives are used to reduce the spreading of the ink (i.e., silver paste) and improve spatial resolution [78, 79]. The viscosity of inkjet printing inks must also be engineered for printability [80]. As a result, in both screen and inkjet printing, ink optimization has a negative impact on the final conductivity.

We developed a technique was inspired from the Japanese kimono dyeing process (the Yuzen method). According to this method, a rice paste is initially painted on the textile surface to form a stencil. The dye is subsequently applied, coating only the areas that are free of rice paste which is subsequently removed in water, resulting in the precise and beautiful patterns of a kimono. In Fig 4.3 we show the adaptation of this technique to the patterning of PEDOT:PSS on textiles. PEDOT:PSS formulation is the same as the one developed in Section 3.2.2, with ethylene glycol, DBSA and GOPS. The textile used was 100% interlock knitted polyester fabric from VWR International (Spec- Wipe® 7 Wipers) with a thickness of 300 μm and a stretch capability up to 50% (in the knit direction). We used polydimethylsiloxane (PDMS, RTV615, elastomer and curing agent kit) as the stencil due to its hydrophobic nature, which can confine the aqueous PEDOT:PSS solution, as well as due to its mechanical properties, which are a good match for the soft and stretchable structure of knitted textiles. The patterning process started by preparing a negative master made of a polyimide (Kapton HN100, DuPont) film on which the outline of the desired pattern was carved by a laser cutting machine (Protolaser S, LPKF, from the same process developed on previous Section 4.1.3). PDMS was subsequently applied on this master by spin coating at 550 rpm for 18 s (step 1). The textile was then placed on top of the PI master, and the PDMS was progressively transferred into the textile in 10 min (step 2). By adjusting PDMS viscosity (using different amount of the curing agent) and thickness (using different spin coating speeds) it is possible to control its diffusion into the textile and to replicate the master design. A short thermal annealing (at 100°C for 10 minute was used to cure the PDMS completing the transfer step. The PI master was then delaminated from the textile surface. Finally, the conducting polymer solution was brush-painted on the textile and baked to dry (at 110°C for 1 hour) (step 3). Contrary to the Yuzen method, in which the rice paste is removed, the PDMS stencil remains in the textile after the patterning process, and can be used to pattern additional layers (see below). Further more this PDMS mask offers some interesting adhesive properties that help fixation to the skin. Typical patterning results can be seen in Fig 4.4. A flower pattern with regularly spaced curved features and a lines-and-spaces test pattern are shown. These results show that patterning of structures as fine as 0.5 mm is possible on tightly woven textiles.

4.2. Introduction of innovative electrodes based on textile substrate

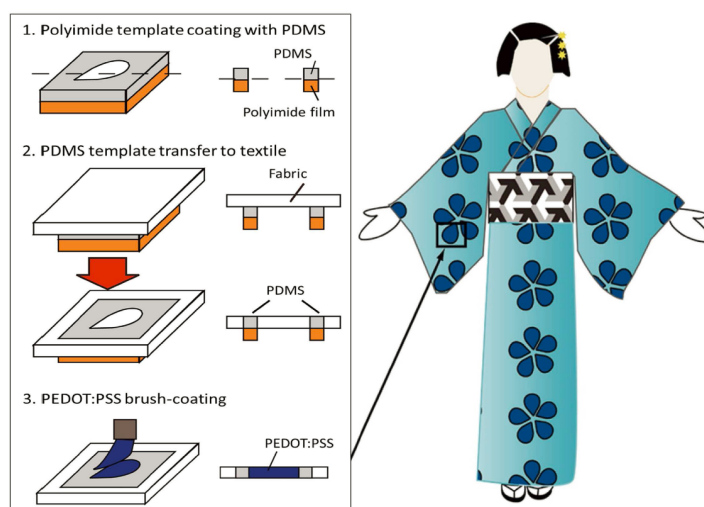


Figure 4.3 – **Process flow for the patterning of PEDOT:PSS on textile.** PDMS is first deposited on a polyimide master defining the outline of the desired pattern. The textile is then placed on the polyimide film and the PDMS is progressively transferred into the bulk of the textile. After a short thermal annealing, the PEDOT:PSS solution is brush-coated on the unprotected area of the textile and dried.

Coating of ion gel to improve cutaneous textile electrodes

Depending on the application, an ion gel layer can be added on top of the PEDOT layer to help establish low-impedance cutaneous contacts. By adding about $45 \mu\text{Lcm}^{-2}$ of ion gel formulation (see Fig 4.5), patterning was achieved on the active area of the electrode. In these textile electrodes, the ion gel was a mixture of ionic liquid 1-ethyl-3-methylimidazolium-ethyl sulfate, poly(ethylene glycol)diacrylate and photoinitiator 2-hydroxy-2-methylpropiophenone at a ratio of 0.6/0.35/0.05. The fabrication method and the properties of this ion gel are presented on Section 3.3.

Connection of the textile electrodes

Because textiles are soft and flexible connection with hard regular electronics is never easy. In our work, electrodes were connected to acquisition systems by regular copper wires. The wire was sewed into the knitted textile on a specific patterned connection pad. To ensure both strong mechanical and electrical connection, a small amount of silver paste and then few drop of PEDOT:PSS solution were deposited between the wire and the PEDOT patterned textile and then hard-baked. To avoid possible contact between the naked wire and the skin, an insulation (such as PDMS or other silicone paste) layer can be added on the connection pad.

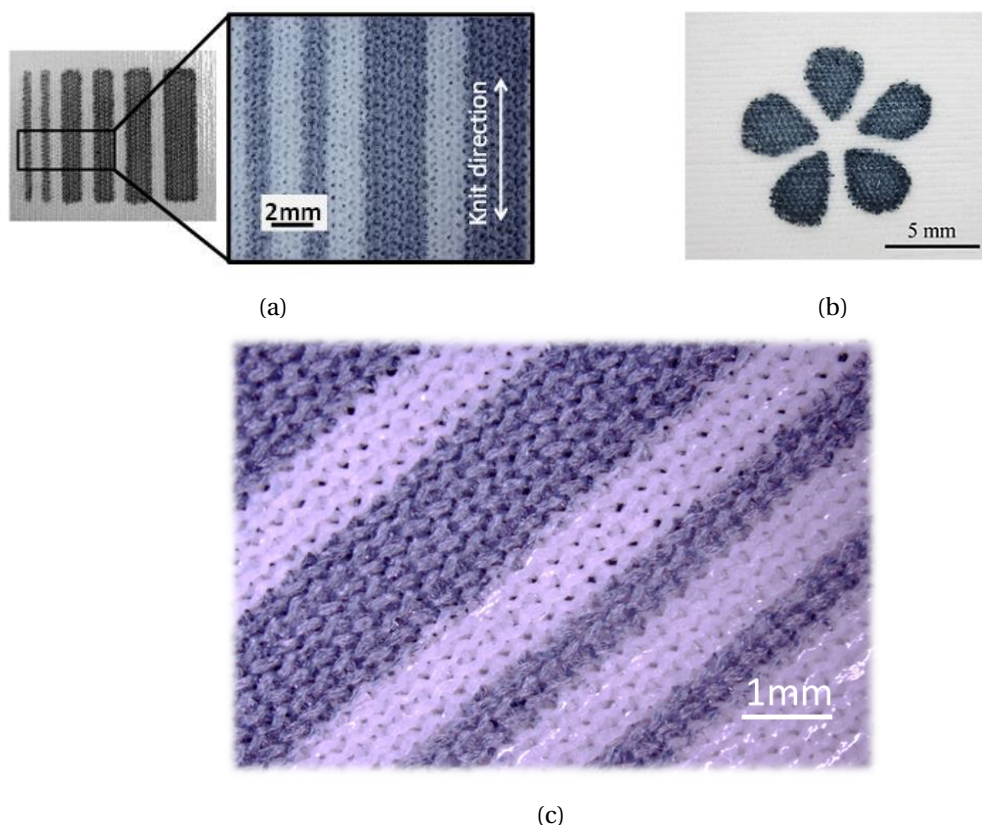


Figure 4.4 – **Examples of PEDOT:PSS-patterned knitted textiles.**(a) (b) Pattern tests with different thickness lines (in blue/purple) (c) Flower pattern to show the possibilities of our patterning process.

4.2.3 Characterization of textile electrodes

Electrical conductivity characterization

The electrical surface conductivity of the samples was measured with a four-probe set-up, made up by four equidistant copper lines on top of which the fabric sample is compressed to make contact in a 3D-printed holder, similarly to what was developed by Hiremath et al. [81]. A constant current source generated applied by a Keithley 2621 is applied between the two outer probes. The voltage drop is measured by a DAQMx between the two inner probes to get the resistance of the fabric. Data are recorded by a LabVIEW software at a 0.5 Hz frequency during 1 minute. The conductivity is then deduced by the formula:

$$\sigma = \frac{L}{t * W * R} \quad (4.1)$$

where L is the spacing between probes, W is the length of the line probe in contact with the

4.2. Introduction of innovative electrodes based on textile substrate

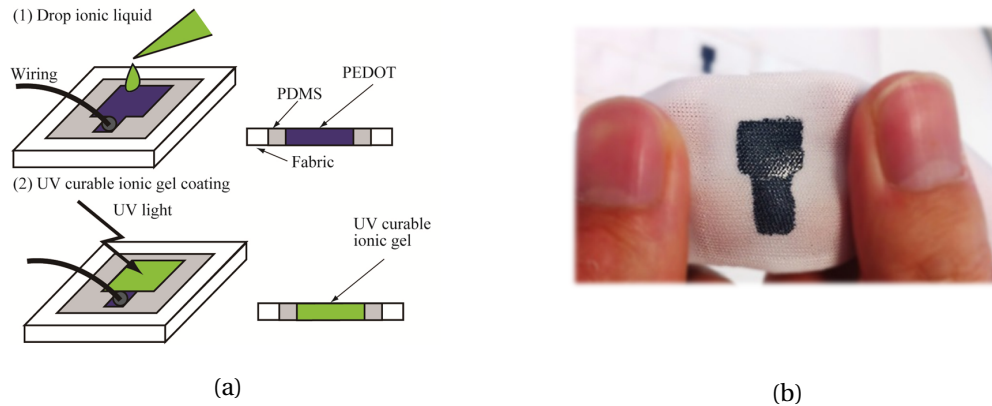


Figure 4.5 – **Integration of ion gel on textile for cutaneous electrodes.** (a) The ion gel mixture is first dropped at the surface of the active area of the electrode. After few minutes of penetration, the gel is polymerised by UV light to be encapsulated inside the knitted textile. (b) Picture of an PEDOT:PSS/ion gel electrode on textile. The top square is the active area coated with ion gel and the bottom square is the connection pad.

sample, t is the thickness of the sample and R is the resistance between the inner probes. For all the samples presented here, $L = 0.4$ cm and $W = 1.5$ cm. The sheet resistance can also be deduced in the same way by the formula:

$$R_s = \frac{W}{L} * R \quad (4.2)$$

The sheet resistance of the patterned PEDOT:PSS stripes was $230 \Omega/\text{sq}$. This value was the same as that of a dip-coated textile, showing that there is no influence of the patterning process on the electrical properties of the conducting polymer.

Mechanical characterization

The use of a knitted textile as a substrate endows stretchability due to its inherent horseshoe-shaped structure, while at the same time offers natural compatibility with a wearable format. The knitted textile consists of loops that provide natural stretchability in both the x and y directions. Coating the fibers with conducting polymers yields electrodes that can be deformed elastically, up to the limit where the fibers are straightened (see Fig 4.6a. This is shown in stretching tests, for which a piece of textile with a width of 0.5 cm and a length of 1 cm was coated with PEDOT:PSS (as described above) and placed in a tensile tester. Fig 4.6b shows a negligible change in resistance when the conducting electrode is stretched with up to 30% applied strain. Beyond this value, the resistance increases nonlinearly as the fibers in the textile are themselves stretched, leading to plastic deformation of the polymer film. For extreme

Chapter 4. Organic conductors in wearable sensors

stretching, the PEDOT:PSS coating breaks apart, as shown in Fig 4.6c. The results of cyclic tests are shown in Fig 4.6d,e, confirming that even after 1000 cycles of 20% applied strain the resistance change is about 10% and the electrode can be stretched repeatedly without plastic deformation, making it suitable for wearable applications.

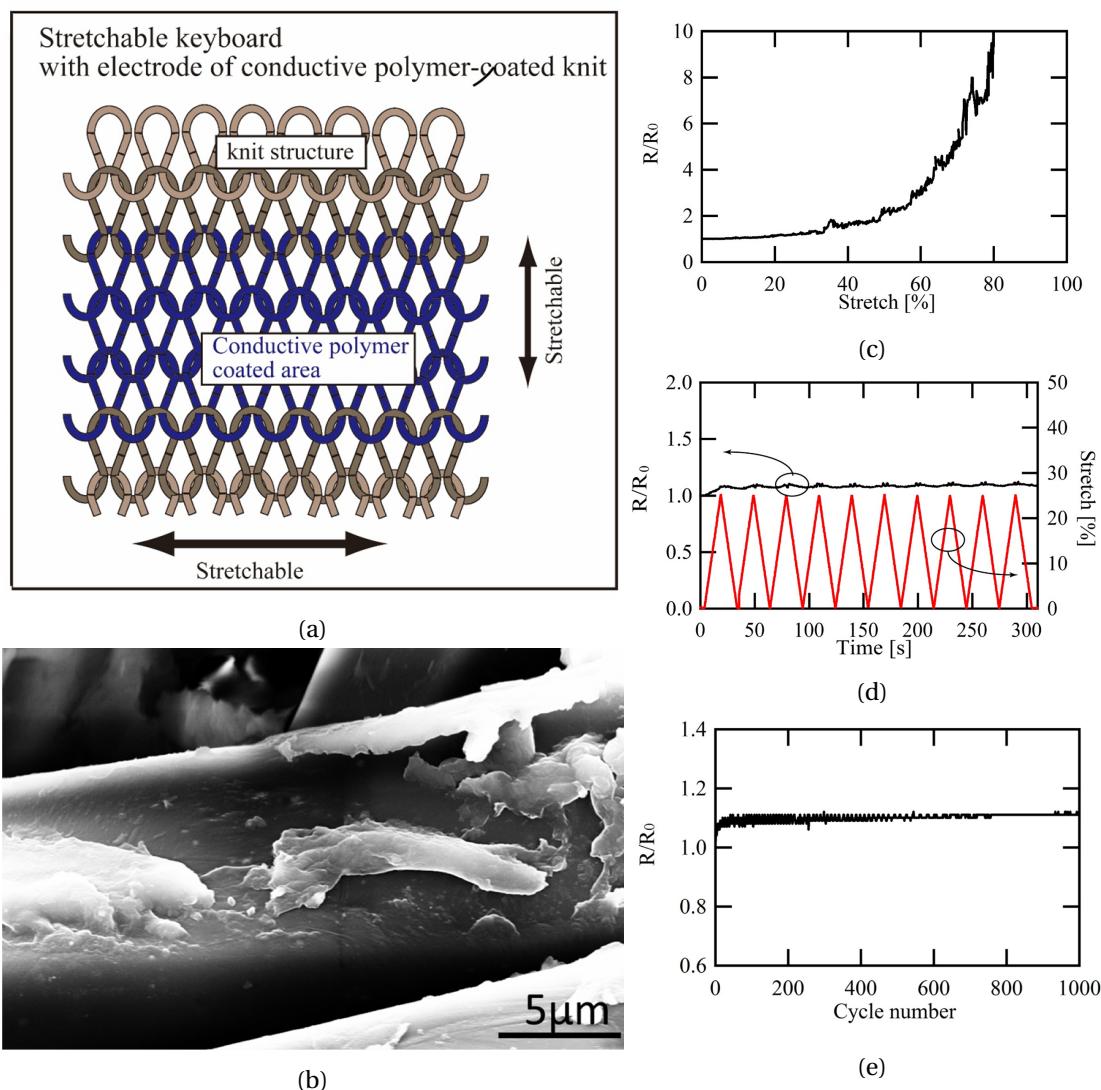


Figure 4.6 – **Mechanical properties of the textile electrode.** (a) Structure of the patterned knitted textile. (b) Stretch test of the PEDOT patterned electrode showing a degradation of the resistivity after 30% stretch. (c) SEM image of the broken PEDOT:PSS coating (bright islands) on a fiber after 80% applied strain. (d) Resistance variation of a PEDOT patterned electrode from 0% to 25% for 10 times. (e) Resistance variation of a PEDOT patterned electrode during a cyclic stretch from 0% to 20% for 1000 times.

4.2.4 Discussion

The technique discussed here allows the patterning of conducting materials with a demonstrated resolution of 0.5 mm, a value that is adequate for the majority of envisioned biomedical applications. These include applications requiring small cutaneous electrodes, such as neonatal care and high-density electroencephalography, where the feature size is larger than several millimeters. In the described patterning process, we were able to combine the direct patterning with relatively thick knitted textiles. We have benefitted from the scalability of this approach and we adopted it for thick structured textiles in a time and cost efficient way. This technique makes use of industrially accepted techniques such as contact printing and deep painting, and can be easily applied not only during textiles manufacturing but also in post manufacturing by processing existing garments. PDMS and PEDOT:PSS materials that are used in the patterning are fully compatible with knitted textile platform thanks to their rheological properties. The rubber-like PDMS stencil integrated with textile conserves the mechanical freedom of its structure. The viscoelastic properties of PEDOT:PSS formulation allows to achieve homogeneous coating of elastic and flexible knitted textiles, in our case, polyester. The technique developed here is generic and would work with any material soluble in aqueous media, provided that post-processing (annealing, sintering, etc.) temperatures stay within the range that the textile can support. The ability to pattern a second layer on top of the conducting polymer paves the way for the development of a wide variety of devices, including organic electrochemical transistors that can be used for simple logic circuits, and biosensors. In addition to applications in healthcare (along the lines of a “smart” bandage), such sensors will extend the scope of bioelectronic textiles to areas including sports and recreation. Finally, the integration of energy and communication modules on textiles represents an important step in the evolution of this technology. Components such as batteries and antennas, which can be made out of conducting polymers, can be patterned in a straightforward way with the technique developed here.

4.3 Bibliography

- [1] M. A. Hopcroft, W. D. Nix, and T. W. Kenny. What is the Young’s Modulus of Silicon? *Journal of Microelectromechanical Systems*, 19(2):229–238, **2010**.
- [2] A. K. Ommaya. Mechanical properties of tissues of the nervous system. *Journal of Biomechanics*, 1(2):127IN23137–136138, **1968**.
- [3] A. Sridharan, S. D. Rajan, and J. Muthuswamy. Long-term changes in the material properties of brain tissue at the implant–tissue interface. *Journal of Neural Engineering*, 10(6):066001, **2013**.
- [4] S. Laurent, X. Girerd, J.-J. Mourad, P. Lacolley, L. Beck, P. Boutouyrie, J.-P. Mignot, and M. Safar. Elastic modulus of the radial artery wall material is not increased in patients with

Chapter 4. Organic conductors in wearable sensors

- essential hypertension. *Arteriosclerosis, Thrombosis, and Vascular Biology*, 14(7):1223–1231, **1994**.
- [5] J. Y. Rho, R. B. Ashman, and C. H. Turner. Young's modulus of trabecular and cortical bone material: ultrasonic and microtensile measurements. *Journal of biomechanics*, 26(2):111–119, **1993**.
- [6] M. Kaltenbrunner, T. Sekitani, J. Reeder, T. Yokota, K. Kuribara, T. Tokuhara, M. Drack, R. Schwödiauer, I. Graz, S. Bauer-Gogonea, S. Bauer, and T. Someya. An ultra-lightweight design for imperceptible plastic electronics. *Nature*, 499(7459):458–463, **2013**.
- [7] S. Takeuchi, D. Ziegler, Y. Yoshida, K. Mabuchi, and T. Suzuki. Parylene flexible neural probes integrated with microfluidic channels. *Lab on a Chip*, 5(5):519, **2005**.
- [8] D. Khodagholy, T. Doublet, P. Quilichini, M. Gurfinkel, P. Leleux, A. Ghestem, E. Ismailova, T. Hervé, S. Sanaur, C. Bernard, and G. G. Malliaras. In vivo recordings of brain activity using organic transistors. *Nature Communications*, 4:1575, **2013**.
- [9] M. Ochoa, P. Wei, A. J. Wolley, K. J. Otto, and B. Ziaie. A hybrid PDMS-Parylene subdural multi-electrode array. *Biomedical Microdevices*, 15(3):437–443, **2013**.
- [10] T.-i. Kim, J. G. McCall, Y. H. Jung, X. Huang, E. R. Siuda, Y. Li, J. Song, Y. M. Song, H. A. Pao, R.-H. Kim, C. Lu, S. D. Lee, I.-S. Song, G. Shin, R. Al-Hasani, S. Kim, M. P. Tan, Y. Huang, F. G. Omenetto, J. A. Rogers, and M. R. Bruchas. Injectable, Cellular-Scale Optoelectronics with Applications for Wireless Optogenetics. *Science*, 340(6129):211–216, **2013**.
- [11] D. Kuzum, H. Takano, E. Shim, J. C. Reed, H. Juul, A. G. Richardson, J. de Vries, H. Bink, M. A. Dichter, T. H. Lucas, D. A. Coulter, E. Cubukcu, and B. Litt. Transparent and flexible low noise graphene electrodes for simultaneous electrophysiology and neuroimaging. *Nature Communications*, 5:5259, **2014**.
- [12] A. A. Guex, N. Vachicouras, A. E. Hight, M. C. Brown, D. J. Lee, and S. P. Lacour. Conducting polymer electrodes for auditory brainstem implants. *J. Mater. Chem. B*, 3(25):5021–5027, **2015**.
- [13] D.-H. Kim, J. Viventi, J. J. Amsden, J. Xiao, L. Vigeland, Y.-S. Kim, J. A. Blanco, B. Panilaitis, E. S. Frechette, D. Contreras, D. L. Kaplan, F. G. Omenetto, Y. Huang, K.-C. Hwang, M. R. Zakin, B. Litt, and J. A. Rogers. Dissolvable films of silk fibroin for ultrathin conformal bio-integrated electronics. *Nature Materials*, 9(6):511–517, **2010**.
- [14] A. Williamson, M. Ferro, P. Leleux, E. Ismailova, A. Kaszas, T. Doublet, P. Quilichini, J. Rivnay, B. Rózsa, G. Katona, C. Bernard, and G. G. Malliaras. Localized Neuron Stimulation with Organic Electrochemical Transistors on Delaminating Depth Probes. *Advanced Materials*, 27(30):4405–4410, **2015**.
- [15] P. Campbell, K. Jones, R. Huber, K. Horch, and R. Normann. A silicon-based, three-dimensional neural interface: manufacturing processes for an intracortical electrode array. *IEEE Transactions on Biomedical Engineering*, 38(8):758–768, **1991**.

- [16] D.-H. Kim, R. Ghaffari, N. Lu, and J. A. Rogers. Flexible and Stretchable Electronics for Biointegrated Devices. *Annual Review of Biomedical Engineering*, 14(1):113–128, **2012**.
- [17] J. Viventi, D.-H. Kim, L. Vigeland, E. S. Frechette, J. A. Blanco, Y.-S. Kim, A. E. Avrin, V. R. Tiruvadi, S.-W. Hwang, A. C. Vanleer, D. F. Wulsin, K. Davis, C. E. Gelber, L. Palmer, J. Van der Spiegel, J. Wu, J. Xiao, Y. Huang, D. Contreras, J. A. Rogers, and B. Litt. Flexible, foldable, actively multiplexed, high-density electrode array for mapping brain activity in vivo. *Nature Neuroscience*, 14(12):1599–1605, **2011**.
- [18] P. Leleux, J.-M. Badier, J. Rivnay, C. Bénar, T. Hervé, P. Chauvel, and G. G. Malliaras. Conducting Polymer Electrodes for Electroencephalography. *Advanced Healthcare Materials*, 3(4):490–493, **2014**.
- [19] T. Roberts, J. B. De Graaf, C. Nicol, T. Hervé, M. Flocchi, and S. Sanaur. Flexible Inkjet-Printed Multielectrode Arrays for Neuromuscular Cartography. *Advanced Healthcare Materials*, 5(12):1462–1470, **2016**.
- [20] S. Imani, A. J. Bandodkar, A. M. V. Mohan, R. Kumar, S. Yu, J. Wang, and P. P. Mercier. A wearable chemical–electrophysiological hybrid biosensing system for real-time health and fitness monitoring. *Nature Communications*, 7:11650, **2016**.
- [21] T. Yamada, Y. Hayamizu, Y. Yamamoto, Y. Yomogida, A. Izadi-Najafabadi, D. N. Futaba, and K. Hata. A stretchable carbon nanotube strain sensor for human-motion detection. *Nature Nanotechnology*, 6(5):296–301, **2011**.
- [22] A. N. Sokolov, B. C.-K. Tee, C. J. Bettinger, J. B.-H. Tok, and Z. Bao. Chemical and Engineering Approaches To Enable Organic Field-Effect Transistors for Electronic Skin Applications. *Accounts of Chemical Research*, 45(3):361–371, **2012**.
- [23] J.-Y. Sun, C. Keplinger, G. M. Whitesides, and Z. Suo. Ionic skin. *Advanced Materials*, 26(45):7608–7614, **2014**.
- [24] Y. Hattori, L. Falgout, W. Lee, S.-Y. Jung, E. Poon, J. W. Lee, I. Na, A. Geisler, D. Sadhwani, Y. Zhang, Y. Su, X. Wang, Z. Liu, J. Xia, H. Cheng, R. C. Webb, A. P. Bonifas, P. Won, J.-W. Jeong, K.-I. Jang, Y. M. Song, B. Nardone, M. Nodzenski, J. A. Fan, Y. Huang, D. P. West, A. S. Paller, M. Alam, W.-H. Yeo, and J. A. Rogers. Multifunctional Skin-Like Electronics for Quantitative, Clinical Monitoring of Cutaneous Wound Healing. *Advanced Healthcare Materials*, 3(10):1597–1607, **2014**.
- [25] M. Drack, I. Graz, T. Sekitani, T. Someya, M. Kaltenbrunner, and S. Bauer. An Imperceptible Plastic Electronic Wrap. *Advanced Materials*, 27(1):34–40, **2015**.
- [26] K.-I. Jang, H. U. Chung, S. Xu, C. H. Lee, H. Luan, J. Jeong, H. Cheng, G.-T. Kim, S. Y. Han, J. W. Lee, J. Kim, M. Cho, F. Miao, Y. Yang, H. N. Jung, M. Flavin, H. Liu, G. W. Kong, K. J. Yu, S. I. Rhee, J. Chung, B. Kim, J. W. Kwak, M. H. Yun, J. Y. Kim, Y. M. Song, U. Paik, Y. Zhang, Y. Huang, and J. A. Rogers. Soft network composite materials with deterministic and bio-inspired designs. *Nature Communications*, 6:6566, **2015**.

Chapter 4. Organic conductors in wearable sensors

- [27] R. Langer and D. A. Tirrell. Designing materials for biology and medicine. *Nature*, 428(6982):487–492, **2004**.
- [28] J.-W. Jeong, W.-H. Yeo, A. Akhtar, J. J. S. Norton, Y.-J. Kwack, S. Li, S.-Y. Jung, Y. Su, W. Lee, J. Xia, H. Cheng, Y. Huang, W.-S. Choi, T. Bretl, and J. A. Rogers. Materials and Optimized Designs for Human-Machine Interfaces Via Epidermal Electronics. *Advanced Materials*, 25(47):6839–6846, **2013**.
- [29] C. Castellini, P. Artemiadis, M. Wininger, A. Ajoudani, M. Alimusaj, A. Bicchi, B. Caputo, W. Craelius, S. Dosen, K. Englehart, D. Farina, A. Gijsberts, S. B. Godfrey, L. Hargrove, M. Ison, T. Kuiken, M. MarkoviÄ, P. M. Pilarski, R. Rupp, and E. Scheme. Proceedings of the first workshop on Peripheral Machine Interfaces: going beyond traditional surface electromyography. *Frontiers in Neurorobotics*, 8, **2014**.
- [30] W.-H. Yeo, Y.-S. Kim, J. Lee, A. Ameen, L. Shi, M. Li, S. Wang, R. Ma, S. H. Jin, Z. Kang, Y. Huang, and J. A. Rogers. Multifunctional Epidermal Electronics Printed Directly Onto the Skin. *Advanced Materials*, 25(20):2773–2778, **2013**.
- [31] X. Huang, Y. Liu, H. Cheng, W.-J. Shin, J. A. Fan, Z. Liu, C.-J. Lu, G.-W. Kong, K. Chen, D. Patnaik, S.-H. Lee, S. Hage-Ali, Y. Huang, and J. A. Rogers. Materials and Designs for Wireless Epidermal Sensors of Hydration and Strain. *Advanced Functional Materials*, 24(25):3846–3854, **2014**.
- [32] A. Zucca, C. Cipriani, Sudha, S. Tarantino, D. Ricci, V. Mattoli, and F. Greco. Tattoo Conductive Polymer Nanosheets for Skin-Contact Applications. *Advanced Healthcare Materials*, 4(7):983–990, **2015**.
- [33] G. A. Salvatore, N. Mnzenrieder, T. Kinkeldei, L. Petti, C. Zysset, I. Strebel, L. Bthe, and G. Trster. Wafer-scale design of lightweight and transparent electronics that wraps around hairs. *Nature Communications*, 5, **2014**.
- [34] J. J. S. Norton, D. S. Lee, J. W. Lee, W. Lee, O. Kwon, P. Won, S.-Y. Jung, H. Cheng, J.-W. Jeong, A. Akce, S. Umunna, I. Na, Y. H. Kwon, X.-Q. Wang, Z. Liu, U. Paik, Y. Huang, T. Bretl, W.-H. Yeo, and J. A. Rogers. Soft, curved electrode systems capable of integration on the auricle as a persistent brain–computer interface. *Proceedings of the National Academy of Sciences*, 112(13):3920–3925, **2015**.
- [35] K.-I. Jang, S. Y. Han, S. Xu, K. E. Mathewson, Y. Zhang, J.-W. Jeong, G.-T. Kim, R. C. Webb, J. W. Lee, T. J. Dawidczyk, R. H. Kim, Y. M. Song, W.-H. Yeo, S. Kim, H. Cheng, S. I. Rhee, J. Chung, B. Kim, H. U. Chung, D. Lee, Y. Yang, M. Cho, J. G. Gaspar, R. Carbonari, M. Fabiani, G. Gratton, Y. Huang, and J. A. Rogers. Rugged and breathable forms of stretchable electronics with adherent composite substrates for transcutaneous monitoring. *Nature Communications*, 5:4779, **2014**.
- [36] A. Campana, T. Cramer, D. T. Simon, M. Berggren, and F. Biscarini. Electrocardiographic Recording with Conformable Organic Electrochemical Transistor Fabricated on Resorbable Bioscaffold. *Advanced Materials*, 26(23):3874–3878, **2014**.

- [37] K. Nagamine, S. Chihara, H. Kai, H. Kaji, and M. Nishizawa. Totally shape-conformable electrode/hydrogel composite for on-skin electrophysiological measurements. *Sensors and Actuators B: Chemical*, 237:49–53, **2016**.
- [38] W. Zeng, L. Shu, Q. Li, S. Chen, F. Wang, and X.-M. Tao. Fiber-Based Wearable Electronics: A Review of Materials, Fabrication, Devices, and Applications. *Advanced Materials*, 26(31):5310–5336, **2014**.
- [39] M. Stoppa and A. Chiolerio. Wearable Electronics and Smart Textiles: A Critical Review. *Sensors*, 14(7):11957–11992, **2014**.
- [40] L. Hu, M. Pasta, F. L. Mantia, L. Cui, S. Jeong, H. D. Deshazer, J. W. Choi, S. M. Han, and Y. Cui. Stretchable, Porous, and Conductive Energy Textiles. *Nano Letters*, 10(2):708–714, **2010**.
- [41] B. S. Shim, W. Chen, C. Doty, C. Xu, and N. A. Kotov. Smart Electronic Yarns and Wearable Fabrics for Human Biomonitoring made by Carbon Nanotube Coating with Polyelectrolytes. *Nano Letters*, 8(12):4151–4157, **2008**.
- [42] F. J. Cunico, J. C. Marquez, H. Hilke, M. Skrifvars, and E. Seoane. Studying the Performance of Conductive Polymer Films as Textile Electrodes for Electrical Bioimpedance Measurements. *Journal of Physics: Conference Series*, 434:012027, **2013**.
- [43] T. Bashir, L. Fast, M. Skrifvars, and N.-K. Persson. Electrical resistance measurement methods and electrical characterization of poly(3,4-ethylenedioxythiophene)-coated conductive fibers. *Journal of Applied Polymer Science*, 124(4):2954–2961, **2012**.
- [44] K. H. Hong, K. W. Oh, and T. J. Kang. Preparation and properties of electrically conducting textiles by in situ polymerization of poly(3,4-ethylenedioxythiophene). *Journal of Applied Polymer Science*, 97(3):1326–1332, **2005**.
- [45] D. Knittel and E. Schollmeyer. Electrically high-conductive textiles. *Synthetic Metals*, 159(14):1433–1437, **2009**.
- [46] A. Laforgue. All-textile flexible supercapacitors using electrospun poly(3,4-ethylenedioxythiophene) nanofibers. *Journal of Power Sources*, 196(1):559–564, **2011**.
- [47] Y. Ding, M. A. Invernale, and G. A. Sotzing. Conductivity Trends of PEDOT-PSS Impregnated Fabric and the Effect of Conductivity on Electrochromic Textile. *ACS Applied Materials & Interfaces*, 2(6):1588–1593, **2010**.
- [48] M. Hamedi, R. Forchheimer, and O. Inganäs. Towards woven logic from organic electronic fibres. *Nature Materials*, 6(5):357–362, **2007**.
- [49] G. Mattana, P. Cosseddu, B. Fraboni, G. G. Malliaras, J. P. Hinestroza, and A. Bonfiglio. Organic electronics on natural cotton fibres. *Organic Electronics*, 12(12):2033–2039, **2011**.

Chapter 4. Organic conductors in wearable sensors

- [50] S. Tsukada, H. Nakashima, and K. Torimitsu. Conductive Polymer Combined Silk Fiber Bundle for Bioelectrical Signal Recording. *PLoS ONE*, 7(4):e33689, **2012**.
- [51] A. J. Granero, P. Wagner, K. Wagner, J. M. Razal, G. G. Wallace, and M. in het Panhuis. Highly Stretchable Conducting SIBS-P3ht Fibers. *Advanced Functional Materials*, 21(5):955–962, **2011**.
- [52] M. Hamed, L. Herlogsson, X. Crispin, R. Marcilla, M. Berggren, and O. Inganäs. Fiber-Embedded Electrolyte-Gated Field-Effect Transistors for e-Textiles. *Advanced Materials*, 21(5):573–577, **2009**.
- [53] R. Gregory, W. Kimbrell, and H. Kuhn. Electrically Conductive Non-Metallic Textile Coatings. *Journal of Industrial Textiles*, 20(3):167–175, **1991**.
- [54] A. Kaynak and R. Foitzik. Methods of coating textiles with soluble conducting polymers. *Research Journal of Textile and Apparel*, 15(2):107–113, **2011**.
- [55] P. Lekpittaya, N. Yanumet, B. P. Grady, and E. A. O’Rear. Resistivity of conductive polymer-coated fabric. *Journal of Applied Polymer Science*, 92(4):2629–2636, **2004**.
- [56] S. McGraw, E. Alocilja, A. Senecal, and K. Senecal. The Effect of 3-Thiopheneacetic Acid in the Polymerization of a Conductive Electrotile for Use in Biosensor Development. *Biosensors*, 3(3):286–296, **2013**.
- [57] M. Skrifvars, W. Rehnby, and M. Gustafsson. Coating of textile fabrics with conductive polymers for smart textile applications. **2008**.
- [58] J. Lee and V. Subramanian. Organic transistors on fiber: a first step towards electronic textiles. pages 8.3.1–8.3.4. IEEE, **2003**.
- [59] K.-Y. Chun, Y. Oh, J. Rho, J.-H. Ahn, Y.-J. Kim, H. R. Choi, and S. Baik. Highly conductive, printable and stretchable composite films of carbon nanotubes and silver. *Nature Nanotechnology*, 5(12):853–857, **2010**.
- [60] K. H. Cherenack, T. Kinkeldei, C. Zysset, and G. Tröster. Woven Thin-Film Metal Interconnects. *IEEE Electron Device Letters*, 31(7):740–742, **2010**.
- [61] T. Kinkeldei, C. Zysset, N. Münzenrieder, and G. Tröster. An electronic nose on flexible substrates integrated into a smart textile. *Sensors and Actuators B: Chemical*, 174:81–86, **2012**.
- [62] B. M. Quandt, L. J. Scherer, L. F. Boesel, M. Wolf, G.-L. Bona, and R. M. Rossi. Body-Monitoring and Health Supervision by Means of Optical Fiber-Based Sensing Systems in Medical Textiles. *Advanced Healthcare Materials*, 4(3):330–355, **2015**.
- [63] T. Yamashita, S. Takamatsu, K. Miyake, and T. Itoh. Fabrication and evaluation of a conductive polymer coated elastomer contact structure for woven electronic textile. *Sensors and Actuators A: Physical*, 195:213–218, **2013**.

- [64] S. Tsukada, H. Nakashima, and K. Torimitsu. Conductive Polymer Combined Silk Fiber Bundle for Bioelectrical Signal Recording. *PLoS ONE*, 7(4):e33689, **2012**.
- [65] S. Takamatsu, T. Yamashita, and T. Itoh. Meter-scale large-area capacitive pressure sensors with fabric with stripe electrodes of conductive polymer-coated fibers. *Microsystem Technologies*, 22(3):451–457, **2016**.
- [66] K. Yang, C. Freeman, R. Torah, S. Beeby, and J. Tudor. Screen printed fabric electrode array for wearable functional electrical stimulation. *Sensors and Actuators A: Physical*, 213:108–115, **2014**.
- [67] P. S. R. Choi, C. W. M. Yuen, S. K. A. Ku, and C. W. Kan. Digital ink-jet printing for chitosan-treated cotton fabric. *Fibers and Polymers*, 6(3):229–234, **2005**.
- [68] A. Soleimani Gorgani and N. Shakib. Single-phase ink-jet printing onto cotton fabric. *Coloration Technology*, 129(2):109–113, **2013**.
- [69] K. Opwis, D. Knittel, and J. S. Gutmann. Oxidative in situ deposition of conductive PEDOT:PTSA on textile substrates and their application as textile heating element. *Synthetic Metals*, 162(21-22):1912–1918, **2012**.
- [70] F. Axisa, P. Schmitt, C. Gehin, G. Delhomme, E. McAdams, and A. Dittmar. Flexible Technologies and Smart Clothing for Citizen Medicine, Home Healthcare, and Disease Prevention. *IEEE Transactions on Information Technology in Biomedicine*, 9(3):325–336, **2005**.
- [71] J. Löfhede, F. Seoane, and M. Thordstein. Textile Electrodes for EEG Recording — A Pilot Study. *Sensors*, 12(12):16907–16919, **2012**.
- [72] G. Cho, K. Jeong, M. J. Paik, Y. Kwun, and M. Sung. Performance Evaluation of Textile-Based Electrodes and Motion Sensors for Smart Clothing. *IEEE Sensors Journal*, 11(12):3183–3193, **2011**.
- [73] J. Coosemans, B. Hermans, and R. Puers. Integrating wireless ECG monitoring in textiles. *Sensors and Actuators A: Physical*, 130-131:48–53, **2006**.
- [74] Y.-P. Hsu and D. J. Young. Skin-Coupled Personal Wearable Ambulatory Pulse Wave Velocity Monitoring System Using Microelectromechanical Sensors. *IEEE Sensors Journal*, 14(10):3490–3497, **2014**.
- [75] K. Cherenack and L. van Pieterse. Smart textiles: Challenges and opportunities. *Journal of Applied Physics*, 112(9):091301, **2012**.
- [76] Y.-L. Zheng, X.-R. Ding, C. C. Y. Poon, B. P. L. Lo, H. Zhang, X.-L. Zhou, G.-Z. Yang, N. Zhao, and Y.-T. Zhang. Unobtrusive Sensing and Wearable Devices for Health Informatics. *IEEE Transactions on Biomedical Engineering*, 61(5):1538–1554, **2014**.

Chapter 4. Organic conductors in wearable sensors

- [77] D. J. Mooney, E. A. Silva, and others. *A glue for biomaterials*. Nature Publishing Group MACMILLAN BUILDING, 4 CRINAN ST, LONDON N1 9XW, ENGLAND, **2007**.
- [78] S. B. Rane, T. Seth, G. J. Phatak, D. P. Amalnerkar, and M. Ghatpande. Effect of inorganic binders on the properties of silver thick films. *Journal of Materials Science: Materials in Electronics*, 15(2):103–106, **2004**.
- [79] T. Sekine, H. Ikeda, A. Kosakai, K. Fukuda, D. Kumaki, and S. Tokito. Improvement of mechanical durability on organic TFT with printed electrodes prepared from nanoparticle ink. *Applied Surface Science*, 294:20–23, **2014**.
- [80] B. Charlot, G. Sassine, A. Garraud, B. Sorli, A. Giani, and P. Combette. Micropatterning PEDOT:PSS layers. *Microsystem Technologies*, 19(6):895–903, **2013**.
- [81] R. K. Hiremath, M. K. Rabinal, and B. G. Mulimani. Simple setup to measure electrical properties of polymeric films. *Review of Scientific Instruments*, 77(12):126106, **2006**.

Cutaneous electrophysiology with organics

From the two previous chapters, we know that organic materials such as conducting polymer PEDOT:PSS and ionic gels can improve the interface with the skin. The choice of substrate such as polyimide or textiles is also important and give the opportunity to consider different applications for ambulatory recording of electrophysiological activity. In collaboration with La Timone Hospital and Aix-Marseille University, in Marseille, we had access to various acquisition systems and recorded ECG or EEG signals to validate the performances of our electrodes. The results and the corresponding analysis are presented in this chapter. We will briefly describe dry electrodes and show their limitations before to demonstrate the excellent electrophysiological recordings obtained with our ion gel-assisted electrodes as well as with our innovative textile electrodes.

Data presented in this chapter were included in the following publications :

M. Isik, T. Lonjaret, H. Sardon, R. Marcilla, T. Herve, G. G. Malliaras, E. Ismailova, and D. Mecerreyes, *Cholinium-based ion gels as solid electrolytes for long-term cutaneous electrophysiology*, J Mater Chem C, 3, 8942–8948 (2015)

S. Takamatsu, T. Lonjaret, D. Crisp, J.-M. Badier, G. G. Malliaras, and E. Ismailova, *Direct patterning of organic conductors on knitted textiles for long-term electrocardiography*, Sci. Rep. 5, 15003 (2015)

M. Papaiordanidou, S. Takamatsu, S. R. Mazinani, T. Lonjaret, A. Martin, and E. Ismailova, *Cutaneous Recording and Stimulation of Muscles Using Organic Electronic Textiles*, Adv. Health. Mater., doi: 10.1002/adhm.201600299 (2016)

5.1 Dry electrodes

5.1.1 State-of-the-art on dry electrodes

To circumvent the long and fastidious preparation for electrode placement (with skin abrasion and potential gel application) and offer the possibility of long-term recordings without gel-evaporation problems, dry electrodes can be used. Three different possibilities of dry-electrodes demonstrated their efficiency:

- **Dry electrodes with micro-structures:** The 3D structure can be at a macro-, micro- or nano-scale, and gives the possibility to penetrate the stratum corneum layer (without involving pain for the patient, at the difference of subdermal electrodes) [1, 2, 3]. This involves a reduced contact impedance. Moreover, the active surface of the electrode is multiplied (but not the effective macro-size of the device) and the impedance is again significantly decreased. Such structured electrodes can even be produced by 3D printing [4]. These electrodes can record high-quality EEG signals, with comparable performances as usual gel-assisted EEG electrodes [5]. However, if long microstructures grant better penetration in the stratum corneum, they also are more fragile and limit the number of utilization of the electrode. Another disadvantage of structured electrodes is that they still need to be in contact with the skin. In case of EEG recording, hair layer restricts the contact with skin instead of being shortcuted by a conductive gel which can penetrate through hair. A solution with macro-pins (at a centimeter-scale) to cross hair was proposed to integrate electrodes in a helmet [6]. EEG was successfully recorded by this solution is painful for the patient, since a pressure needs to be applied by the helmet to ensure a permanent contact.
- **Capacitive non contact electrodes:** It is possible to record electrophysiological signals by using capacitive coupling between the body and an electrode. In this case, the electrode is not in direct contact with skin, thus can be separated from the epidermis by a fabric or hair layer. Such a non-contact capacitive electrode is made of conductive part insulating from the body by a thin plastic layer or a metal oxide. Lopez and Richardson conceived one of the first capacitive electrode in 1969 and successfully demonstrated its performances similar to those of a gel-assisted Ag/AgCl medical electrode on ECG recordings [7]. Capacitive electrodes are able to record α and β waves associated to EEG [8] and can be integrated to BCI system [9]. However, the use of a capacitive electrode imply to deal with a high impedance. Only *in situ* electronics can adapt the impedance to fit with input impedance of the amplifier. These capacitive electrodes have to be "active" (see Section 6.4.1) and thus very expensive, which limits the diffusion of their use.
- **Dry electrodes on flexible substrates:** By taking advantage of the conformity properties of the substrate, it is possible to perform high-quality electrophysiological recordings with dry electrodes. Both the unique properties of organic conducting polymers (see

Section 3.1.2) and a better conformity to the skin facilitate the acquisition of high-quality signals, as it was demonstrated on PEDOT:PSS-coated polyimide electrodes [10]. Next generation sensors, with ultra-thin substrates, facilitate a perfect conformity with the skin and a maximum surface of contact. In this case, gel are not useful anymore and performing EMG, ECG or EEG can be recorded [11, 12, 13]. However, these electrodes are still sensible to motion artifact.

5.1.2 Discussion

If dry electrodes present important advantages, their massive use is still limited by high-price or difficulties of fabrication or manipulation. We decided to focus on gel-assisted electrodes, which allow better performances for ambulatory recordings where constraints are numerous. Since the user is moving as soon as he is active, a maximum reduction of motion artifact effects is necessary. From an industrial point of view, the use of substrate such as polyimide or fabric can be justified by their flexibility, low-cost, ease of process and ease of integration in clothes for fast integration in a future medical device.

5.2 Ionic gel-assisted electrodes

5.2.1 Experimental

Preparation of electrodes

The same electrodes than the one presented on Section 4.1.3 were used as substrates, with polyimide, chromium, Gold and PEDOT:PSS layers.

Choice of the ion gels

Cholinium-based ion gel, developed on Section 3.4 was incorporated onto electrodes. It is then used as the electrolytic interface between the skin and the electrode itself. This interface is an important element in successful transcutaneous signal transduction. As a reminder, this ion gel is made of an ionic liquid polymer (cholinium lactate methacrylate, to give the matrix structure), a changeable amount of ionic liquid (cholinium lactate, to improve conductivity), a crosslinker (ethylene glycol demethacrylate, to help polymerization) and a photoinitiator (to initiate polymerization).

15 mL of cholinium ion gel solution mixed with the photoinitiator were deposited on top of the PEDOT:PSS layer of 0.5 cm² (size of the recording area) and UV cured until the full polymerization, as described above. The resulting layer of ion gel was around 2 mm thick.

Acquisition systems and signal processing

Gel-to-gel and skin impedance spectra were acquired using a potentiostat (Autolab equipped with FRA module, Metrohm B.V.). The CardioTOMM acquisition system was provided by Microvitae Technologies and allowed ECG recordings. Signals were then filtered and processed by LabVIEW software using a standard wavelet approach.

Signal-to-Noise Ratio (SNR) was calculated by using the Crest factor, or Peak-to-RMS value, which is the ratio between the R peak amplitude and the RMS value of the signal all along a PQRST complex [14].

5.2.2 Electrode characterization

Gel-to-gel characterization

The electrodes were characterized accordingly to the ANSI/AAMI EC12:2000/(R)2005 norm: AC impedance and DC offset voltage are 300 Ω and 25.4 mV, respectively.

Skin impedance characterization

In order to compare the performance of these electrodes in cutaneous recordings, we tested the electrode/skin impedance on a healthy volunteer, following the protocol described on Section 2.2.2. The electrodes were placed on the subject's arm using a three-electrode configuration, where both counter and reference electrodes were commercial Ag/AgCl electrodes. Fig 5.1] shows typical electrical impedance spectra, both magnitude and phase angle, for the electrodes tested including different ion gels with different free IL contents. To record physiological potential variations, a good contact with the skin and low impedance are important to ensure a good ionic/electronic translation. All the tested cholinium ion gels showed good long-term adhesion to the skin. This is an important factor since in long-term recordings the electrodes have to endure some mechanical constraints during movements such as friction and delamination from the skin. Interestingly, impedance values obtained using electrodes containing different cholinium ion gel compositions are comparable to the ones from regular medical electrode, as shown in Fig 5.1. Similar to the data presented above the impedance measurements of the ion gels coated electrodes containing different amounts of the free IL displayed a slight decrease of impedance magnitude at low frequency range with increasing the free IL amount. The phase curves show that ion gel electrodes behave similarly to standard Ag/AgCl electrodes, i.e. their phase shift is close to 0 π at low frequencies, as mostly non-polarizable electrodes. The comparison of impedance values with the commercial Ag/AgCl electrode standard indicated that cholinium ion gels can effectively be used in electrophysiological recordings. Although impedance of all gels was comparable to the commercial Ag/AgCl electrode, the lowest impedance was obtained with IG-50 ion gel formulation. This composition presented a good compromise between mechanical properties and ionic conductivity of the material.

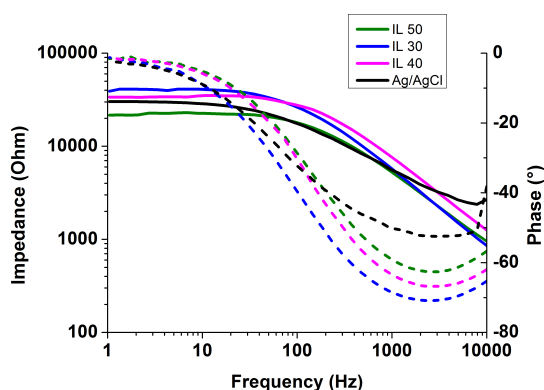


Figure 5.1 – **Skin impedance characterization of cholinium-based ion gels.** Impedance values on skin over frequencies for different ion gels and comparison with a standard medical Ag/AgCl electrode.

5.2.3 ECG recordings

The performance of the cholinium ion gel IG-50 was evaluated in cutaneous electrophysiology. ECG recordings were performed by placing one electrode on each wrist of a healthy volunteer to form a bipolar Limb Lead I derivation, one of the 12 ECG lead configurations used in clinics (see Section 1.1.2). Medical electrodes (Sensor N medical grade Ag/AgCl electrodes, Ambu) were placed as close as possible to the IG-50 electrodes to form a parallel bipolar Limb Lead I. Signals from both leads were recorded at the same time, facilitating comparison of signals from the same heart beats.

Comparison of ECG signals with medical electrodes

Short-term evaluation of this electrode demonstrated similar performance in comparison with medical standard (Sensor N medical grade Ag/AgCl electrodes, Ambu) after 3 h of contact with the skin, shown in Fig 5.2. Processing of 48 seconds of signals confirmed that mean SNR (6.41 dB and 6.51 dB for medical and IG-50 electrodes, respectively) and mean R-peak amplitude (430.9 μ V and 451.4 μ V for medical and IG-50 electrodes, respectively) are equivalent.

Long-term ECG recording

Then, a long-term study was done with cholinium ion gel coated electrodes. To avoid any loose of contact due to the possible mechanical displacement of the electrode connected to electrical wires during long-term evaluations, the electrodes were fixed to the skin with 3 M Steri-Strip and a protective bandage was rolled around each wrist. The ECG was then recorded for 48 seconds several times a day during 72 hours. ECG signals recorded from our electrodes are shown in Fig 5.3a. The PQRST complexes, corresponding to the different depolarization phases of the heart, can be easily identified. Fig 5.3b shows the evolution of the

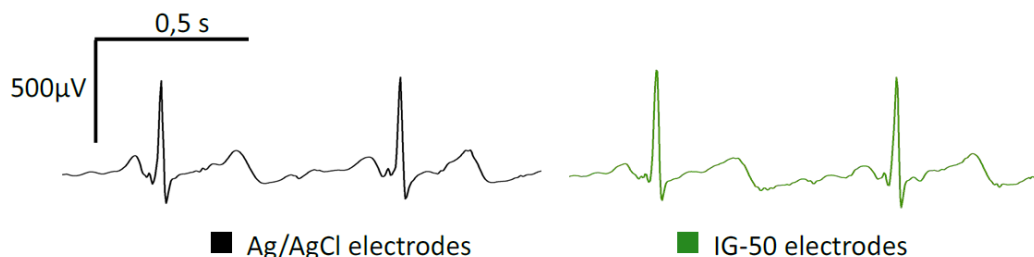


Figure 5.2 – **Comparison of ECG signals between medical electrode and cholinium ion gel electrodes.** ECG signals (from Ag/AgCl medical standard electrodes in Black, and from cholinium ion gel IG50-assisted electrodes in Green) simultaneously after 3h of contact with the skin.

ECG signal with time. Amplitudes of R-peaks and evolution of SNR over time are shown. As the recordings were carried out on a person performing regular activities (walking, office working, taking shower...) many reasons cause daily variations of SNR and R-peaks amplitudes. The physiological change of the skin impedance, the noise from different electronic sources can interfere with the signal and modify the recording quality. However, the electrodes containing cholinium ion gel allowed obtaining good quality electrophysiological recordings during 72 hours long with the reliable detection of the PQRST cardiac complex.

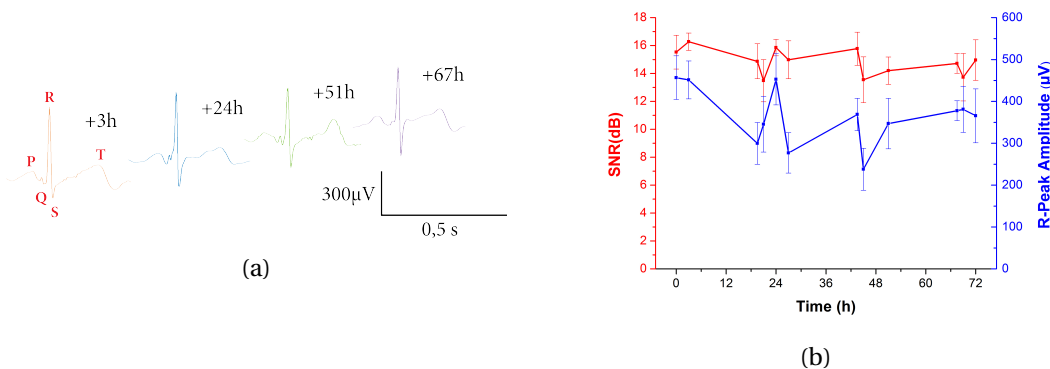


Figure 5.3 – **Cholinium-based ion gel electrode evaluation for long-term ECG evaluation.** Long-term ECG measurement performed with IG-50. (A) ECG signals recorded on skin with highlighted PQRST complexes. (B) Stability of the ECG signals over 72 hours with SNR (red) and R-peaks amplitudes (blue) evolutions.

5.2.4 Discussion

Cholinium ion gels showed good long term adhesion to the skin without any loss of properties caused by the evaporation of the electrolyte in commercial electrodes. Accurate physiologic signals were recorded for a long period of time with a remarkable stability that outperforms

the short-term stability of medical electrodes. Due to the recognized low toxicity of cholinium ionic liquids, these ion gels are ideal candidates to assist the long-term cutaneous recordings. However, further evaluations are required to assess the dermatotoxicology of the ion gels in clinical applications. The Kapton substrate we used proved to be a good candidate for fast industrialization of such organic electrodes.

5.3 Wearable textile electrodes

We reported in Section 4.2.2 a simple and reliable fabrication process that allows the patterning of conducting polymers on thick knitted textiles, thereby yielding wearable and conformal electronic devices for healthcare monitoring. We applied this process to the fabrication of cutaneous electrodes using the commercially available, high conductivity polymer PEDOT:PSS, and an ionic liquid gel that promotes better skin contact. We evaluated the performance of these devices in electrophysiological recordings of a human heart. A particular interest was given to ambulatory conditions.

5.3.1 Experimental

Preparation of electrodes

Textile electrodes were made accordingly to the protocol described on 4.2.2. Shortly, a conductive layer of PEDOT:PSS was coated on knitted fabric thanks to a PDMS pattern. Then, an ion gel made of ionic liquid (1-ethyl-3-methylimidazolium-ethyl sulfate), poly(ethylene glycol)diacrylate and photoinitiator 2-hydroxy-2-methylpropiophenone is deposited on top of the active area. This active area is a square of 1 cm^2 . Connection is made by a sewed copper wire.

Acquisition systems and signal processing

Electrode characterization: Impedance spectrum was acquired using an Autolab potentiostat, equipped with FRA module (Metrohm B.V.), applying sinusoidal voltage of 0.01 V.

Evaluation of ECG for ambulatory conditions: Textile electrodes were connected to a SandResearch system using EA68 or EA136 amplifiers during the 3 hours of evaluation sessions. Signals were processed and filtered using LabVIEW (National Instruments) software with a third-order Butterworth filter (passband with low and high cutoff of 0.5 Hz and 40 Hz, respectively). To compare the signal quality recorded from textile electrodes with medical electrodes, SNR values were calculated after filtering. A feature recognition program first isolated each PQRST complexes and then found the Crest Factor, or peak-to-RMS ratio, which is the ratio between the amplitude of the R peak (which is the peak with the highest amplitude) and the RMS value of the signal all along the complex [14]. To extract baseline from ECG signals we used a wavelet approach corresponding to a low-pass filter with a cutoff of 1.93 Hz). The

algorithm for the calculation of heartbeat (R peak) frequency is a feature extractor LabVIEW software (available in BioMedical Toolkit from National Instrument) with intern filters between 10 and 25 Hz.

long-term ECG evaluation: ECG signals were recorded with a portable and wireless RF-ECG2 acquisition system (from GM3 Corporation, intern passband with low and high cutoff of 0.16 and 100 Hz, respectively).

5.3.2 Electrode characterization on skin

As described in Section 2.2.2, impedance is an important characterization to define the quality of contact between the electrode and the material to be measured. We placed medical cutaneous Ag/AgCl electrodes (Sensor N medical grade Ag/AgCl electrodes, Ambu) on the skin as counter and reference electrodes. Working and counter electrodes were placed 2 cm away from each other on the forearm, and the reference electrode was placed 30 cm away on the arm. The Ambu electrodes were 0.95 cm diameter gel-assisted electrodes. Results from 3 different volunteers are presented on Fig 5.4. In agreement with previous results [15], the impedance of the PEDOT/ion gel electrodes is lower (2.5 times lower at 10 Hz) than the one from medical electrode all over the frequency spectrum. This demonstrates the quality of contact between textile electrode and skin.

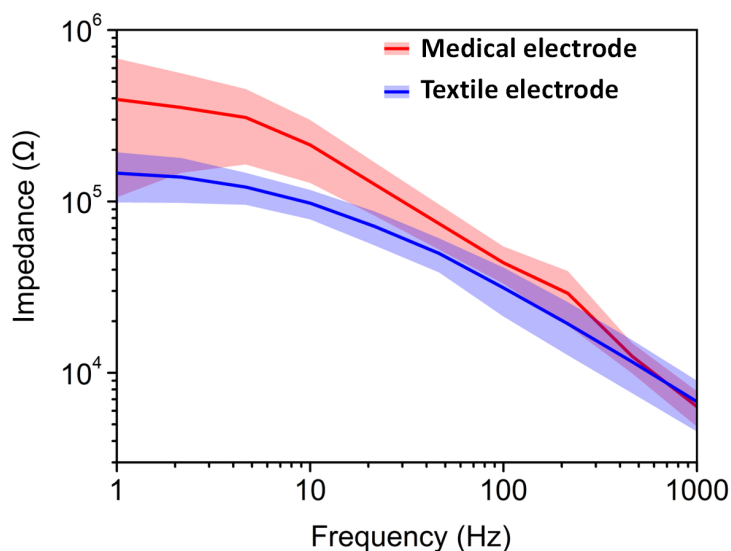


Figure 5.4 – **Impedance spectra of textile and medical electrodes.** Impedance results were recorded in the 1 Hz to 1 kHz frequency range on 3 different volunteers (mean (straight line) and standard deviation (confidence area)).

5.3.3 ECG recording

The potential of the textile electrodes in biomedical monitoring was assessed using electrocardiography recordings. ECG is a common diagnostic technique in the clinic, and is also used to monitor heart rate during exercise. ECG measurements in dynamic conditions are usually performed with electrodes placed on the chest, in order to reduce motion artifacts. To evaluate the performance of the textiles electrodes in a wearable configuration, we used the limb lead II configuration (one electrode worn on the right wrist and a second one worn on the left ankle) (see Section 1.1.2) and performed measurements on volunteers at rest and various states of movement consecutively during 3 hours. In this study, conventional medical electrodes were placed next to the textile ones for comparison.

Evaluation of textile electrodes in ECG monitoring at rest

During a first measurement, the volunteer was sitting at rest, to reduce muscle movements and respiratory artifacts. This position allows obtaining high quality recordings that can be used to detect heart function anomalies. Both, the textile and the medical electrodes show the typical waveform of the heart activity with similar amplitudes (Fig 5.5a). High resolution PQRST complexes, corresponding to the different phases of polarization and depolarization of cardiac cells, can be clearly detected with both electrodes. The SNR value is averaged over 25 different complexes obtained with textile and medical electrodes and found to be equal to 16.3 dB (± 0.1 dB) for both electrodes.

Evaluation of textile electrodes under ambulatory conditions

The evaluations were performed first in the movement and then during long-term experiments. Fig 5.5b shows recorded signals obtained while the volunteer was standing up and moving. Movement can have a large impact on ECG recordings, inducing an undulating baseline that can disturb the acquisition of the PQRST complex. This is evident in the recording obtained by the medical electrode (in red), where the R peak is barely visible. In contrast, the influence of motion is significantly lower on the recordings from the textile electrode (in blue), which show richer signal content, with a well-defined R peak and even a visible T wave (the positive wave following the R peak). We calculated that the baseline noise (low frequencies) is 13.1 dB higher for the medical electrode. As a result, a standard algorithm for the calculation of heartbeat frequency fares considerably better with recordings from the textile electrode. On a subject with a mean heartbeat of 70 bpm (at rest or during low-level activity), Fig 5.5c demonstrates that R peaks are more accurately detected in recordings obtained with the textiles electrodes for a panel of different types of motion.

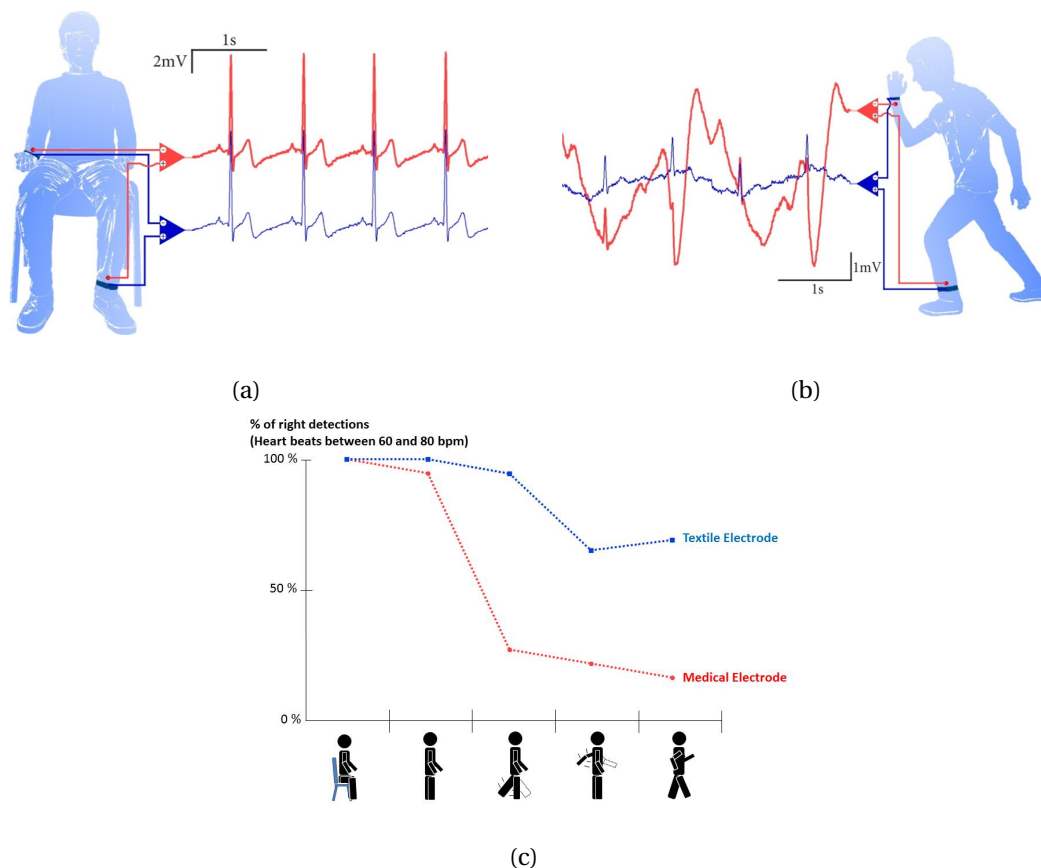
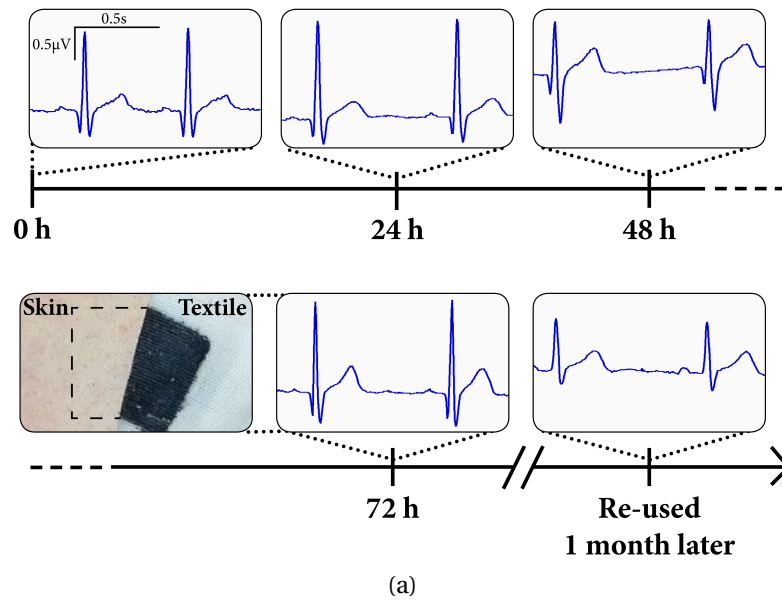


Figure 5.5 – **Textile electrode evaluation for ambulatory ECG monitoring.** ECG recordings performed with the PEDOT:PSS ion gel textile electrode (in blue), and medical Ag/AgCl electrodes (in red), (a) from volunteers sitting at rest and (b) during movement. (c) Percentage of accuracy of heartbeat detection during different types of activity (seating, standing up, leg moving, arm moving, walking) with medical and textile electrodes during a 50 s epoch.

Long-term stability evaluation of textile electrodes

The long-term signal stability is assessed by continuously placing two textile electrodes on a volunteer's chest during 3 days. ECG recordings from these electrodes are presented in Fig 5.6 and demonstrate that the signals are highly consistent during this recording time. The SNR and R-Peak amplitude evolutions are presented in Table S1. Despite the signal variations from day to day related with the skin hydration changes and environmental noise, their amplitude and noise level remain stable. There was no skin reaction to the electrodes observed after 3 days. Moreover, the same electrodes were stored in ambient air for 1 month and then were re-used in ECG recordings in the same setup. These electrodes were still able to record well defined PQRST complexes, highlighting the long-term stability of the textile PEDOT:PSS/IL gel electrodes.



ECG SIGNAL EVOLUTION	Continuously in contact with the skin						Re-used 1 month
	0h	1h	12h	24h	48h	72h	
R-Peak Amplitude (mV)	1.27 (±0.09)	1.13 (±0.05)	1.45 (±0.04)	1.45 (±0.03)	0.76 (±5)	1.23 (±0.08)	0.67 (±0.03)
SNR (dB)	4.64 (±0.53)	4.53 (±0.38)	6.45 (±0.12)	6.07 (±0.07)	4.01 (±0.16)	4.88 (±0.5)	4.33 (±0.33)

(b)

Figure 5.6 – **Textile electrode evaluation for for long-term ECG evaluation.** ECG signal evolutions obtained with textile electrodes in permanent contact with skin over three days. The inset shows a picture of the skin under the electrode after 72 h. The last ECG signals were obtained from re-used textile electrodes stored in ambient air for one month.

5.3.4 Discussion

The combination of a low contact impedance provided by the PEDOT:PSS/IL gel electrode and of a conformable support provided by the textile was shown here to diminish the impact of motion artifacts, which paves the way for a variety of applications, including electromyography (EMG). The high tolerance of textile electrodes to low frequency motion artifacts makes them well-suited for this application. Finally, electroencephalography (EEG) is another obvious application for these textile electrodes. EEG measurements are currently performed using electrodes mounted on casks, then filled with gel. The monolithic fabrication of a cask with integrated electrodes will make these measurements easier to perform. Such measurements are currently ongoing in our own lab. As textile electrodes can be easily integrated with hats, they can be used to render EEG electrodes imperceptible to the wearer. As a result, this can increase the acceptance of EEG in applications beyond healthcare, such as gaming and fatigue monitoring. In conclusion, we developed a technique that allows the simple

patterning of conducting polymers on knitted textiles. The technique uses a PDMS stencil to confine the spreading of the polymer to dimensions as small as 0.5 mm. PEDOT:PSS electrodes fabricated this way and coated with an ionic liquid gel showed a low impedance contact with the skin. They were able to record high quality electrocardiograms in clinic and ambulatory conditions, and accurately determine heart rate, even when the wearer was in motion. Moreover, these electrodes demonstrated high performance long-term stability during 3 days of ECG recordings and after extended ambient storage without any special reconditioning.

5.4 Recording and stimulation performances of textile electrodes

In this study we evaluated the potential of conducting polymercoated textiles in monitoring and stimulating muscle activity. We first demonstrated the performance of textile electrodes in surface electromyography of the lower limb during voluntary and electrically evoked contractions. Then, we further test these electrodes in stimulating the tibial nerve in order to elicit neuromuscular responses.

5.4.1 Experimental

Preparation of electrodes

Textile electrodes were made the same way as in previous Section 5.3.1.

Acquisition systems and signal processing

Electrode characterization: CV measurements were performed with an Autolab potentiostat, equipped with FRA module (Metrohm B.V.) *Electrical stimulation for EMG recordings:* The tibial nerve was stimulated by means of a high-voltage, constant-current stimulator (DS7AH, Digitimer, Hertfordshire, UK), delivering monophasic, rectangular, 1 ms pulses. The anode (10 × 5 cm) was placed 2 cm distally to the patella, after verification of an appropriate reflex acquisition in the SOL muscle, and the cathode (an Ag/AgCl surface electrode, 9 mm diameter or the textile electrode, 9 mm²) was fixed in the popliteal fossa.

EMG acquisition and analysis: Surface EMG was recorded from the soleus (SOL) muscle bipolarly. To minimize impedance (<5 kΩ), the skin was shaved, abraded, and cleaned with alcohol. Electrodes were placed along the mid-dorsal line of the leg, about 5 cm distally to the insertion point of the two gastrocnemii to the Achilles tendon. Medical electrodes were Ag/AgCl electrodes, with a recording diameter of 9 mm and an inter-electrode distance of 20 mm (Contrôle Graphique Medical, Brie-Compte-Robert, France). Electrode position was secured after verification of an appropriate M-wave acquisition (single response, highest amplitude for a given intensity). Textile electrodes were placed in the same configuration with 9 × 9 mm² recording surface and 20 mm inter-electrode distance. The connection to

5.4. Recording and stimulation performances of textile electrodes

the acquisition system was provided by a metallic wire attached to the conducting textile inter-pad. The ground electrode was placed on the contralateral patella. EMG signals were amplified (x 500), sampled (5 kHz) and stored to computer via an analog-to-digital interface (Biopac, MP150, Santa Barbara, CA). The EMG activity of the SOL muscle was quantified by the root mean square (RMS) value of the filtered signal (10–500 Hz) at the 500 ms interval preceding the stimulation artifact. The RMS value was subsequently normalized to M_{sup} (RMS/M_{sup}).

Mechanical data acquisition and analysis: Voluntary and electrically evoked torque was obtained from the right plantar flexors using a calibrated dynamometric pedal (Celiens-Meiri, France) interfaced with an acquisition system (Biopac, MP150, Santa Barbara, CA). Subjects were comfortably seated on an adjustable chair with their right foot attached to the pedal using Velcro straps to secure ankle positioning. The ankle joint was set at 90° and the knee joint at 110° (180° full extension). The axis of the dynamometer was aligned with the anatomical ankle plantarand dorsiflexion axis. The amplitude of the torque evoked by each 1 s stimulation train for the force-frequency relationship was analyzed for the maximal value at 100 Hz.

5.4.2 Electrode characterization for stimulation

We quantified textile electrode properties in electrical stimulation by measuring their electrochemical behavior in an electrolyte solution during cyclic voltammetry (CV) measurements (Fig 5.7). CV were performed between potential limits of –0,6 and 0,8 V, with a three-electrode cell with an Ag/AgCl reference electrode, a large Pt mesh counter electrode and the immersed textile electrode as a working electrode, in a 0,01 M NaCl solution. In our study, the charge transfer profile of textile PEDOT:PSS-coated electrodes follows Faradaic behavior while defined by a rectangular shape of the CV profile. The CV data obtained at different scan rates indicate capacitive charge storage with larger CV curve area for faster sweep rate. The CV profile of PEDOT:PSS-coated textile electrodes with a scan rate of 0,01 Vs⁻¹ was used to estimate the charge-injection capability of 56 mC cm⁻². This value is close to the previously reported in the literature [16], however its calculation is based on the planar surface area of the electrode without taking into account the knitted textile structure, which in reality increases electrode's effective area.

5.4.3 EMG recording and stimulation

Set-up and validation of EMG recordings from textile electrodes

One healthy subjects participated in the study. He was physically active with no history of injury of the lower limb. After having received information on the study, he gave their written consent. All experimental procedures were approved by the local ethics committee and were in accordance with the principles of the Declaration of Helsinki for human studies. Mechanical and electrophysiological data were recorded from the right plantar flexors. In our experiments,

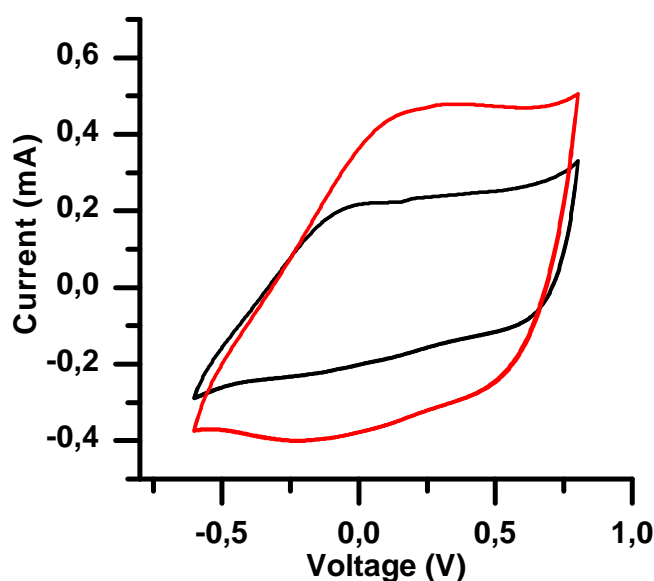


Figure 5.7 – **Cyclic voltammetric measurement on textile electrode.** Cyclic voltammetry measurements with textile electrodes at different scan rate (0.01 Vs^{-1} in black and 0.02 Vs^{-1} in red).

EMG monitoring is performed bipolarly, i.e., two electrodes are placed over the soleus (SOL) muscle of the lower limb. The schematic representation of the experimental setup is shown in Fig 5.8a. In general, electrical stimulation is largely used to boost muscular activity and to produce functional movements by recruiting motor units and triggering neural response. As shown in Figure 1A, when an electrical stimulus is applied over the motor nerve (in this example over the tibial nerve), the direct activation of motor axons and indirect activation of the muscle via spinal loops can be achieved. The performance of these electrodes in EMG monitoring can be seen in Fig 5.8b, where the mechanical torque, the muscle force output produced by the leg during a plantar-flexion movement, is presented with concomitant recordings of the electrical potentials produced by the firing motor units during voluntary contraction. The two textile electrodes are able to monitor the potential variation of the recruited motor units of the SOL muscle while a subject performs an effort to produce steady-state contraction and then slowly increasing the level of contraction force.

Evaluation of stimulation performances for textile electrodes

Textile electrodes were then tested in terms of stimulation performance. The main requirement in cutaneous stimulations is for the electrode to provide optimum performance with a negligible skin damage and pain [17]. In most applications, electrical stimulation is applied as a series of biphasic current pulses [18]. The geometric surface area of the electrode defines the charge and current densities [19]. We evaluated the performance of the conducting polymer-coated textile electrodes to evoke a muscle contraction. In order to compare the stimulation

5.4. Recording and stimulation performances of textile electrodes

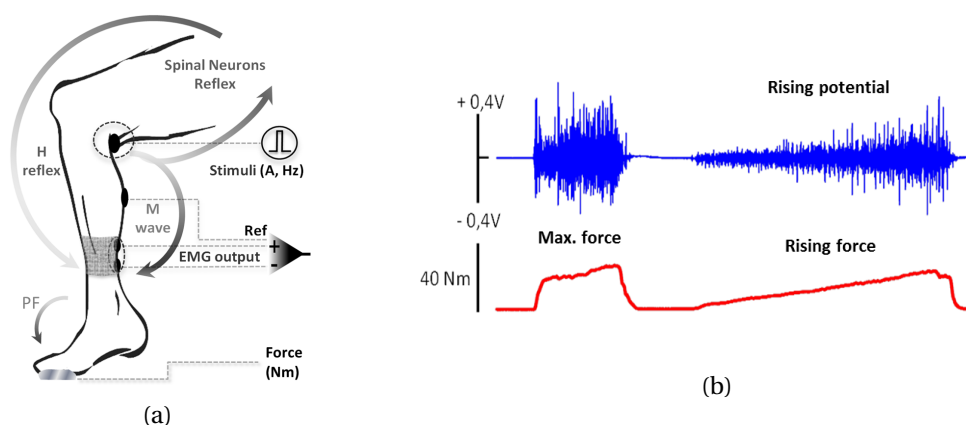


Figure 5.8 – **EMG recording with textile electrode.** (a) Schematic representation of the EMG experimental setup and the pathway of the neuromuscular response associated with a stimulated tibial nerve of the lower limb. The stimulation electrode is placed behind the knees in the location of the tibial nerve. The reference and two textile electrodes are placed in the lower part of the leg. (b) Raw EMG (in blue) and Torque data (in red) recorded with textile electrodes during voluntary plantar-flexion contraction and then repeated after a short pause with a slowly rising force.

performance of medical and textile electrodes, the relationship between the mechanical force and the stimulation at different frequencies was established in one subject. This relationship was obtained by stimulation trains of 1 s duration, delivered at an intensity of 9 mA and with a pulse width of 1 ms, at different frequencies (1, 5, 10, 30, 50, 80, and 100 Hz). The evoked mechanical response produced by the stimulation with medical Ag/AgCl and textile electrodes is shown in Fig 5.9a. Fig 5.9 shows the normalized torque with respect to the torque produced at 100 Hz, for both types of electrodes. These comparisons show that the performance of conducting polymer-coated textiles electrodes is in general comparable with medical electrodes in terms of the recruiting motor units needed to produce a muscle contraction.

5.4.4 Discussion

We have presented an approach which offers countless possibilities to directly integrate conducting polymer-based electrodes in sport wears and monitor electrophysiological activities during physical exercise. We evaluated the performance of PEDOT:PSS-coated textile electrodes in recording voluntary and induced muscle activities in the human lower limb. These electrodes were assisted with an ionic liquid gel to provide better contact of the textile structure with the human skin. The recordings of voluntary and evoked activity in muscles from coated textiles are comparable with those obtained from standard medical electrodes. Transcutaneous stimulations using PEDOT:PSS textile electrodes confirm their efficiency in evoking mechanical contractions triggered by electrically excited tissues with stimulation frequencies up to 100 Hz. Electrical characterizations of textile electrodes support these physiological data, and show that these organic electrodes are able to efficiently conduct an electrical stimulus.

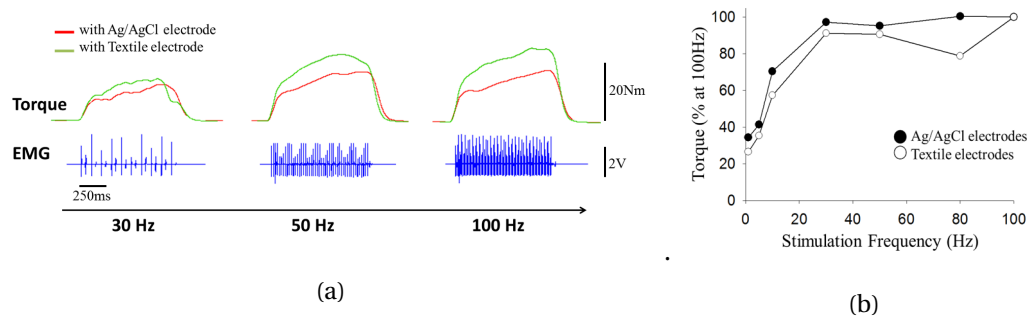


Figure 5.9 – Performance of conducting polymer textile electrode in muscular stimulation. (a) Raw torque response (Nm) and EMG signals (V) obtained at different stimulation frequencies with stimulation trains of 1 s duration, delivered at an intensity of 9 mA and with a pulse width of 1 ms. Torque curves show the difference in the mechanical force produced by the stimulation using medical Ag/AgCl and textile electrodes; (b) Normalized torque at 100 Hz versus stimulation frequency relationship is showing comparable behavior between medical and textile electrodes in recruiting motor units to produce a muscle contraction.

The developed technology in this study provides an affordable electrofunctional textile platform for electrophysiological applications. It can be easily used in order to evaluate muscle function and provide electrotherapeutical assistance in case of post-traumatic rehabilitation. The potential of these electrodes in wearable applications has been demonstrated in the previous Section 5.3, showing their outstanding long-term performance in cardiac monitoring. Future applications will involve integrating these organic electronic textiles in garments with bifunctional electrical capabilities. Such smart textiles are highly demanded in biomedicine where wearable cutaneous electrodes are needed to diagnostic electrophysiological pathologies, provide electrotherapeutic assistance of electroexcitable tissues, survey bioimpedance on damaged epidermis, and to locally deliver chemicals by electrophoresis.

5.5 Bibliography

- [1] Chin-Teng Lin, Li-Wei Ko, Jin-Chern Chiou, Jeng-Ren Duann, Ruey-Song Huang, Sheng-Fu Liang, Tzai-Wen Chiu, and Tzyy-Ping Jung. Noninvasive Neural Prostheses Using Mobile and Wireless EEG. *Proceedings of the IEEE*, 96(7):1167–1183, **2008**.
- [2] P. Fiedler, S. Griebel, C. Fonseca, F. Vaz, L. Zentner, F. Zanow, and J. Haueisen. Novel Ti/TiN dry electrodes and Ag/AgCl: A direct comparison in multichannel EEG. In *5th European conference of the international federation for medical and biological engineering*, pages 1011–1014. Springer, **2011**.
- [3] P. Fiedler, C. Fonseca, P. Pedrosa, A. Martins, F. Vaz, S. Griebel, and J. Haueisen. Novel flexible Dry multipin electrodes for EEG: signal quality and interfacial impedance of Ti and TiN coatings. In *2013 35th Annual International Conference of the IEEE Engineering in Medicine and Biology Society (EMBC)*, pages 547–550. IEEE, **2013**.

-
- [4] P. Salvo, R. Raedt, E. Carrette, D. Schaubroeck, J. Vanfleteren, and L. Cardon. A 3d printed dry electrode for ECG/EEG recording. *Sensors and Actuators A: Physical*, 174:96–102, **2012**.
- [5] J.-C. Chiou, L.-W. Ko, C.-T. Lin, C.-T. Hong, T.-P. Jung, S.-F. Liang, and J.-L. Jeng. Using novel MEMS EEG sensors in detecting drowsiness application. In *2006 IEEE Biomedical Circuits and Systems Conference*, pages 33–36. IEEE, **2006**.
- [6] R. Matthews, P. J. Turner, N. J. McDonald, K. Ermolaev, T. Mc Manus, R. A. Shelby, and M. Steindorf. Real time workload classification from an ambulatory wireless EEG system using hybrid EEG electrodes. In *2008 30th Annual International Conference of the IEEE Engineering in Medicine and Biology Society*, pages 5871–5875. IEEE, **2008**.
- [7] A. Lopez and P. C. Richardson. Capacitive electrocardiographic and bioelectric electrodes. *IEEE Transactions on Biomedical Engineering*, (1):99–99, **1969**.
- [8] C. J. Harland, T. D. Clark, and R. J. Prance. Remote detection of human electroencephalograms using ultrahigh input impedance electric potential sensors. *Applied Physics Letters*, 81(17):3284, **2002**.
- [9] M. Oehler, P. Neumann, M. Becker, G. Curio, and M. Schilling. Extraction of SSVEP signals of a capacitive EEG helmet for human machine interface. In *2008 30th Annual International Conference of the IEEE Engineering in Medicine and Biology Society*, pages 4495–4498. IEEE, **2008**.
- [10] P. Leleux, J.-M. Badier, J. Rivnay, C. Bénar, T. Hervé, P. Chauvel, and G. G. Malliaras. Conducting Polymer Electrodes for Electroencephalography. *Advanced Healthcare Materials*, 3(4):490–493, **2014**.
- [11] W.-H. Yeo, Y.-S. Kim, J. Lee, A. Ameen, L. Shi, M. Li, S. Wang, R. Ma, S. H. Jin, Z. Kang, Y. Huang, and J. A. Rogers. Multifunctional Epidermal Electronics Printed Directly Onto the Skin. *Advanced Materials*, 25(20):2773–2778, **2013**.
- [12] A. Zucca, C. Cipriani, Sudha, S. Tarantino, D. Ricci, V. Mattoli, and F. Greco. Tattoo Conductive Polymer Nanosheets for Skin-Contact Applications. *Advanced Healthcare Materials*, 4(7):983–990, **2015**.
- [13] J. J. S. Norton, D. S. Lee, J. W. Lee, W. Lee, O. Kwon, P. Won, S.-Y. Jung, H. Cheng, J.-W. Jeong, A. Akce, S. Umunna, I. Na, Y. H. Kwon, X.-Q. Wang, Z. Liu, U. Paik, Y. Huang, T. Bretl, W.-H. Yeo, and J. A. Rogers. Soft, curved electrode systems capable of integration on the auricle as a persistent brain–computer interface. *Proceedings of the National Academy of Sciences*, 112(13):3920–3925, **2015**.
- [14] G. D. Clifford, editor. *Advanced methods and tools for ECG data analysis*. Engineering in medicine & biology. Artech House, Boston, Mass., **2006**. OCLC: 255369607.

Chapter 5. Cutaneous electrophysiology with organics

- [15] P. Leleux, C. Johnson, X. Strakosas, J. Rivnay, T. Hervé, R. M. Owens, and G. G. Malliaras. Ionic Liquid Gel-Assisted Electrodes for Long-Term Cutaneous Recordings. *Advanced Healthcare Materials*, 3(9):1377–1380, **2014**.
- [16] S. Wilks. Poly(3,4-ethylene dioxythiophene) (PEDOT) as a micro-neural interface material for electrostimulation. *Frontiers in Neuroengineering*, 2, **2009**.
- [17] T. Keller and A. Kuhn. Electrodes for transcutaneous (surface) electrical stimulation. *Journal of Automatic Control*, 18(2):35–45, **2008**.
- [18] D. R. Merrill, M. Bikson, and J. G. Jefferys. Electrical stimulation of excitable tissue: design of efficacious and safe protocols. *Journal of Neuroscience Methods*, 141(2):171–198, **2005**.
- [19] S. F. Cogan. Neural Stimulation and Recording Electrodes. *Annual Review of Biomedical Engineering*, 10(1):275–309, **2008**.

Potential of OECT for next generation electrophysiology

In the last years, active devices like transistors have shown their advantage of providing increased SNR due to local amplification compared to simple electrodes. These devices combine ease of fabrication, compatibility with mechanically flexible substrates, facile miniaturization, stable operation in aqueous environments, and high transconductance, thereby constituting a low-cost and efficient means to transduce low amplitude signals of biological origin. In this work, we show that Organic ElectroChemical Transistors can also be used as active sensors to monitor vital cutaneous electrophysiological information. After an introduction on organic transistors, we will confirm that OECT can record a wide range of signals with applications in multiple fields of electrophysiology. Then, we will show how it is possible to use it as a simple voltage amplifier to enable direct connection with clinical acquisition systems.

Data presented in this chapter were included in the following publications :

P. Leleux, J. Rivnay, T. Lonjaret, J.-M. Badier, C. Bénar, T. Hervé, P. Chauvel, and G. G. Malliaras, *Organic Electrochemical Transistors for Clinical Applications*, Adv. Healthc. Mater. 4, 142–147 (2015)

M. Braendlein, T. Lonjaret, P. Leleux, J.-M. Badier, and G. G. Malliaras, *Voltage amplifier based on organic electrochemical transistor*, Adv. Science, doi: 10.1002/advs.201600247 (2016)

P. Gkoupidenis, D. A. Koutsouras, T. Lonjaret, J. A. Fairfield, and G. G. Malliaras, *Orientation selectivity in a multi-gated organic electrochemical transistor*, Sci. Rep. 6, 27007 (2016)

Integration of Organic Electrochemical and Field-Effect Transistors for Ultraflexible, High Temporal Resolution Electrophysiology Arrays, W. Lee, D. Kim, J. Rivany, N. Matsuhisa, **T. Lonjaret**, T. Yokota, M. Sekino, G. G. Malliaras and T. Someya, Adv. Mater., doi: 10.1002/adma.201602237 (2016)

6.1 Introduction on Organic ElectroChemical Transistors

6.1.1 Organic transistors

The field-effect transistor (FET) is used for amplification and switching. This transistor is nowadays omnipresent in all digital electronic devices. It is a three-terminal device, with drain (D), source (S) and gate (Gate). Usually, source and drain electrodes are symmetric (in design and fabrication) and connected by the channel region. Because FETs are unipolar transistors, the channel is a semi-conductor made of only one charge carrier (n-doped transistor in case of electrons, p-doped transistor in case of holes). The FET is regulated by an applied gate voltage, V_{gs} , which allows an electrical current, I_{ds} , to flow through the channel by increasing its conductivity (enhancement mode transistor) or conversely by reducing the current flow (depletion mode transistor). The gate is insulated from the device. For the most common FET, the MOSFET (for metal-oxide-semiconductor field-effect transistor), this insulating layer is typically made of SiO_2 . Main advantages of FETs are their high input impedance (ratio of gate potential versus drain current), low noise production, immunity to radiations, no offset voltage at zero drain current and low-power switching. FETs integrated on planar and flexible devices have been successfully used to record *in vitro* and *in vivo* neural signals from brain slices and full brain [1, 2, 3, 4]. However, the integration on flexible substrate is not obvious. Moreover, some oxide layer of FETs are not biocompatible and then need to be encapsulated. TFTs (for Thin-film transistors) are another kind of FET made by successive deposition of nanometers-thick layers (metal, semi-conductor and insulator) on a non-conductive supporting substrate (unlike other FETs where substrate is the semi-conductor material). The main application for TFTs is for display matrix for LCD (liquid-crystal display) screens.

An organic field-effect transistor, or OFET, is a FET with a channel made of a conjugated organic semi-conductor material. Mass fabrication in a cost effective manner of large-area organic products is possible since they can be solution processed. Moreover, organic technologies permit flexible, biocompatible and biodegradable OFET. Many OFET are based on the TFT model. In order to reduce the number of wires in experiments with multi-electrode arrays, pentacene-based OFETs were successfully used to build active switching matrices and presented low toxicity to surrounding cell networks [5, 6]. OFETs can be integrated into flexible ultra-thin substrates for e-skin applications, such as pressure, temperature and optical sensors [7].

6.1.2 The Organic ElectroChemical Transistors

A schematic representation of the Organic electrochemical transistor (OECT) is given in Fig 6.1a, b. The OECT is a three terminal device with electrodes called Drain, Source and Gate. A semiconductor film, the channel, connects Source and Drain. It is usually made of a conjugated polymer, typically PEDOT:PSS. The main difference between an OECT and an OFET is that for the OECT, channel and Gate electrode are immersed directly in an electrolyte,

6.1. Introduction on Organic ElectroChemical Transistors

instead of being separated by a dielectric. Thereby, OECTs are part of the family of electrolyte-gated transistors [8][9]. In a basic configuration, a voltage, V_{ds} , is applied between Source and Drain while Source is grounded. This involves a current, I_{ds} , and thus electronic charges (usually holes) flow through the channel. When a voltage is applied between Source and Gate, V_{gs} , channel resistance (and then I_{ds}) is modulated: ions from the electrolyte are injected in the bulk material and change the number of holes by dedoping the conducting polymer [10]. The OECT can work in both accumulation [11] or depletion mode. In the case of a PEDOT:PSS channel, a p-type semiconductor, the OECT works in a depletion mode. In this thesis, OECT channel are always made of PEDOT:PSS, a depletion mode will always be described. When no gate voltage is applied, I_{ds} reaches its maximum amplitude and the device is ON. If a gate voltage is applied, cations compensate sulfonate anions on the PSS chain. When the channel is fully dedoped, I_{ds} is very low and the device is OFF [12].

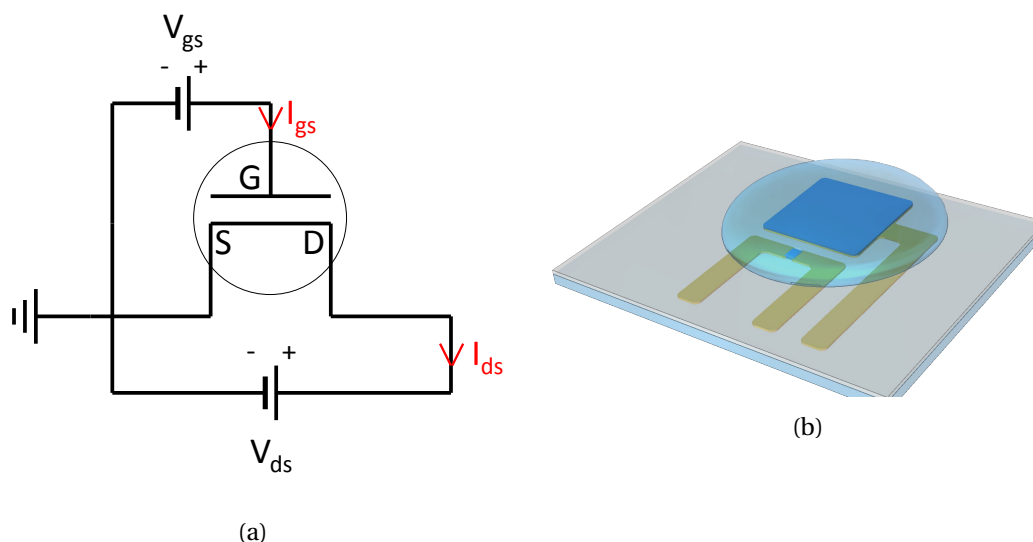


Figure 6.1 – **Schematic of the OECT.** (a) Electric configuration of the OECT for measurement. (b) Cartoon of an OECT with Source and Drain gold lines, PEDOT:PSS channel, planar Gold/PEDOT:PSS Gate and the electrolyte.

6.1.3 Fabrication process

Standard fabrication process by photolithography

Initially developed for photography [13], photolithography is a process used in microfabrication to pattern thin film on a substrate. A light-sensitive photoresist is deposited on the substrate and then exposed to UV light through a photomask to define patterns. The substrate is then immersed in a developer solution. If the photoresist is positive, exposed parts will be removed by the developer solution. In the case of a negative photoresist, only the exposed parts will stay. Another material is then coated on the substrate. After removal of the remaining photoresist, this new material is patterned according to the initial pattern on the photomask.

Chapter 6. Potential of OECT for next generation electrophysiology

This fabrication process is used everyday in microelectronics field to pattern conducting lines and components for circuits. The pattern resolution is now pushed down to 15 nm [14].

The use of organic materials for OECTs allows easy fabrication with low temperature processing techniques, such as photolithography, screen printing or inkjet printing. It provides a future perspective for large scale manufacturing of flexible, disposable and reasonably priced sensor devices on a broad range of substrates [15, 16, 17]. OECTs have even be made by using plants components such as xylem, leaves, veins, and plant signals after soaking them in a PEDOT solution [18]. The fabrication process herein presented, including photolithography and etching steps, was first developed by Sessolo et al. [19] to pattern Gold/PEDOT electrodes and then adapted for OECT fabrication [20, 21, 22, 23].

All of this protocol was developed in a clean room environment in order to prevent any contamination of micro-particles that could disturb the uniformity of the surfaces or induce resistance on electrical lines. Standard microscope glass slides are cleaned via sonication in an acetone and isopropyl alcohol solution and dried with nitrogen (Fig 6.2a) to remove dust and contamination from the surface of the substrate. Positive S1813 photoresist is spin-coated, baked and then exposed to UV with a SUSS MBJ4 broad band UV light mask aligner. It is developed with MF-26 developer to remove exposed photoresist parts (Fig 6.2b). This facilitates the patterning of connection pads and interconnects. After thermal evaporation of 10 nm of Chromium (Fig 6.2c) as a bonding layer, followed by evaporation of 100 nm of Gold (Fig 6.2d), the conductive lines are defined by lift-off: acetone is used to remove the resist, and only the metal layers deposited directly on the glass stay (Fig 6.2e). A first 2 μm thick layer of parylene C, deposited via a SCS Labcoater 2 together with a small amount of 3-(trimethoxysilyl)propyl methacrylate (A-174 Silane) to enhance adhesion, acts as an insulator to define the active area and to prevent disturbing capacitive effects at the metal liquid interface (Fig 6.2f). Subsequently, an anti-adhesive layer is spin coated using a 2% dilution of industrial cleaner (Micro-90) (Fig 6.2g). A second 2 μm parylene C sacrificial layer is evaporated (Fig 6.2h). The final photolithographic patterning step is that of the PEDOT:PSS channel and gate. AZ9260 photoresist is spin-coated, baked, exposed, and developed in AZ developer (Fig 6.2i). The resist is then used to protect the Parylene C layer from a subsequent plasma reactive ion etching (15 min) via an Oxford 80 Plasmalab plus. Where no photoresist is present, the layers of Parylene C and soap are removed by etching, but not the gold (Fig 6.2j). A dispersion of PEDOT:PSS with ethylene glycole, DBSA and GOPs (as presented in 3.2.2) is spin-coated (3000 rpm), on top of the device and soft-baked (Fig 6.2k). Changing speed and time of spin-coating give the opportunity to tune the PEDOT:PSS thickness and so the geometry and performances of the OECT [24]. The PEDOT:PSS thus covers the whole glass slide and fills the “wells” defined in the second photolithographic patterning step. The sacrificial top Parylene C layer is mechanically peeled off to pattern the PEDOT:PSS channel (Fig 6.2l). The completed device is hard-baked (annealed) at 130 °C for 1 h, and then rinsed/soaked in DI water overnight to remove excess low molecular weight components.

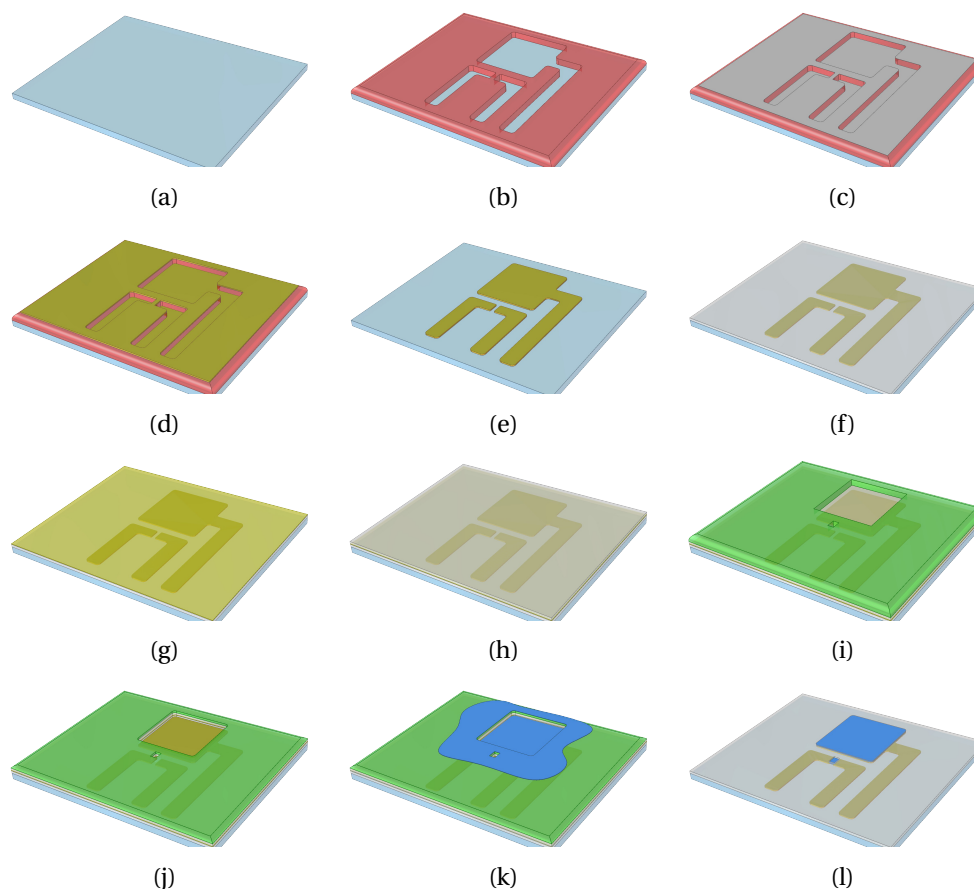


Figure 6.2 – **OECT fabrication process with photolithography.** (a) Blank glass slide. (b) Positive developed resist. (c) Evaporated layer of Chromium. (d) Evaporated layer of Gold. (e) Device after liftoff (f) Evaporated insulating Parylene C layer. (g) Deposition of a soap layer. (h) Evaporated sacrificial Parylene C layer. (i) Positive developed resist. (j) Etched device. (k) Spin-coated PEDOT:PSS. (l) Final device after peel-off of the sacrificial layer.

Modification of the annealing temperature of the channel

For some specific reasons, other materials present on the device could not be able to keep their properties during the usual annealing of the PEDOT:PSS channel (130 °C during 1 h). We showed that, if needed, the hard-baking of the channel can be reduced to 55 °C for 12 h. To investigate the stability of this PEDOT:PSS low temperature cross-linking, transconductance of OECTs achieved by this method was continuously measured for 8h (Fig 6.3a). The result showed minimal changes (1.7%) all along the measurements and prove long-term stability of the transconductance. In addition, there was only a 15% change in the transconductance and a 1.5% change in the response time between the typical condition and the low temperature condition, obtained by comparing the data for each condition of the OECT with a channel width (W)/length (L) = 32 μm /8 μm (Fig 6.3b, c). This result allows the integration of different materials, less resistive to heat, during the fabrication process.

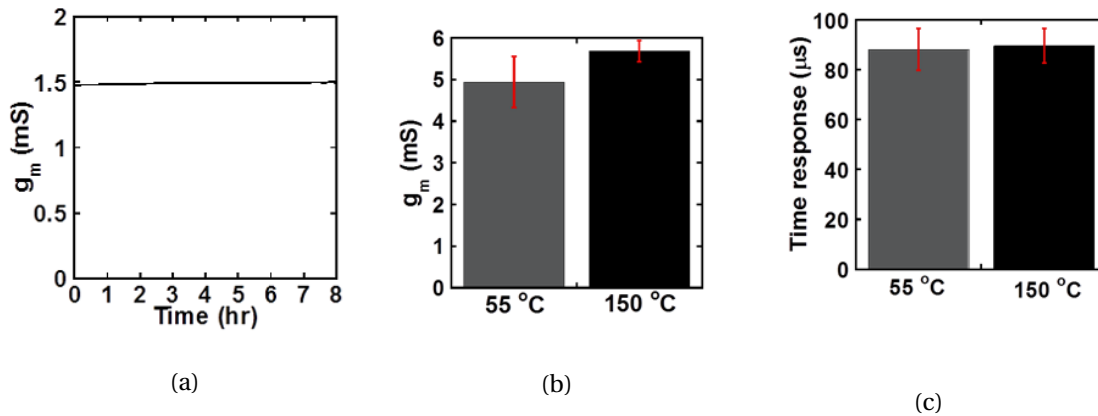


Figure 6.3 – **Characteristics of low temperature annealed OECTs.** (a) Long-term stability of the transconductance of an OECT annealed at 55 °C for 12 h ($V_{ds} = -0.6$ V; Channel Width = 100 μ m; Channel Length = 100 μ m). (b) Transconductance comparison in the same condition of the OECTs annealed at 55 °C and 150 °C ($V_{ds} = -0.6$ V; Channel Width = 32 μ m; Channel Length = 8 μ m). (c) Transconductance comparison in the same condition of the OECTs ($V_{ds} = -0.6$ V; Channel Width = 32 μ m; Channel Length = 8 μ m).

6.1.4 Applications of the OECT

Matured by Wrighton's group in 1984 [25], the OECT has been improved, characterized and included in multiple devices for the last 15 years. Its numerous advantages such as low-cost and adjustable fabrication processes, biocompatibility, high-transconductance and tunable response –time pave the way for a broader use of the OECT in fields as different as bio-sensors and neuromorphic computing. It can be used as a regular transistor and then be included in logic circuits (inverter, NAND or NOR gates...)[26]. Recent works showed that neuromorphic functions can be realized from OECTs [23][27]. In this case, the OECT can process spatiotemporal information the same way as neurons are processing the same information: short-term depression, dynamic filtering, orientation selectivity and short- to long-term memory transition. The OECT is also a useful tool to verify and dynamically measure the integrity of a cultured cell layer located between the channel and the Gate electrode. Here, a phosphate-buffered saline acts both as media for cells and electrolyte to de-dope the PEDOT:PSS channel. The presence of the cell barrier reduces the mobility of ions in the electrolyte and thus increases the response time of the OECT. Then, toxins for the cell layer (ethanol, H_2O_2 , thylene glycol-bis(beta-aminoethyl ether)-N,N,N',N'-tetra acetic acid (EGTA) for the gastrointestinal epithelium for instance) can disrupt the tight junctions between the cells and increase the response time back to the initial value [28][29]. Compared to conventional methods for measuring barrier tissue integrity, the OECT presents an increased temporal resolution and greater or equal sensitivity. It can detect bacteria such as *Salmonella typhimurium* in a complex media (milk) [21] and this electrical sensing can be combined with optical sensing to follow evolution of kidney cell layers [30]. By adding (functionalize) new components on the OECT components, it is possible to modify its behavior and to make it sensitive to specific biological

6.2. OECT as a pre-amplifier for electrophysiological recordings

components. A chitosan-ferrocene solution can be added to a solid-state electrolyte in order to develop a screen-printed glucose and lactate sensor [31]. Most of time, the Gate electrode is functionalized to facilitate reactions with the electrolyte that contains the component to be measured. Tang et al. showed a great-performing glucose-oxidase Platinum Gate for glucose sensing [32]. Lin et al. demonstrated the feasibility of a flexible OECT integrated onto a micro-fluidic channel to detect DNA targets [33]. In this case, the Gate electrode was functionalized with DNA probes and the hybridization with the complementary DNA target changed Gate properties and then channel current. A new technique involving poly(vinyl alcohol) (PVA) addition on the PEDOT:PSS-coated Gate was developed by Strakosas et al. to help bio-functionalization of the Gate and anchorage of biomolecules while maintaining OECTs performance [34]. It allowed the fabrication of a sensing platform for glucose, lactate and cholesterol using OECT and able to sense at the same time these components from few drops of saliva [35]. Recently, OECT were used as neuro-sensors. If an OECT is placed close to a neuron or any electroactive cell, the generated electric field will overlap the Gate signal and then modulate the channel current. Since bio-fluids (Cerebrospinal fluid, blood...) can conduct electrical currents, they can act as electrolyte for the OECTs and these OECTs are then able to measure *in vivo* electrophysiological activity. Khodagholy et al., presented organic transistors integrated on a flexible and biocompatible substrate that gave the opportunity to record brain activity from the surface of the brain with signal-to-noise ratio compared to surface electrodes, which hold great promise for diagnostic purpose and brain-machine interfaces [36]. It is also possible to integrate OECTs on delaminating depth probes to interact and measure from inside the brain [37]. In this case, the transistors can measure activity or stimulate a small population of neurons without affecting the nearby other neurons.

6.2 OECT as a pre-amplifier for electrophysiological recordings

Results from other teams, coupled with the potential for low-cost fabrication, show that OECTs constitute a promising solution as amplifying transducers for electrophysiology and calls for a broader investigation of their capabilities to record cutaneous electrical signals of relevance to the clinic. In this section, we show that OECTs are able to measure a wide range of typical clinical physiological signals of a human volunteer: ECG, EOG and EEG.

6.2.1 Connection set-up and Characterization

Experimental part for cutaneous recordings

OECT fabrication: OECT were fabricated following the protocol presented on Section 6.1.3. *OECT electrical characterization:* All characterization was done with a solution of 0.1 M NaCl in DI water as the electrolyte and a Ag/AgCl wire (Warner Instruments) as the gate electrode. The measurements were performed using a National Instruments PXIe-1062Q system. The channel of the OECT was biased using one channel of a source-measurement unit NI PXIe-4145. The gate voltage was applied using a NI PXI-6289 modular instrument. Output and transfer curves

were collected using the SMU channel used to apply the bias. For time response and bandwidth characterization of the OECT, one NI-PXI-4071 digital multimeter measured the drain current, and a channel of the NI PXI-6289 measured the gate voltage. The bandwidth measurements were performed by applying a sinusoidal modulation (10 mV peak-to-peak), $V_{ds} = -0.6$ V, and measuring the modulation in the drain current, and therefore g_m as a function of frequency. All the measurements were triggered through the built-in PXI architecture. The recorded signals were saved and analyzed using customized LabVIEW software.

In vivo recordings: All patients provided informed signed consent to participate in the study. Commercially available Ag/AgCl electrodes (Comepa Industries) were used to establish contact between the skin and the appropriate terminals of the transistors. The measurements were performed using a National Instruments PXIe-1062Q system. In both cases, the channel of the OECT ($V_{ds} = -0.6$ V) was biased using one channel of a source-measurement unit NI PXIe-4145 and the recording of the drain current was made using the same SMU channel with a sampling rate of 1 kHz. All the measurements were triggered through the built-in PXI architecture. The acquisition system was controlled using customized LabVIEW software.

Post-acquisition data treatment: All recordings were digitally filtered using a 0.1 Hz high pass filter (in principle, an appropriate low pass filter could also be used to reject high frequency noise). The data were analyzed using custom-written tools in MATLAB (Mathworks). Spectral analysis was performed using fast Fourier transform of the EEG signal between 0.1 and 50 Hz. A Gabor wavelet time–frequency analysis was used to determine the frequency content of the recordings.

***in vitro* characterization of the OECT**

As shown in Section 1.1, electrophysiological signals recorded from skin range from a millivolt to tens of microvolts, a range that is representative of the majority of the noninvasive signals measured in the field of electrophysiology. EEG, in particular, represents a challenge, as it requires the ability to measure signals that are two orders of magnitude lower than the ones usually measured by OECTs [36, 38]. We used an OECT that shows a high transconductance at zero gate voltage, [39]. The OECT had a PEDOT:PSS channel with length of 100 μm , width of 100 μm , and thickness of 140 nm, and a Ag/AgCl external gate electrode. Its output curves, shown in Fig 6.4b, are typical for operation in the depletion mode. The transfer curve and corresponding transconductance for $V_{ds} = -0.6$ V are shown in Fig 6.4c. At zero gate voltage, the OECT shows a high transconductance of 1.3 mS. The frequency response of the transconductance was measured by applying $V_{ds} = -0.6$ V and using a small AC modulation at the gate, as shown in Fig 6.4a. The resulting bandwidth is shown to exceed 100 Hz 6.4d, and is therefore adequate for the applications pursued herein.

6.2.2 Results on ECG

After *in vitro* characterization, we wired the transistor as shown in Fig 6.4a and 6.5a, using electrical potentials of the human body to drive the gate circuit. We first demonstrate the

6.2. OECT as a pre-amplifier for electrophysiological recordings

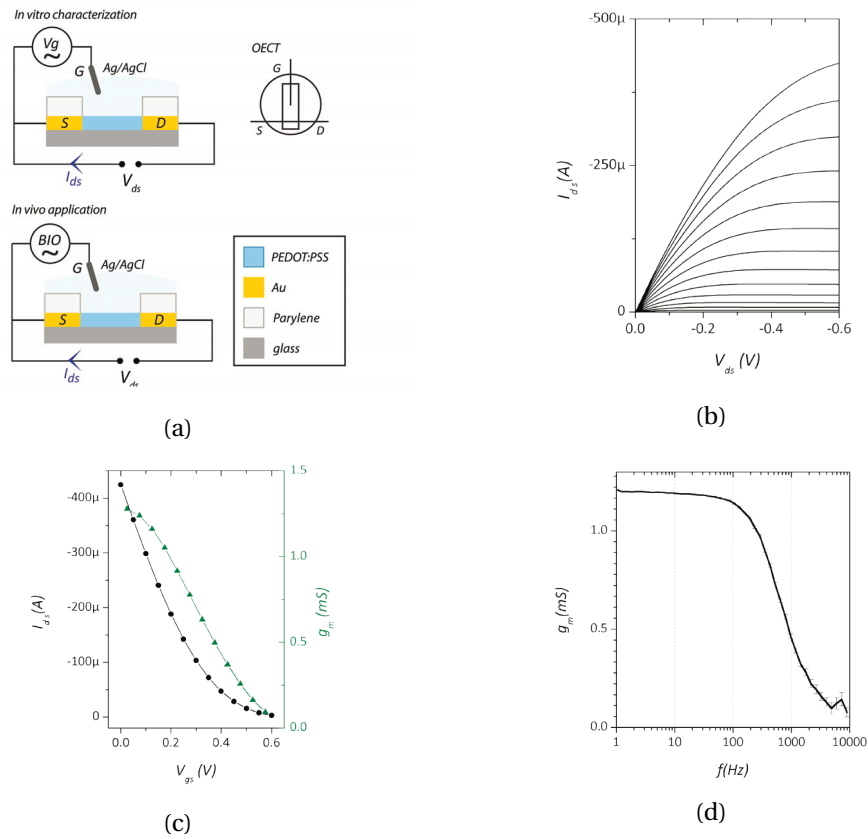


Figure 6.4 – **Set-up of the OECT as pre-amplifier and characterization.** (a) Schematic of an OECT and the wiring diagrams used in vitro (top) and in vivo (bottom). (b) Output characteristics for V_{gs} varying from 0 (top curve) to +0.6 V (bottom curve) with a step of +0.05 V. (c) Transfer curve for $V_{ds} = -0.6$ V, and the associated transconductance. (d) Frequency dependence of the transconductance. The device was biased with $V_{ds} = -0.6$ V and $V_{gs} = 0$ V, and an additional 10 mV peak-to-peak gate voltage oscillation was applied to measure the small signal transconductance.

application of OECTs in electrocardiography, which corresponds to the signal with the largest amplitude among the ones considered here. Here we measure ECG in the standard configuration used in the clinic. The measurement configuration, shown in FIG 6.5a, consisted of two identical OECTs making four contacts to the body. The first OECT measured the voltage difference between electrodes placed at the left and right arms, while the second one measures the voltage difference between the left leg and left arm. This is the standard two main limb lead configuration, however, the setup can be extended in a straightforward way to the full “12-lead” system for diagnosis purposes (see Section 1.1). Representative recordings of the drain current of the two OECTs are shown in Fig 6.5b. The temporal coincidence of the peaks in the traces recorded by the two OECTs confirms the biological origin of the recorded activity. The recorded traces correspond to the expected electrical activity of a human heart: The main peak, called the QRS complex, reflects the depolarization of the ventricles. It has a peak-to-

peak amplitude of the order of a mV, and a duration around 100 ms. The P and T waves correspond to normal atrial depolarization and repolarization of the ventricles, respectively. They are usually around 200 μV in peak-to-peak amplitude with a duration around 80 and 160 ms, respectively. These peaks are well resolved with the OECT, with the QRS complex corresponding to an easily readable change of 1 μA in the drain current, demonstrating the potential of this device for measurements at a clinical setting.

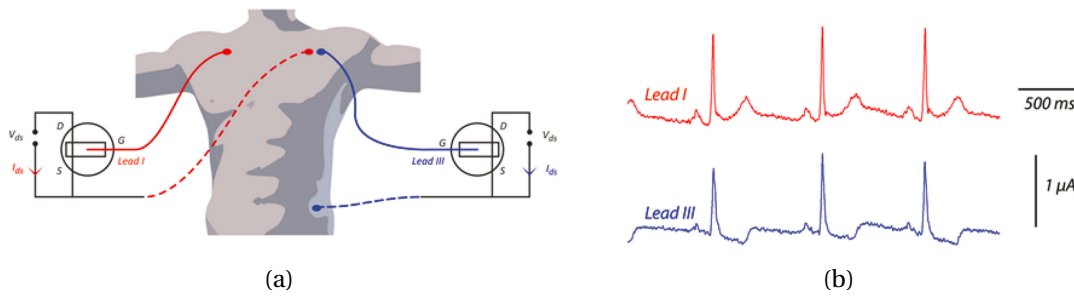


Figure 6.5 – **ECG with OECT as pre-amplifier.** (a) Wiring configuration of the OECT for spontaneous ECG recordings. (b) Spontaneous heart activity measured on a human volunteer.

6.2.3 Results on EOG

We investigated the suitability of OECTs for the application of electrooculography by measuring both horizontal and vertical eyeball movements. We used two OECTs, wired as shown in Fig 6.6a, to simultaneously track both the horizontal (blue traces) and vertical (red traces) movements of the eyes of a human volunteer. The volunteer looked straight in front of him at a specific marker, and was then asked to move his eyes into extreme positions. Fig 6.6b,c shows the recorded signal, in the case of horizontal and vertical eye movement, respectively. The baseline corresponds to the eyes looking at the central position. The amplitude of the recorded signal is larger on the channel following the movement direction: The blue trace, following horizontal eye movements is larger in Fig 6.6b than in Fig 6.6c, and vice versa for the red trace. In the case of the horizontal eye movements, the signal presents an equal amplitude change around the baseline when the eyes move to extreme left and extreme right positions. This symmetry is lost in the case of the up/down eyeball movement, which is expected due to the presence of the supraorbital ridge that limits the movement of the eyeball in the up direction. These recordings, which show drain current changes in the range of hundreds of nA, confirm that the OECT can be used to monitor eye movement. It should be noted that diagonal or unusual movements of the eyeballs could also be tracked by analyzing the horizontal and vertical components of the movement registered on the two transistors.

As explained in Section 1.1.2, an additional use of EOG is to detect drowsiness, which is extracted from the amplitude, frequency, and duration of spontaneous blinking. We measured the blinking pattern of an awake human volunteer, and compared it to the pattern corresponding to the intentional closing of the eye in Fig 6.7 (The wiring configuration used here is the same as for the EOG measurement (see Fig 6.6a). The OECT was able to record both of

6.2. OECT as a pre-amplifier for electrophysiological recordings

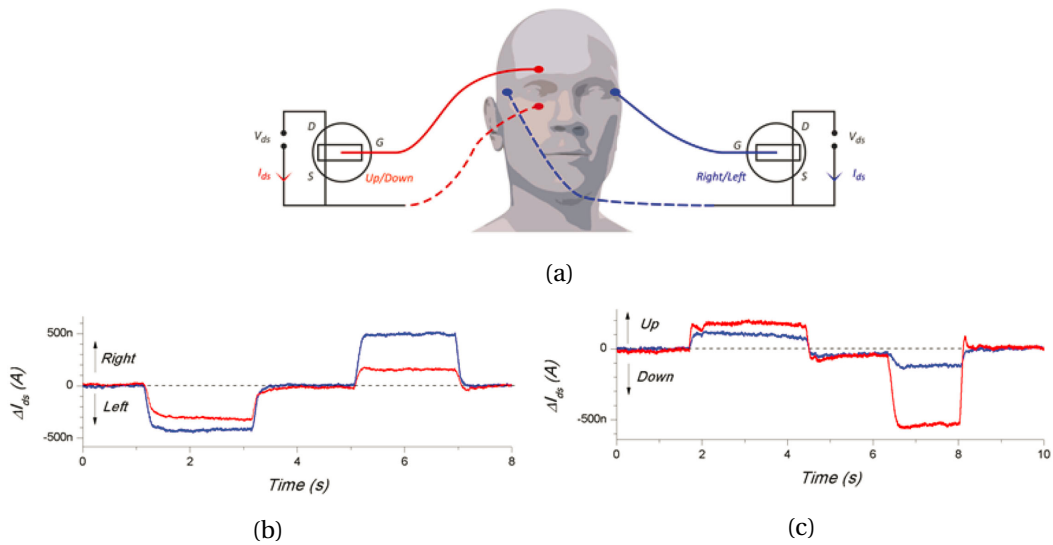


Figure 6.6 – **EOG with OECT as pre-amplifier.** (a) Wiring configuration of the OECT for EOG recordings. (b) Recording of electrical activity during left/right eyeball movements. (c) Recording of electrical activity during up/down eyeball movements. Both up/down (red) and left/right (blue) activities are measured.

these signals, showing a larger amplitude in the vertical direction, which corresponds to the direction of eyelid movement. The blinking pattern shows a rise time around 100 ms whereas response time was about three times longer when the eye was closed intentionally. OECTs, therefore, can accurately resolve eye blinking and are suitable for applications in the detection of drowsiness.

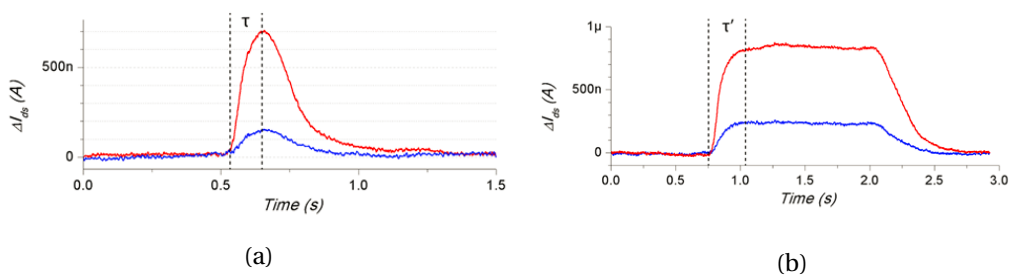


Figure 6.7 – **Eye blinking and closing recorded with OECT as pre-amplifier.** (a) Electrical recording of eye blinking, where τ corresponds to the rise time of the signal (approximately 100 ms). (b) Electrical recording of eye closing, where τ' corresponds to the rise time of the signal (approximately 300 ms). The red curves correspond to the vertical direction recording and the blue curves correspond to the horizontal direction recording.

6.2.4 Results on EEG

The last clinical diagnostic technique we investigated is electroencephalography. We measured alpha rhythm on an awake human volunteer using the recording configuration shown in Fig 6.8a. A sample extracted from a recording is shown in Fig 6.8b (top), demonstrating that spontaneous brain activity induces drain current changes of the order of tens of nA. The corresponding time–frequency analysis (bottom) reveals frequency components corresponding to the alpha rhythm, as expected regarding the behavior of the subject during the measurement [40]. The high quality of the signal can be seen in Fig 6.8c, which displays the fast Fourier transform of a 3 min recording: A clear peak corresponding to the alpha rhythm is well resolved over the $1/f$ background activity of the brain. This confirms that OECT provides sufficient resolution to successfully capture brain oscillations.

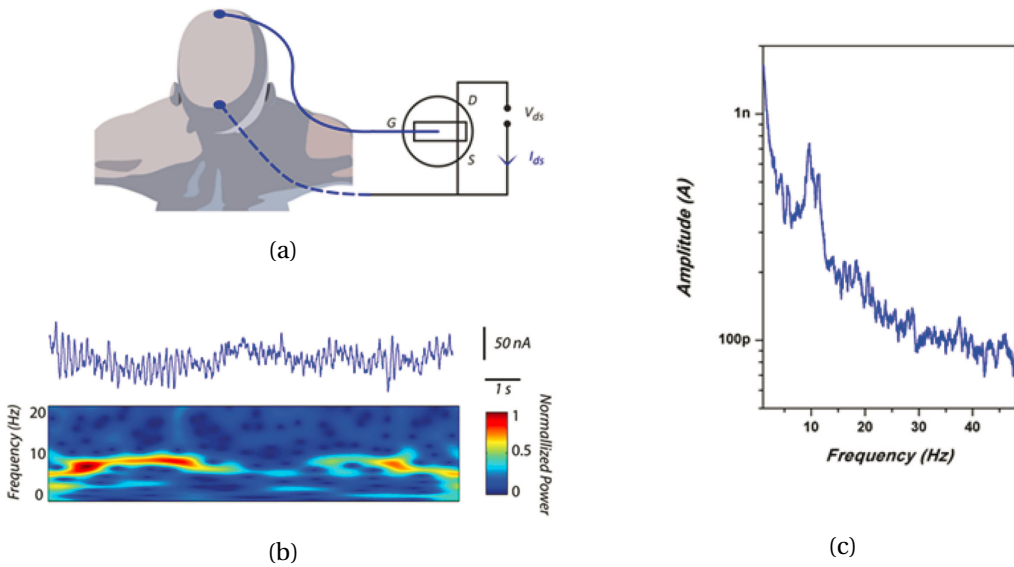


Figure 6.8 – EEG with OECT as pre-amplifier. (a) Wiring configuration of the OECT for EEG recordings. (b) Recording of spontaneous brain activity (top) showing the alpha rhythm, and associated time-frequency spectrogram (bottom). (c) Fourier analysis of a 3 min recording.

6.2.5 Discussion

In this work, we showed the ability to perform high-quality and clinically relevant recordings, with an OECT. We used an OECT that shows a high (>1 mS) transconductance at zero applied gate voltage, which necessitated only one power supply to bias the drain, while the gate circuit was driven by cutaneous electrical potentials. The OECT was successful in recording cardiac rhythm, eye movement, and brain activity of a human volunteer. In each case, the OECT was connected to patient’s body through cutaneous electrodes that were peaking up potentials. It means we were using the OECT as a pre-amplifier. However, the recorded signal was a

current and thus not compatible with standard medical acquisition systems, which amplify and process voltage signal.

6.3 Enabling the compatibility of OECT technology with medical systems

As shown in previous section 6.2, a key limitation of OECT, lies in the fact that their output is a current, while most electrophysiology equipment requires a voltage input. In this section, we focus on the integration of the OECT into a simple voltage amplifier circuit (with a drain resistor) to provide a voltage-to-voltage transduction, as first introduced by Rivnay et al. [39]. A simple circuit is built and modeled that uses a drain resistor to produce a voltage output.

6.3.1 Experimental part

OECT fabrication: OECT were fabricated following the protocol presented on Section 6.1.3.
Device characterization: All experiments were done using a NaCl solution (0.1 M) as electrolyte and a Ag/AgCl pellet (Warner Instruments) as gate electrode. The IV curves were recorded using a Keithley 2612A dual SourceMeter. For the pre-characterization experiments with the drain load a Voltcraft R-BOX 01 decade resistor box was connected to the OECT and a Keithley 2612A dual SourceMeter was used for the supply voltage, the output voltage was recorded using a National Instruments USB- 6251 BNC data acquisition system and a customized LabVIEW software. The ECG recordings were done in a low noise room at the hospital La Timone in Marseille, France. Ambu sensor N medical Ag/AgCl electrodes with 0.95 cm diameter gel-assisted contact area were used as standard ECG electrodes to make contact with the skin. A battery was used for the supply voltage to reduce the noise coming from building ground and the output voltage was recorded using a Braintronics voltage recording system with Brainbox EEG-1166 amplifiers. The data were treated subsequently using a 49–51 Hz band block fast Fourier transform (FFT) filter, a 100 Hz low pass FFT filter, and a 0.05 Hz high pass FFT filter.

6.3.2 Addition of a load resistor

As described in Fig 6.9a, a resistor, called load resistor R_{load} , is added on the drain side of the OECT. Resistance of the channel is represented by R_0 . With V_{supply} as the supply voltage of the circuit, it forms a voltage divider and the drain voltage V_{out} floats and depends on the drain current I_{ds} , which itself depends on both gate Voltage V_{gs} and V_{out} :

$$V_{out} = V_{supply} - R_{load} \cdot I_{ds}(V_{gs}, V_{out}) \quad (6.1)$$

This circuit forms a voltage amplifier since any modification of gate voltage is related to a

Chapter 6. Potential of OECT for next generation electrophysiology

change in V_{out} . An operation point (OP), depending on R_{load} and V_{supply} , can be defined because each gate voltage is related to a specific output voltage. By solving Eq 6.1 for I_{ds} :

$$I_{ds}(V_{gs}, V_{out}) = \frac{V_{supply} - V_{out}}{R_{load}} \quad (6.2)$$

a so called load line can be plotted on top of the IV curve of the OECT (see Fig 6.9b). The operation point is then extracted at the intersection between the load line and the specific IV curve. It is important to take into account that the resulting transconductance $g_m = \delta I_{ds} / \delta V_{gs}$ can be modified because V_{out} is linearly dependent of I_{ds} . A distinction is done between linear and saturation regime of the OECT and two corresponding operation points are chosen: $OP_{lin} = -0.2V$ (at $V_{gs} = 0V$) and $OP_{sat} = -0.8V$ (at $V_{gs} = 0V$) (circles on Fig 6.9b). Corresponding transconductance curves are calculated and presented on Fig 6.9c, d with and without load resistor. In the linear regime the peak transconductance is shifted toward a higher voltage compare to the same OECT without load resistor. This involves the transconductance at $V_{gs} = 0V$ dropping by more than 50%. However, in the saturation regime, the transconductance is identical to an unload OECT for positive voltages. It can be seen that it deviates only for negative gate voltage. This can be explained by the fact that at negative gate voltage, the OECT operates back at linear regime. Because working at $V_{gs} = 0V$ avoid the use of a supplementary power source and because targeting electrophysiological signals are small (from few μV to few mV), we are mainly interested in operating the device in the saturation regime.

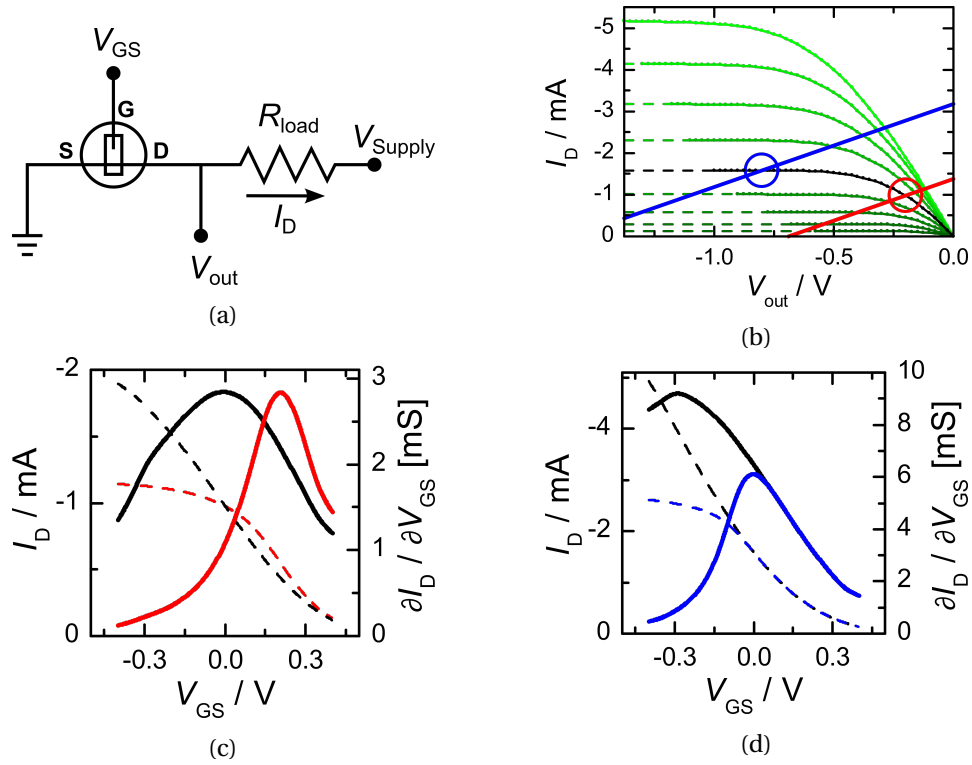


Figure 6.9 – **Characterization of an OECT with drain load resistor.** (a) Voltage amplifier schematic. (b) Load line diagram and IV characterization of the OECT. The gate voltage is varied from $V_{gs} = +0.4$ V (top green curve) to $V_{gs} = -0.4$ V (bottom green curve) in steps of 0.1 V. The black lines indicates the output as $V_{gs} = 0$ V and the open circles denote the operation points. A load resistor of $R_{load} = 500 \Omega$ is used for saturation (blue) and linear (red) regimes. OECT characteristics are $W/L = 2$ and thickness $d = 70$ nm. A solution of 100 mmol NaCl is used as electrolyte. (c) Dashed lines represent transfer curve and solid lines represent transconductance of the unloaded OECT (black) versus the loaded OECT (red) for linear regime. (d) Same as (c) with loaded OECT (blue) in saturation regime. For (c) and (d), values of I_{ds} are extracted from (b) via the intersection of the load line with IV curve for each value of V_{gs} .

6.3.3 Voltage gain in linear and saturation regimes

Because drain current is depending on both gate voltage and source-drain bias, we can use the differential form of $I_{ds}(V_{gs}, V_{out})$ to write:

$$\begin{aligned} dI_{ds} &= \left. \frac{\partial I_{ds}}{\partial V_{gs}} \right|_{V_{out}} dV_{gs} + \left. \frac{\partial I_{ds}}{\partial V_{out}} \right|_{V_{gs}} dV_{out} \\ &= g_m \cdot dV_{gs} + g_d \cdot dV_{out} \end{aligned} \quad (6.3)$$

Chapter 6. Potential of OECT for next generation electrophysiology

where g_d and g_m are the intrinsic transconduction and drain conductance respectively. Eq 6.1 can be derived:

$$dI_{ds} = -\frac{1}{R_{load}} \cdot dV_{out} \quad (6.4)$$

And by inserting Eq 6.4 in Eq 6.3, we get:

$$dV_{out} = -\frac{dV_{out}}{R_{load} \cdot g_d} - \frac{g_m \cdot dV_{gs}}{g_d} \quad (6.5)$$

Which leads us to:

$$Gain = \left| \frac{dV_{out}}{dV_{gs}} \right| = \left| \frac{g_m}{\frac{1}{R_{load}} + g_d} \right| \quad (6.6)$$

In case of saturation regime, the drain current is independent of source-drain bias so it means that $g_d = 0$. Then, from [equation 6] it appears that gain is directly proportional to the transconductance times the load resistor. But in linear regime, the gain is far less important and saturates for high load resistor since $1/R_{load}$ goes to zero. This model and corresponding experimental data are shown on Fig 6.10. A 2 Hz sinusoidal signal with an amplitude of $\Delta V_{gs} = 1$ mV was applied at the gate. Linear and saturation regime are again distinguished: V_{out} was adjusted to obtain OP_{lin} and OP_{sat} for each values of the load resistor. The experimental data fits very well with the model, except for the high load resistor in saturation regime. It could be due to small drift of drain current induced by evaporation of electrolyte and amplified. This would cause the shift toward higher source-drain bias of the operation point at zero gate bias.

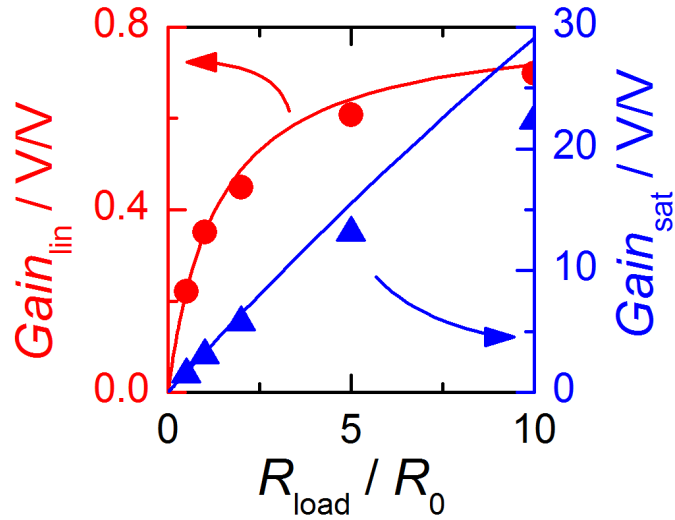


Figure 6.10 – **Experimental data versus model for amplification gain.** Voltage gain $\delta V_{out} / \delta V_{gs}$ for different load resistor for an input signal of $\delta V_{gs} = 1 mV$ in both the linear regime (red, $OP_{lin} = -0.2 V$) and the saturation regime (blue, $OP_{sat} = -0.8 V$). The solid line shows an analytical model extracted from Eq 6.6.

6.3.4 Voltage amplification of ECG signals

In the same manner as in Section 6.2.2, we record heart activity by connecting the body to the OECT through cutaneous medical electrodes. One electrode is likewise connected to source and ground (to simulate $V_{gs} = 0 V$ while the second electrode is connected to an immersed Ag/AgCl gate. Then heart activity is doping and dedoping the OECT channel. In this configuration, the OECT is still not in contact with the skin and acts as an external amplifier but it allows us to modify the load resistor value. Thanks to the voltage conversion carried out by the circuit, we can directly connect the output voltage V_{out} to a medical acquisition system and supply the circuit with a battery to avoid supplementary noise. We record ECG signal with OECT in saturation and linear regime for comparison (see Fig 6.11). As expected, variations of load resistor affect the amplification of the ECG signal. Even if all relevant features of ECG (such as PQRST complexes) can be seen in the case of linear regime, amplification saturates for values of $R_{load} > 5 * R_0$ (see Fig [FIGURE]). At best, a one-to-one amplification is done. The use of the OECT in saturation regime shows stronger amplification of ECG signal, up to 30 V/V. The fact that the experiment was conducted in a low-noise environment (inside Faraday cage) could explain why the SNR seems not to change for the different recordings.

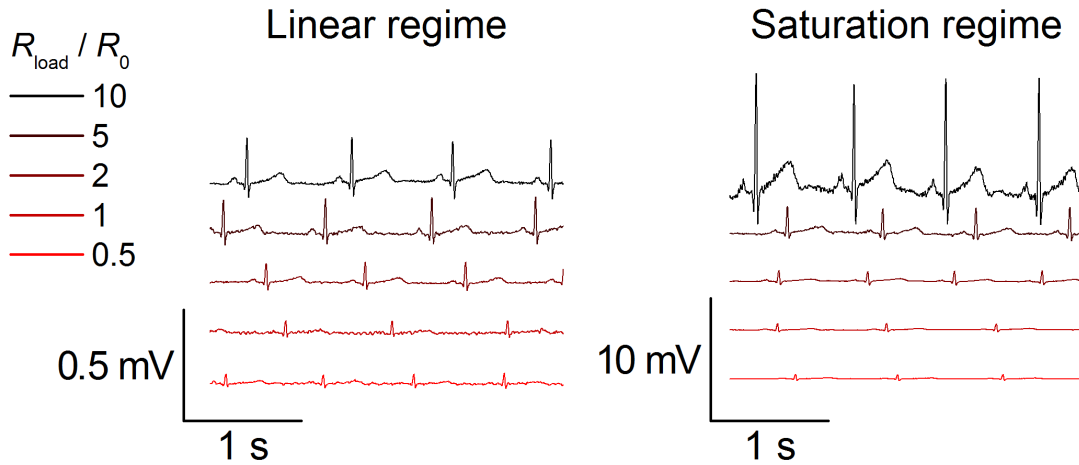


Figure 6.11 – **Amplification of ECG signals in saturation and linear regimes.** (a) ECG recordings for different load resistors from OECTs in linear and (b) in saturation regime. OECT characteristics are $W/L = 2$ and thickness $d = 70$ nm.

6.3.5 Discussion

In this work, we showed the working principle of a voltage amplifier circuit based on a high-transconductance OECT and a simple resistor in series. A floating voltage point is generated, linearly depends on drain current and transduces signal picked up by the OECT. We demonstrated that much better performance was achieved upon driving the transistor in saturation regime. In this case, I_{ds} is independent of V_{ds} and thus output voltage is only dependent on the gate voltage input. Thanks to the voltage-to-voltage amplification of cutaneous signals, we were able to record and save high-quality ECG by using clinical recording systems. To our knowledge, this is the first time voltage-to-voltage amplifying transduction of electrophysiological activity has been demonstrated with an OECT, rendering this device directly useful in a clinical setup. Similarly to what was done in previous Section sec:OECTasPreamplifier, the OECT-based voltage amplifier was deployed from the patient and connected to him by cutaneous electrodes.

6.4 Outlook: Improved OECT in direct contact with skin as active electrodes

This section will present a work that is on going, the integration of OECT and drain load resistor on flexible substrate for cutaneous recordings. Results are not obtained yet, but we give an overview of the working principle of the promising device.

6.4.1 OECT and active electrodes

For most of the electrophysiological recordings, clinicians prefer the use of “passive” electrodes. These passive electrodes are only recording a potential and delivering it to the acquisition system. They are usually cheap, easy to fabricate and for single-use only. An “active” electrode is actually a device containing a passive electrode as well as embedded electronics, all in one package. This on-board electronics usually consists on filters, amplifiers and potentially wireless systems, to *in situ* improve signal quality before it gets disturbed by any external noise [41, 42]. Miniaturized bipolar transistors can be embedded with the electrode, as well as power supply. State-of-the-art active electrodes are less sensible to electromagnetic perturbations and are compatible with clinical recording systems for electrophysiology. Because active electrodes can adapt their impedance to the skin, a conductive gel is unnecessary. Research on active electrodes was initiated at the end of the 60s, but their use was limited to signals with high amplitude such as ECG (see Section 5.1.1). The use of active electrodes for EEG measurements was validated in the 90s. Nowadays, recording systems with active electrodes are available on the market (BioSemi from The Netherlands, Acticap (BrainProduct) from Germany or g.SAHARA (Cortech Solutions), USA). They are performing as good as conventional electrodes but are much more expensive and have difficulties to find their public.

As it was demonstrated in the two previous Sections 6.2 and 6.3, OECT can be used as a voltage amplifier for clinically relevant electrophysiology recordings. It is possible to remove the cutaneous electrode that was connected to the Gate of the OECT, and to bring the electrolyte in contact with skin at the same place where was the electrode. The local potential changes at the interface skin-electrolyte will modulate the drain current, as the Gate electrode was doing. In a sense, the same set-up that was previously explained can be used, minus a wire and a cutaneous electrode. The working principle of the OECT for cutaneous recordings was demonstrated by Campana et al. [38]. They realized a cross-thoracic recording by placing the channel of their OECT on a forearm of a volunteer and a ground electrode connected to the Source on the chest. They were able to record ECG with performances similar to recordings from conventional electrodes. However, transconductance of their OECT was not high and they had to apply two voltage bias (V_{gs} and V_{ds}).

6.4.2 Integration on flexible substrate for skin contact

A permanent contact with the skin cannot be done with a rigid glass slide and thus integration of OECT on conformable substrate is needed. Integration of OECT on flexible substrates were mostly done on Parylene C (see Section 4.1.1 for more details). However, a few micrometer-thick device is actually too thin to be easily manipulated by clinicians. We aim to integrate our device on a flexible 15 μm -thick polyimide (Kapton) for easier handling during fabrication steps and further manipulations. To improve the lift-off fabrication step (to pattern gold lines on the substrates), the first photolithography step (see Fig 6.2b) needs to be modified by the deposition of a lift-off resist (LOR 5A) layer beneath S1813 layer [43, 44]. The drain load resistor

will be also integrated to the flexible substrate and made of gold or PEDOT for a resulting device presented on the cartoon of Fig 6.12

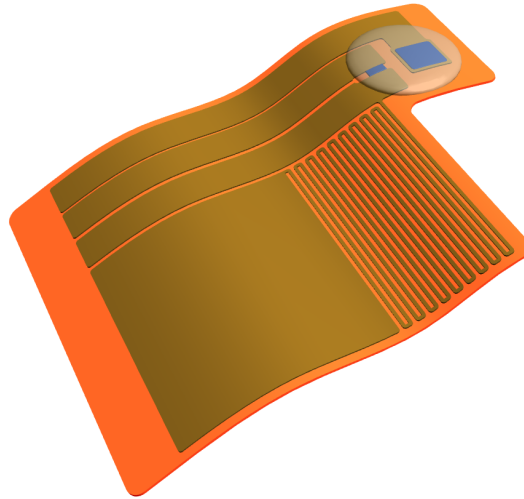


Figure 6.12 – **Cartoon of an active electrode with an OECT.** Source and drain electrodes are visible as well as the channel, the electrolyte which will make contact with the skin, and drain load resistor. The PEDOT-coated electrode close to the channel can be used for *in vitro* characterization of the OECT but also as a passive electrode to compare signal recorded from the OECT.

6.4.3 Work on going

Based on our previous work, we make the hypothesis that it is possible to perform high-quality electrophysiology recordings with a high-transconductance OECT which works at zero gate bias and associated to a drain load resistor. The resulting electrode will be only made of an OECT, an electrolyte, a resistor and one battery. The recorded potential will be amplified by the OECT at the place of the recording, before the addition of external noise to the signal of interest. It is possible to tune the low-pass filtering effect of the amplification by playing with the OECT channel dimensions [24]. Thus we can adapt our active electrode for ECG or EEG specifications and remove frequencies higher than the ones of interest. The use of a liquid electrolyte is impossible for cutaneous applications because it will dry out or leak, and signal recording will be deteriorated or lost. Based on our previous work on gel electrolyte for cutaneous electrodes, an electrolyte made of ion gel or hydrogel will grants an improved contact with the skin as well as the possibility of long-term recordings. The recording area of such a device will be made of a small channel (typically, values of $100\mu\text{m} * 50\mu\text{m} * 100\text{nm}$ are adapted to EEG monitoring) and of the electrolyte drop. The microscopic size of this sensor will give the possibility of EEG recordings between hair or high-density EEG arrays.

6.5 Bibliography

- [1] M. Hutzler and P. Fromherz. Silicon chip with capacitors and transistors for interfacing organotypic brain slice of rat hippocampus. *European Journal of Neuroscience*, 19(8):2231–2238, **2004**.
- [2] B. P. Timko, T. Cohen-Karni, G. Yu, Q. Qing, B. Tian, and C. M. Lieber. Electrical Recording from Hearts with Flexible Nanowire Device Arrays. *Nano Letters*, 9(2):914–918, **2009**.
- [3] Q. Qing, S. K. Pal, B. Tian, X. Duan, B. P. Timko, T. Cohen-Karni, V. N. Murthy, and C. M. Lieber. Nanowire transistor arrays for mapping neural circuits in acute brain slices. *Proceedings of the National Academy of Sciences*, 107(5):1882–1887, **2010**.
- [4] J. Viventi, D.-H. Kim, L. Vigeland, E. S. Frechette, J. A. Blanco, Y.-S. Kim, A. E. Avrin, V. R. Tiruvadi, S.-W. Hwang, A. C. Vanleer, D. F. Wulsin, K. Davis, C. E. Gelber, L. Palmer, J. Van der Spiegel, J. Wu, J. Xiao, Y. Huang, D. Contreras, J. A. Rogers, and B. Litt. Flexible, foldable, actively multiplexed, high-density electrode array for mapping brain activity in vivo. *Nature Neuroscience*, 14(12):1599–1605, **2011**.
- [5] D. Feili, M. Schuettler, and T. Stieglitz. Matrix-addressable, active electrode arrays for neural stimulation using organic semiconductors—cytotoxicity and pilot experiments *in vivo*. *Journal of Neural Engineering*, 5(1):68–74, **2008**.
- [6] E. Bystrenova, M. Jelitai, I. Tonazzini, A. N. Lazar, M. Huth, P. Stoliar, C. Dionigi, M. G. Cacace, B. Nickel, E. Madarasz, and F. Biscarini. Neural Networks Grown on Organic Semiconductors. *Advanced Functional Materials*, 18(12):1751–1756, **2008**.
- [7] M. Kaltenbrunner, T. Sekitani, J. Reeder, T. Yokota, K. Kuribara, T. Tokuhara, M. Drack, R. Schwödiauer, I. Graz, S. Bauer-Gogonea, S. Bauer, and T. Someya. An ultra-lightweight design for imperceptible plastic electronics. *Nature*, 499(7459):458–463, **2013**.
- [8] J. H. Cho, J. Lee, Y. Xia, B. Kim, Y. He, M. J. Renn, T. P. Lodge, and C. Daniel Frisbie. Printable ion-gel gate dielectrics for low-voltage polymer thin-film transistors on plastic. *Nature Materials*, 7(11):900–906, **2008**.
- [9] S. H. Kim, K. Hong, W. Xie, K. H. Lee, S. Zhang, T. P. Lodge, and C. D. Frisbie. Electrolyte-Gated Transistors for Organic and Printed Electronics. *Advanced Materials*, 25(13):1822–1846, **2013**.
- [10] J. D. Yuen, A. S. Dhoot, E. B. Namdas, N. E. Coates, M. Heeney, I. McCulloch, D. Moses, and A. J. Heeger. Electrochemical Doping in Electrolyte-Gated Polymer Transistors. *Journal of the American Chemical Society*, 129(46):14367–14371, **2007**.
- [11] S. Inal, J. Rivnay, P. Leleux, M. Ferro, M. Ramuz, J. C. Brendel, M. M. Schmidt, M. Thelakkat, and G. G. Malliaras. A High Transconductance Accumulation Mode Electrochemical Transistor. *Advanced Materials*, 26(44):7450–7455, **2014**.

- [12] D. Bernards and G. Malliaras. Steady-State and Transient Behavior of Organic Electrochemical Transistors. *Advanced Functional Materials*, 17(17):3538–3544, **2007**.
- [13] C. G. Willson, R. R. Dammel, and A. Reiser. Photoresist materials: a historical perspective. volume 3051, pages 28–41. **1997**.
- [14] J. Dong, J. Liu, G. Kang, J. Xie, and Y. Wang. Pushing the resolution of photolithography down to 15nm by surface plasmon interference. *Scientific Reports*, 4, **2014**.
- [15] P. Andersson, D. Nilsson, P.-O. Svensson, M. Chen, A. Malmström, T. Remonen, T. Kugler, and M. Berggren. Active Matrix Displays Based on All-Organic Electrochemical Smart Pixels Printed on Paper. *Advanced Materials*, 14(20):1460–1464, **2002**.
- [16] D. Nilsson, T. Kugler, P.-O. Svensson, and M. Berggren. An all-organic sensor–transistor based on a novel electrochemical transducer concept printed electrochemical sensors on paper. *Sensors and Actuators B: Chemical*, 86(2):193–197, **2002**.
- [17] L. Basiricò, P. Cosseddu, A. Scidà, B. Fraboni, G. Malliaras, and A. Bonfiglio. Electrical characteristics of ink-jet printed, all-polymer electrochemical transistors. *Organic Electronics*, 13(2):244–248, **2012**.
- [18] E. Stavrinidou, R. Gabrielsson, E. Gomez, X. Crispin, O. Nilsson, D. T. Simon, and M. Berggren. Electronic plants. *Science Advances*, 1(10):e1501136–e1501136, **2015**.
- [19] M. Sessolo, D. Khodagholy, J. Rivnay, F. Maddalena, M. Gleyzes, E. Steidl, B. Buisson, and G. G. Malliaras. Easy-to-Fabricate Conducting Polymer Microelectrode Arrays. *Advanced Materials*, 25(15):2135–2139, **2013**.
- [20] D. Khodagholy, J. Rivnay, M. Sessolo, M. Gurfinkel, P. Leleux, L. H. Jimison, E. Stavrinidou, T. Herve, S. Sanaur, R. M. Owens, and G. G. Malliaras. High transconductance organic electrochemical transistors. *Nature Communications*, 4, **2013**.
- [21] S. A. Tria, M. Ramuz, M. Huerta, P. Leleux, J. Rivnay, L. H. Jimison, A. Hama, G. G. Malliaras, and R. M. Owens. Dynamic Monitoring of *Salmonella typhimurium* Infection of Polarized Epithelia Using Organic Transistors. *Advanced Healthcare Materials*, 3(7):1053–1060, **2014**.
- [22] J. T. Friedlein, S. E. Shaheen, G. G. Malliaras, and R. R. McLeod. Optical Measurements Revealing Nonuniform Hole Mobility in Organic Electrochemical Transistors. *Advanced Electronic Materials*, 1(11):1500189, **2015**.
- [23] P. Gkoupidenis, N. Schaefer, B. Garlan, and G. G. Malliaras. Neuromorphic Functions in PEDOT:PSS Organic Electrochemical Transistors. *Advanced Materials*, 27(44):7176–7180, **2015**.
- [24] J. Rivnay, P. Leleux, M. Ferro, M. Sessolo, A. Williamson, D. A. Koutsouras, D. Khodagholy, M. Ramuz, X. Strakosas, R. M. Owens, C. Benar, J.-M. Badier, C. Bernard, and G. G.

- Malliaras. High-performance transistors for bioelectronics through tuning of channel thickness. *Science Advances*, 1(4):e1400251–e1400251, **2015**.
- [25] H. S. White, G. P. Kittlesen, and M. S. Wrighton. Chemical derivatization of an array of three gold microelectrodes with polypyrrole: fabrication of a molecule-based transistor. *Journal of the American Chemical Society*, 106(18):5375–5377, **1984**.
- [26] D. K. Rayabarapu, B. M. J. S. Paulose, J.-P. Duan, and C.-H. Cheng. New Iridium Complexes with Cyclometalated Alkenylquinoline Ligands as Highly Efficient Saturated Red-Light Emitters for Organic Light-Emitting Diodes. *Advanced Materials*, 17(3):349–353, **2005**.
- [27] P. Gkoupidenis, N. Schaefer, X. Strakosas, J. A. Fairfield, and G. G. Malliaras. Synaptic plasticity functions in an organic electrochemical transistor. *Applied Physics Letters*, 107(26):263302, **2015**.
- [28] S. A. Tria, L. H. Jimison, A. Hama, M. Bongo, and R. M. Owens. Validation of the organic electrochemical transistor for in vitro toxicology. *Biochimica et Biophysica Acta (BBA) - General Subjects*, 1830(9):4381–4390, **2013**.
- [29] S. Tria, L. Jimison, A. Hama, M. Bongo, and R. Owens. Sensing of EGTA Mediated Barrier Tissue Disruption with an Organic Transistor. *Biosensors*, 3(1):44–57, **2013**.
- [30] M. Ramuz, A. Hama, M. Huerta, J. Rivnay, P. Leleux, and R. M. Owens. Combined Optical and Electronic Sensing of Epithelial Cells Using Planar Organic Transistors. *Advanced Materials*, 26(41):7083–7090, **2014**.
- [31] G. Scheiblin, A. Aliane, X. Strakosas, V. F. Curto, R. Coppard, G. Marchand, R. M. Owens, P. Mailley, and G. G. Malliaras. Screen-printed organic electrochemical transistors for metabolite sensing. *MRS Communications*, 5(03):507–511, **2015**.
- [32] H. Tang, F. Yan, P. Lin, J. Xu, and H. L. W. Chan. Highly Sensitive Glucose Biosensors Based on Organic Electrochemical Transistors Using Platinum Gate Electrodes Modified with Enzyme and Nanomaterials. *Advanced Functional Materials*, 21(12):2264–2272, **2011**.
- [33] P. Lin, X. Luo, I.-M. Hsing, and F. Yan. Organic Electrochemical Transistors Integrated in Flexible Microfluidic Systems and Used for Label-Free DNA Sensing. *Advanced Materials*, 23(35):4035–4040, **2011**.
- [34] X. Strakosas, M. Sessolo, A. Hama, J. Rivnay, E. Stavrinidou, G. G. Malliaras, and R. M. Owens. A facile biofunctionalisation route for solution processable conducting polymer devices. *J. Mater. Chem. B*, 2(17):2537–2545, **2014**.
- [35] A.-M. Pappa, V. F. Curto, M. Braendlein, X. Strakosas, M. J. Donahue, M. Fiocchi, G. G. Malliaras, and R. M. Owens. Organic Transistor Arrays Integrated with Finger-Powered Microfluidics for Multianalyte Saliva Testing. *Advanced Healthcare Materials*, **2016**.

- [36] D. Khodagholy, T. Doublet, P. Quilichini, M. Gurfinkel, P. Leleux, A. Ghestem, E. Ismailova, T. Hervé, S. Sanaur, C. Bernard, and G. G. Malliaras. In vivo recordings of brain activity using organic transistors. *Nature Communications*, 4:1575, **2013**.
- [37] A. Williamson, M. Ferro, P. Leleux, E. Ismailova, A. Kaszas, T. Doublet, P. Quilichini, J. Rivnay, B. Rózsa, G. Katona, C. Bernard, and G. G. Malliaras. Localized Neuron Stimulation with Organic Electrochemical Transistors on Delaminating Depth Probes. *Advanced Materials*, 27(30):4405–4410, **2015**.
- [38] A. Campana, T. Cramer, D. T. Simon, M. Berggren, and F. Biscarini. Electrocardiographic Recording with Conformable Organic Electrochemical Transistor Fabricated on Resorbable Bioscaffold. *Advanced Materials*, 26(23):3874–3878, **2014**.
- [39] J. Rivnay, P. Leleux, M. Sessolo, D. Khodagholy, T. Hervé, M. Fiocchi, and G. G. Malliaras. Organic Electrochemical Transistors with Maximum Transconductance at Zero Gate Bias. *Advanced Materials*, 25(48):7010–7014, **2013**.
- [40] G. Pfurtscheller, A. Stancák Jr., and C. Neuper. Event-related synchronization (ERS) in the alpha band — an electrophysiological correlate of cortical idling: A review. *International Journal of Psychophysiology*, 24(1–2):39–46, **1996**.
- [41] J. Xu, R. F. Yazicioglu, B. Grundlehner, P. Harpe, K. A. A. Makinwa, and C. Van Hoof. A $160\text{-}\mu\text{m}$ 8-Channel Active Electrode System for EEG Monitoring. *IEEE Transactions on Biomedical Circuits and Systems*, 5(6):555–567, **2011**.
- [42] S. Patki, B. Grundlehner, A. Verwegen, S. Mitra, J. Xu, A. Matsumoto, R. F. Yazicioglu, and J. Penders. Wireless EEG system with real time impedance monitoring and active electrodes. In *2012 IEEE Biomedical Circuits and Systems Conference (BioCAS)*, pages 108–111. IEEE, **2012**.
- [43] Y. Chen. A lift-off process for high resolution patterns using PMMA/LOR resist stack. *Microelectronic Engineering*, 73-74:278–281, **2004**.
- [44] D. Khodagholy, T. Doublet, M. Gurfinkel, P. Quilichini, E. Ismailova, P. Leleux, T. Herve, S. Sanaur, C. Bernard, and G. G. Malliaras. Highly Conformable Conducting Polymer Electrodes for In Vivo Recordings. *Advanced Materials*, 23(36):H268–H272, **2011**.

Conclusion and outlook

The work presented in this thesis contributed to the development of improved interfaces between electrophysiological sensors and skin for healthcare applications. We first introduced the field of electrophysiology, to explain the genesis of electrical signals that can be recorded from the skin. We defined the medical and technological needs for cutaneous recording sensors, as well as the industrial conception steps for medical devices. The fundamental working principle of electrodes was described, particularly for cutaneous recordings. Commercially available medical electrodes used in clinics were presented for comparison. Once technology challenges and medical context understood, we focused our work on the development of innovated cutaneous sensors. We demonstrated the efficiency of conducting polymers such as PEDOT:PSS to better interface with biological tissue than medical standard do. We developed a new cholinium-based ion gel, with low toxicity, to replace traditional conductive gel in medical electrode. If a polyimide substrate is adapted for a fast industrialization of organic cutaneous electrodes, we also introduced an innovative process to coat organic materials within a knitted stretchable fabric. Then, we successfully evaluated the performance of our polyimide- and textile-based organic electrodes by the recording of electrophysiological signals on human volunteers. High-resolution, long-term and clinically relevant ECG and EMG were performed and compared with standard medical electrodes. Textile electrodes proved their ability in muscle stimulation and showed a strong resistance to motion artifacts, making them suitable as wearable healthcare sensors, integrated into clothes. Finally we explored the use of OECTs as active electrodes. We established their performance as pre-amplifier for clinical EEG, EOG and ECG recordings and studied their association with a drain load resistor for voltage-to-voltage amplification. Integration of OECTs and resistors on flexible substrates is now under development, to create active devices that can be in direct contact with the skin and connected to medical acquisition systems. Properties of OECTs such as *in situ* amplification and filtering will increase the sensibility of cutaneous recordings, particularly in EEG.

Our organic materials-based sensors exhibit an improved interface with the skin and can participate in the development of wearable sensors for long-term ambulatory monitoring. Our collaboration with an hospital facilitated the comprehension of medical requirements. Methods and materials presented in this thesis are now being integrated on medical devices for future industrialization.

NNT : 2016LYSEM021

Thomas Lonjaret

MICRO-FABRICATION OF WEARABLE AND HIGH-PERFORMING
CUTANEOUS DEVICES BASED ON ORGANIC MATERIALS FOR HUMAN
ELECTROPHYSIOLOGICAL RECORDINGS

Speciality: Microelectronics / Bioelectronics

Keywords: Medical Device, electrode, electrophysiology, organic electronics, organic electrochemical transistor, wearable sensor

Abstract: In our medicalized world, human-monitoring sensors can be found everywhere, from a smart-watch to a life-saving pacemaker. They facilitate direct recordings of our electrophysiological activity, in the hospital as well as in our everyday life. Electrophysiology is the study of electrical and electrochemical signals generated by specific cells or whole organs. It gives doctors the opportunity to track the physiological behavior of a single neuron, a muscle tissue or the integral brain. The recording of these activities is essential to diagnose and better understand diseases like cardiac arrhythmias, epilepsy, muscular degeneration and many more. In this thesis, we study different types of cutaneous electrodes based on organic materials, from conception to pre-clinical evaluation. The main focus of this work is to enable high-quality electrophysiological recordings through soft and flexible devices compatible with human skin.

Our approach is based on the usage of PEDOT:PSS conducting polymer and ionic gels in order to reduce impedance at the skin-electrode interface. Moreover, the substrate of our electrodes is made with different materials such as thin and conformable plastics and textiles. Our devices are then flexible, motion resistant and can be integrating into clothes. We developed new fabrication processes, considering the different substrates and organic materials specifics. The electrodes were characterized and then tested on human volunteers to show their excellent performance in comparison to standard medical electrodes. The evaluation of noise reduction capabilities and possibilities to perform long-term recordings were established on signals coming from muscles, heart and brain. In order to further reduce noise and to increase wearability, we present a hundred micrometer-small “active” electrode, based on the organic electrochemical transistor. It enables in situ amplification and filtering of recorded signals. The wearable organic electrodes developed in this work are of great industrial and clinic interest. Future work will aim to integrate these technologies into state-of-the-art medical devices.

École Nationale Supérieure des Mines
de Saint-Étienne

NNT : 2016LYSEM021

Thomas Lonjaret

MICRO-FABRICATION DE DISPOSITIFS AMBULATOIRES, CUTANÉS,
HAUTEMENT PERFORMANTS ET À BASE DE MATÉRIAUX ORGANIQUES
POUR L'ENREGISTREMENT DE SIGNAUX ÉLECTROPHYSIOLOGIQUES SUR
L'HOMME

Spécialité: Microélectronique / Bioélectronique

Mots clefs : Dispositif Médical, Electrode, Electrophysiologie, Electronique Organique,
Transistor Organique Electrochimique, Capteurs Flexibles Intégrés

Résumé : L'ensemble du corps humain est surveillé par différents capteurs médicaux connectés, que ce soit depuis une montre connecté ou par un pacemaker. Ces capteurs permettent une nette amélioration du suivi de notre santé, à l'hôpital, mais surtout dans notre vie de tous les jours, notamment en enregistrant les signaux électrophysiologiques. L'électrophysiologie consiste à étudier les signaux électriques et électrochimiques générés aussi bien par certaines cellules spécifiques que par des organes entiers. Elle donne donc aux médecins l'opportunité de suivre le fonctionnement du corps à plusieurs échelles. L'enregistrement de ces activités par des électrodes est essentiel pour le diagnostic et la compréhension de pathologies aussi diverses que les arythmies cardiaques, l'épilepsie ou la dégénération musculaire. Dans cette thèse, nous étudions différents types d'électrodes cutanées à base de matériaux organiques, de leur conception à leur évaluation préclinique. Le principal but de ce travail est de développer une interface souple et compatible avec la peau humaine, afin de réaliser des mesures électrophysiologiques performantes. Notre approche est basée sur l'utilisation du polymère conducteur PEDOT:PSS et de gels ioniques, qui réduisent l'impédance de l'interface électrode-peau. Différents substrats fins et souples, plastiques ou textiles, composent nos électrodes. Cela leur confère une importante flexibilité et permet même de les intégrer à des vêtements. De nouvelles techniques de fabrications, adaptées à ces substrats et aux matériaux organiques, sont présentées. Afin de démontrer les excellentes performances de nos capteurs innovants par rapport aux électrodes médicales usuelles, ceux-ci sont intégralement caractérisés, puis testés sur des volontaires. L'enregistrement de signaux cutanés issus des tissus musculaires, cardiaques et cérébraux permet d'évaluer la stabilité sur plusieurs jours et la qualité de nos électrodes. Nous introduisons également le transistor organique électrochimique, utilisé pour la première fois comme une électrode cutanée microscopique dite « active ». Celui-ci permet d'amplifier et de filtrer in situ le signal afin d'augmenter sa qualité. Du fait de leurs forts potentiels industriels et cliniques, nous étudions maintenant l'intégration de nos électrodes organiques cutanées dans des produits médicaux de pointe.